# VAPA, THE MAJOR VIRULENCE DETERMINANT OF *RHODOCOCCUS EQUI*, BINDS PHOSPHOLIPIDS AND ALTERS PHAGOSOMAL MATURATION

by

#### LINDSAY MICHELLE WRIGHT

(Under the Direction of Mary K. Hondalus and Vincent J. Starai)

#### **ABSTRACT**

Rhodococcus equi is a ubiquitous organism that causes pyogranulomatous pneumonia in foals. Previous work on R. equi has ascertained that the organism carries an ~80 kb virulence plasmid known as pVapA; within this plasmid, is a region that contains features consistent with a pathogenicity island. This pathogenicity island encompasses a family of virulence associated proteins, or Vaps, that do not share sequence homology with any other proteins nor have an identified function. Investigation of these Vap proteins has determined that VapA is able to allow intramacrophage replication of R. equi, wherein none of the remaining Vap proteins on pVapA share this capacity. Further studies with a vapA deletion mutant of R. equi have determined the importance of this protein during inhibition of phagosomal maturation; however, it has yet to be defined how VapA functions to promote bacterial virulence. Experimentation within has shown the capacity of recombinant VapA (rVapA) to rescue the  $\Delta vapA$  deletion mutant of R. equi during macrophage infection. Subsequently, this protein was assessed for its ability to bind host phospholipids to better understand VapA's mechanism of action. It was seen that rVapA was able to interact with phosphatidic acid. Furthermore, staining for VapA during intramacrophage replication or in vitro expression of the protein in the model organism Saccharomyces cerevisiae

revealed the presence of VapA at the surface of eukaryotic membranes. Consequently, the basic amino acid residues within VapA were mutated in an attempt to hinder VapA membrane localization and phosphatidic acid binding, as it is hypothesized that VapA's interaction with phosphatidic acid is at least partially responsible for the ability of VapA to alter the outcome of *R. equi* intramacrophage replication. Mutating residues within the conserved domain of VapA prohibited bacterial replication within the macrophage and disrupted the membrane localization during yeast expression. It remains to be proven whether these mutations alter the ability of the protein to bind phosphatidic acid. Together, these findings suggest that VapA is able to bind phosphatidic acid and that amino acid residues located within the conserved domain of the protein are important for VapA's ability to alter macrophage infection with *R. equi*.

INDEX WORDS: Rhodococcus equi, VapA, Phosphatidic acid, Macrophage, Conserved domain

# VAPA, THE MAJOR VIRULENCE DETERMINANT OF *RHODOCOCCUS EQUI*, BINDS PHOSPHOLIPIDS AND ALTERS PHAGOSOMAL MATURATION

by

### LINDSAY MICHELLE WRIGHT

B.S., Clemson University, 2012

A Dissertation Submitted to the Graduate Faculty of The University of Georgia in Partial

Fulfillment of the Requirements for the Degree

DOCTOR OF PHILOSOPHY

ATHENS, GEORGIA

2018

© 2018

Lindsay Michelle Wright

All Rights Reserved

# VAPA, THE MAJOR VIRULENCE DETERMINANT OF *RHODOCOCCUS EQUI*, BINDS PHOSPHOLIPIDS AND ALTERS PHAGOSOMAL MATURATION

by

## LINDSAY MICHELLE WRIGHT

Major Professor: Mary Hondalus

Vincent Starai

Committee: Barbara Reaves

Steeve Giguère Richard Steet

Electronic Version Approved:

Suzanne Barbour Dean of the Graduate School The University of Georgia May 2018

## **DEDICATION**

This dissertation is dedicated to my parents, Cindy and Stephen Wright. They not only supported me through my education but always promoted my passion for science.

#### **ACKNOWLEDGEMENTS**

I would first and foremost like to thank Dr. Mary Hondalus who gave me the opportunity to work in her lab and on this project. Throughout this process she has been a supportive foundation from which I was able to grow and expand my scientific knowledge. Additionally, she has guided me through the critical examination of produced data as well as improved my ability to communicate my findings with others. I am honored to have been able to work with her during my graduate education.

I have also had the privilege of having a co-major professor, Dr. Vincent Starai, whom I would like to thank for his constant encouragement and help in learning to assess all angles of an obstacle. I thank the members of my committee, Dr. Barbara Reaves, Dr. Steeve Giguère, and Dr. Richard Steet, for their time spent advising and mentoring me.

# TABLE OF CONTENTS

		Page
ACKNO	WLEDGEMENTS	v
LIST OF	TABLES	viii
LIST OF	FIGURES	ix
СНАРТЕ	ER	
1	INTRODUCTION	1
2	REVIEW OF THE LITERATURE	2
	Taxonomical Analysis	2
	Epidemiology	2
	Microbial Features	6
	Capsule	6
	Cell Envelope	7
	Chromosomal Virulence Determinants	11
	Virulence Plasmid	14
	Pathogenesis of Rhodococcus equi	23
	Macrophage Microbicidal Tactics	32
	Host Response	36
	Clinical Disease and Pathology	39
	Diagnosis and Treatment	41
	Bacterial Effectors	43

		Saccharomyces cerevisiae as a Model Organism	40
		Mammalian Membranes	47
	3	VAPA OF RHODOCOCCUS EQUI BINDS PHOSPHATIDIC ACID	54
		Abstract	55
		Introduction	55
		Results	59
		Discussion	66
		Experimental Procedures	74
	4	MUTATIONAL ASSESSMENT OF VAPA OF RHODOCOCCUS EQUI	97
		Introduction	98
		Results	99
		Discussion	104
		Experimental Procedures	106
	5	CONCLUSION	124
REFE	REI	NCES	133

# LIST OF TABLES

	Page
Table 1: Bacterial and yeast strains	93
Table 2: Plasmids used in this study	94
Table 3: Primers used in this study	95
Table 4: Bacterial and yeast strains	119
Table 5: Primers used in this study	120
Table 6: Plasmids used in this study	122

## LIST OF FIGURES

Page
Figure 1: Recombinant VapA <sup>32-189</sup> and VapK2 <sup>32-202</sup> complement the replication defect of <i>R. equi</i>
$\Delta vapA$ 83
Figure 2: Proteinase K digestion of each recombinant Vap shows a stable protein core84
Figure 3: Recombinant VapA <sup>32-189</sup> enhances intracellular persistence of nonpathogenic <i>E. coli</i> in
J774A.1 cells85
Figure 4: VapA associates with the RCV membrane during infection
Figure 5: GFP-VapA binds to the yeast plasma membrane upon expression <i>in vivo</i>
Figure 6: rVapA binds phosphatidic acid containing liposomes90
Figure 7: The presence of VapA prevents the accumulation of LAMP1 within the RCV 48 and
72h post infection91
Figure 8: Comparison of $\Delta vapA$ with strains expressing wild type or mutated versions of
vapA112
Figure 9: Expression of <i>vapA</i> containing mutations within the conserved domain is unable to
rescue the replication defect of $\Delta vapA~R.~equi$
Figure 10: GFP-VapA mutated within the conserved domain fails to localize to the plasma
membrane in saccharomyces cerevisiae116
Figure 11: GFP-VapA <sup>R99A</sup> mimics the localization of GFP-VapA.Conserved when expressed in
Saccharomyces cerevisiae118

Figure 12: Model for VapA's mechanism of action during macrophage infection with	
Rhodococcus equi	132

#### CHAPTER 1

#### INTRODUCTION

Rhodococcus equi is a soil dwelling Gram-positive bacterium that can cause disease in a variety of hosts species; including but not limited to equine, bovine, swine, and human. In the foal (young horse) and human, the bacterium causes pyogranulomatous pneumonia, characterized by the marked influx of macrophages and neutrophils. Within the host, the bacterium replicates inside of alveolar macrophages, generating a niche in which the bacterium can avoid clearance. Intramacrophage replication of R. equi relies on the presence of a virulence plasmid. Isolates from foals contain a pVapA type virulence plasmid, but research has shown that there are also pVapB and pVapN type virulence plasmids in isolates from other species. Located on each of these plasmids is a pathogenicity island carrying a unique family of genes denoted as the virulence associated protein, or vap, genes. The generated virulence associated proteins do not share an extensive amount of homology with any other studied proteins besides one another. Previous research has established the importance of certain Vap proteins and their requirement for R. equi to replicate within the macrophage. pVapA containing R. equi isolates, express multiple vap genes including vapG, vapH, vapC, vapD, vapE, and vapA, yet only the latter is essential for intramacrophage replication. Characterization of the R. equi containing vacuole has revealed an alteration in phagosome maturation in the presence of VapA. Currently, the mechanism by which VapA alters the killing capacity of the macrophage is unknown. The following work was initiated to better understand host: VapA interaction.

#### CHAPTER 2

#### REVIEW OF THE LITERATURE

#### **Taxonomical Analysis**

Rhodococcus equi belongs to the nocardioform actinomycete group encompassing the Mycobacterium, Corynebacterium, Nocardia, Gordonia, Rhodococcus, and Tsukamurella genera. It is widely accepted that Magnusson first isolated R. equi from a pneumonic foal in 1923, where he identified the bacterium as Corynebacterium equi [1-4]. Over the years, other taxonomic names were given to the bacterium including, but not limited to, Corynebacterium hoagii, Nocardia restricta, and Mycobacterium equi [2, 4, 5]. Of these, C. equi was the most widely used, but shuffling of the organism between taxa caused turmoil in the field. Goodfellow and Alderson would later relieve this confusion by establishing the Rhodococcus genus and reclassifying C. equi as Rhodococcus equi [2]. About 40 years have passed since the classification of R. equi and until recently, 2013, there were no attempts made to reassign its taxonomic location [1]. The name proposed by Jones and colleagues in 2013 was neither legitimate nor accepted by the field [1]. While classification has not yet been fully resolved, Rhodococcus equi will remain the identifying name for the bacterium for the foreseeable future [5-8].

### **Epidemiology**

Like other actinomycetes, *R. equi* is a soil-dwelling bacterium that is ubiquitous in nature [9-11]. Typically, *R. equi* is found replicating in topsoil that is neutral in pH, but isolation of the bacterium from more acidic soil is also possible [10-13]. As a topsoil inhabitant, *R. equi* is able

to come into contact with the feces of grazing herbivores. This is beneficial to the bacterium as it uses organic fatty acids present in the manure as a carbon source [10, 11]. In fact, *R. equi* replicates to a much higher degree in the excrement found on pastures, than in soil alone, making the bacterium a coprophile [11]. Additionally, the bacterium has been isolated from the intestinal tracts of a variety grazing animals [cattle, horse, sheep, pigs, and goats] [10, 11, 14]. Infection by *R. equi* occurs in a wide variety of animals [cattle, goats, swine, buffalo, sheep, crocodiles, wild birds, deer, seals, marmosets, and koala bears], but disease predominates in immunocompromised hosts and in foals [9, 15].

#### Horses

R. equi disease is most common in foals, and therefore, most epidemiological studies have been done on horse farms. 50-95% of farms studied have had R. equi identified in environmental isolates [9]. Consistent with this, is the ability of horses on these farms to generate a delayed-type hypersensitivity (DTH) response to bacterial antigens, indicating immunological exposure to R. equi [11, 16]. Despite the magnitude of R. equi exposure, disease is considered sporadic, with only certain farms reaching an endemic state [12, 16-18]. Furthermore, the mortality rate can range from 12-80% once clinical disease is established [18].

Development of disease has been associated with the proportion of virulent *R. equi*, specifically aerosolized *R. equi*, present on the farm [12, 13, 16, 19]. These findings are in agreement with the contention that inhalation of aerosolized bacteria is the major route of infection, as ingestion is typically self-limiting [14, 17, 20, 21]. Simultaneously, the underdeveloped gastrointestinal tract of foals has been suggested to allow bacterial replication in the gut, and therefore, higher amounts of *R. equi* are present in the feces of foals compared to adults [12, 17, 22]. This leads to increased deposition of *R. equi* onto the pasture and greater

opportunity for bacterial exposure. In addition, the tendency of a pneumonic foal to swallow R. equi containing sputum permits infected foals to excrete the highest amounts of R. equi at  $10^6$ - $10^8$  bacteria/gram feces [12].

Approaches to lessen the burden and spread of virulent *R. equi* on the farm have been recommended. These methods consist of removing manure from the pasture, maintaining ground cover for paddock areas, altering horse mating season such that foals are borne in colder months when levels of airborne *R. equi* are lower, and keeping horses/foals in smaller groups [12, 16, 17, 19]. Advisement to use these methods comes from studies showing that there is a higher amount of airborne *R. equi* on dry, windy, and hot days [12, 16]. Generally, the theory maintains that greater amounts of virulent *R. equi* allow for a higher probability of infection, with larger bacterial challenges more likely to cause disease [16, 22].

## Pigs and Cattle

R. equi has the ability to infect a wide variety of animals, where, behind foals and man, cattle and swine are the most commonly affected species [9]. Studies discerning the presence of virulent R. equi in the soil and air on cattle and pig farms are scant; however, there are studies documenting the isolation of R. equi from swine and bovine tissues [15, 23-25]. In swine, R. equi was found in both domesticated livestock and in wild boars [25]. Cattle have a very low prevalence of R. equi as only .008% of 3,263,622 animals screened were culture positive for the bacterium [24]. Swine and cattle will carry the bacterium in their submaxillary lymph nodes and appear healthy. Although not all colonized lymph nodes will have lesions, when lesions are present, they can be tuberculosis-like in nature [12, 17, 23, 24]. Unlike foals, the route of infection for cattle and swine is unknown. Experiments attempting to replicate infection in

swine, via aerosolized or fed *R. equi*, were unsuccessful [15, 26]. Despite the failure to mimic disease progression in swine, it is accepted that ingestion is the likely route of infection.

#### Humans

With the rise in immunocompromised individuals has come the increased occurrence of *R. equi* disease in humans [9]. The first case of *R. equi* pneumonia in a human patient was documented in 1967 and occurred in a 29-year-old man being treated for chronic hepatitis C. This individual was presumably exposed to *R. equi* during a prolonged period of time spent on a horse farm [27]. Since then, *R. equi* has become a recognized agent of human disease and not just a laboratory-identified contaminant [9, 28]. HIV-infected individuals represent the principal group affected by *R. equi*, at ~66% of cases. Other predisposing host factors for disease caused by *R. equi* include organ transplantation, presence of traumatic wounds, and ongoing chemotherapy. Mortality is a common outcome of *R. equi* infection, with HIV patients exhibiting a 55% mortality rate. Immunocompetent individuals are also at risk for acquiring *R. equi*, representing 10-15% of cases [9]. Cavitary pneumonia comprises the majority of both immunocompromised and immunocompetent cases; however, there are a plethora of other clinical manifestations documented [9, 29, 30].

Like the swine and bovine hosts, the route of infection in people is unknown but presumed to be most commonly via inhalation or wound contamination. Bacterial exposure probably occurs through contact with soil, livestock, or through nosocomial introduction [9, 28, 29]. Analysis of soil and sand specimens from a park in Japan determined that *R. equi* could be isolated from this environmental setting; however, of the bacteria isolated none expressed the virulent or intermediately virulent markers making it unclear if this bacteria is relevant to infection [31]. More recently, cattle, swine, and horses destined as a food source were examined

for the presence of virulent *R. equi* as a potential exposure risk to humans. It was determined, that approximately 25% of swine submaxillary lymph nodes had pVapB carrying *R. equi* present, while horse and bovine species had 0.5% and 1.3% of virulent *R. equi* isolated respectively [32].

## **Microbial Features**

Characteristically, *R. equi* is an aerobic, Gram-positive, non-motile, partially acid-fast bacterium that is coccobacillus in shape [1, 2, 10, 33]. It possesses urease, lipase, catalase, and phosphatase; and lacks DNase, oxidase, protease, and elastase [1-3, 9, 34]. When grown on agar, colonies will be mucoid and produce a pink to orange-red color, as suggested by the name *Rhodococcus*, meaning red coccus [1, 2].

#### **Capsule**

Examination of the capsular polysaccharide encompassing *R. equi* has thus far resolved the presence of 27 serotypes [34, 35]. Of the seven serotypes described by Prescott in 1981, six were analyzed and determined to be acidic in nature [34-36]. This acidity is achieved through acetal-linked pyruvic or lactic acid and an acidic sugar, like glucuronic or rhodaminic acid, in the polysaccharide repeating unit [35, 36].

Capsules of other bacteria have been shown to play a role in virulence. Some immune system functions known to be inhibited by the presence of certain capsules are serum lytic activity, phagocytosis, and immune cell activation. For instance, the K antigen of *E. coli* is a well-studied capsule carbohydrate that can interfere with the lytic capabilities of complement [37]. It was initially believed that the *R. equi* capsule would also contribute to virulence, but this theory has since been disproven. The leading observation dismissing *R. equi*'s capsule as a virulence factor was the lack of a serotype correlating with virulent isolates and instead with geographical location [17, 38]. Sydor and colleagues later deleted the mycolyl transferase gene,

*fbpA*, generating a mutant *R. equi* that could no longer produce a capsule. Macrophage infections done with this *fbpA* mutant showed that the bacterium could replicate and avoid phagolysosomal fusion to the same capacity as the wild type bacterium [39].

## **Cell Envelope**

*R. equi*'s cell envelope has been modeled by Iain Sutcliffe, wherein the models were based off of experimental studies [35, 40, 41]. As a Gram-positive bacterium belonging to the mycolata subset, *R. equi*'s cell envelope contains the mycolyl-arabinogalactan-peptidoglycan complex [35, 40, 42]. This complex provides extensive layering outside of the bacterial plasma membrane, producing a somewhat impermeable and protective coat [42-44]. Moving from the plasma membrane to the extracellular environment, the initial layer present in the cell envelope is the peptidoglycan structure [35, 40].

#### Peptidoglycan

The general structure of peptidoglycan consists of a disaccharide polymer linked via pentapeptide chains [43]. Typically, the disaccharide is made up of N-acetylglucosamine-N-acetylmuramic acid, but *R. equi* will contain an N-glycolylmuramic acid instead [35, 40, 43]. Pentapeptide crosslinks between the disaccharide polymers will occur through mesodiaminopimelic acid, making *R. equi*'s peptidoglycan the A1 Y type [35].

#### Arabinogalactan

Moving outward from the peptidoglycan layer, the next structural component is the polysaccharide arabinogalactan (AG), which makes up 35% of the cell wall mass [35, 40, 42, 45]. Covalent attachment of AG to peptidoglycan occurs through the linker unit rhamnosyl- $(1\rightarrow 3)$ -N-acetyl-glucosamine. AG is a heteropolymer consisting of a galactan and an arabinan domain. The galactan domain consists of a 35-50 residue polymer of  $\beta$ -galactofuranosyl with

alternating 1-5 and 1-6 linkages or 1-5 and 1-3 linkages, off of which α-arabinofuranosyl will branch [35, 45]. The *R. equi* arabinan domain consists of a linear 5-linked chain with branches at the third carbon. This arabinose organization is similar between *R. equi* and other actinobacteria, including *Mycobacterium* and *Nocardia*; however, the arabinose non-reducing ends vastly differ between these genera [45]. Capping of *R. equi*'s arabinose chain can occur in one of two ways. The first of which is via a triarabinosol branch and the second of which is a mannose cap [35, 40, 45]. When the triarabinosol non-reducing end is present, it can result in the esterification of two mycolic acid chains, described next [35].

#### Mycolic Acids

Mycolic acids form the basis of *R. equi*'s outer membrane, a characteristic feature of the mycolata subset. Mycolic acids are characterized by their 2-alkyl, 3-hydroxy long chain fatty acid composition. The 3-hydroxy long chain fatty acid is known as the meromycolate chain, which can differ in length depending on the bacterial genus or species [35, 40, 42, 46]. As a genus, *Rhodococcus* has an intermediate meromycolate chain length at 28-54 carbons, where *R. equi* resides on the lower end of this spectrum containing 14-36 carbons [35, 39, 42, 46, 47]. Respectively, the longest and shortest meromycolate chain lengths will be found in the *Segniliparus* (40-76 carbons) and *Corynebacterium* (8-18 carbons) genera [42]. Genera specific alterations at the distal end of the meromycolate chain also occur, with the *Mycobacterial* genus having the highest capacity for chain modification [35, 42]. Specifically, the distal end of *R. equi*'s meromycolate chain will contain 0-2 degrees of unsaturation [42, 46].

Synthesis of mycolic acids begins in the cytoplasm of the bacterium through the use of the eukaryotic-like fatty acid synthase, FAS-I [35, 42]. FAS-I will generate the 2-alkyl chain or the foundation of the meromycolate chain via the attachment of 10-18 carbons to acetyl-CoA

[42]. This acyl-CoA, produced by FAS-I, will be condensed with malonyl-CoA to enter the FAS-II multistep pathway, responsible for elongation of the meromycolate chain [35, 42]. *M. tuberculosis* viability depends on the presence of the FAS-II pathway, as shown by gene deletion and metabolic inhibitor studies [42]. Sydor's group has demonstrated that this is not the case for *R. equi*, as neither deletion of *kasA*, from the FAS-II complex, nor addition of thiolactomycin, a *kasA* inhibitor, could arrest bacterial growth in broth. In contrast, FAS-I function is essential for *R. equi* replication as the triclosan compound, responsible for inhibition of the FAS-I and FAS-II pathways, prohibited growth [39].

Polyketide synthases will assemble the FAS-I and FAS-II products through Claisen condensation, in order to generate mycolic acid [42, 48]. Exportation of mycolic acid to the extracellular space occurs via a trehalose carrier [35, 42]. At the cell wall, the mycolic acid may either be covalently bound to the free arabinose of arabinogalactan or remain as a free glycolipid [35, 42]. Work by Hsu and associates demonstrated that the mycolic acids are predominantly attached to the cell wall, where linkage occurs via the *fbp* family of mycolyltransferases [35, 46]. It has yet to be determined whether the outer membrane of *R. equi* is an asymmetrical bilayer, with an inner leaflet of mycolic acids and an outer leaflet of glycolipids, or a monolayer of mycolic acids [35]. *M. tuberculosis* has been found to have a bilayer outer membrane, known as the mycomembrane, allowing speculation that the same may be true for *R. equi* [42]. The relatively impermeable mycolic acid containing outer membrane may provide a protective layer for *R. equi* [35, 40, 44]. Relevance of mycolic acids as a virulence determinant for *R. equi* will be discussed later.

#### Other Cell Wall Constituents

The above malonyl-arabinogalactan-peptidoglycan complex provides the scaffolding for other components of the cell wall. Free glycolipids, mentioned earlier, represent one of these components [35, 42]. It is unknown how these glycolipids associate with the outer membrane of *R. equi*, but a favored theory suggests that these molecules will form an outer leaflet to fill the exposed mycolic acid containing layer [35].

Protein factors are also present in the cell envelope of *R. equi*; however, due to the vast amount of proteins contained, only a small discussion will ensue. Attachment of proteins to the cell wall may occur through covalent bonding to the peptidoglycan structure or through lipid modification [35, 40, 48]. Lipoproteins represent the lipid bound polypeptides, which make up ~2% of the total protein produced by the bacterium [35, 40]. It was once postulated, that the major virulence determinant VapA, discussed later, was a lipoprotein, but further work did not support this theory [49]. Additionally, a family of non-covalently attached proteins in the cell wall, known as porins, are important for acquiring nutrients from the bacterium's environment [35].

The last constituent of the cell envelope that requires discussion is the lipoglycan lipoarabinomannan (LAM). LAM is found in other actinobacterial species, like *M. tuberculosis*, and has been known to facilitate the phagocytosis of invading pathogens by macrophages [35, 40, 50, 51]. *R. equi*'s LAM molecule has also been notated as ReqLAM [51]. Phosphatidylinositol mannoside provides the base of this LAM molecule, allowing for interaction with bacterial membranes. Off this foundation resides an alpha-1, 6- linked mannopyranose (Man*p*) chain, originating from the sixth carbon of the inositol base [35, 40, 51]. Branching from the Man*p* linear chain will occur ~44% of the time via attachment of a Man*p* 

sugar to the second carbon. Of these branch events, half will remain with the added Man*p* as the terminal sugar and the other half will undergo addition of a terminal arabinofuranosyl group. Overall, LAM is a highly variable macromolecule, where ReqLAM is considered a truncated version due to a ~9kDa difference between *M. tuberculosis* LAM and *R. equi* LAM, presumably caused by a lack of arabinose branching in the ReqLAM molecule [51].

### **Chromosomal Virulence Determinants**

R. equi has a circular genome that is ~5Mb in size with 4,525 predicted genes. This genome is smaller than that of other *Rhodococcus* species. The larger genomes of other Rhodococci are due to acquisition of redundant genes through gene duplication and horizontal gene transfer. In general, the *Rhodococcus* genus possesses numerous metabolic pathways allowing survival in different environmental niches. Annotation of the R. equi genome revealed the most predominant gene ontologies to be genes involved in metabolism and regulation, those encoding surface proteins, and those of unknown function [48].

The *narGHIJ* operon is one genomic region that may contribute to virulence in that it is responsible for denitrification under anaerobic conditions. Through this process, *R. equi* can acquire nitrogen as a food source and reduce nitric oxide, both of which are important during intramacrophage survival [48]. Evidence supporting the importance of the *narGHIJ* operon includes deletion of *narG* decreasing bacterial liver burden during *R. equi* infection of mice [52]. A second region of interest, containing a 9kb horizontal gene transfer (HGT) region, exclusive to *R. equi*, was found to harbor genes essential for pilus formation. This area of the genome is known as the *rpl* island, where *R. equi* may use the encoded pilus to adhere to host cells, promoting invasion [48]. Other chromosomal virulence determinants supported by experimental evidence include isocitrate lyase, mycolic acids, and a hydroxamate siderophore [39, 53, 54].

#### Isocitrate Lyase

It has been suggested that R. equi uses host lipids available in the phagosomal compartment in order to generate energy during macrophage infection [48, 53, 55, 56]. Cholesterol is one lipid present in the macrophage membrane, and it has been shown by Geize and colleagues that cholesterol can be used as a carbon source for R. equi [57, 58]. In agreement with this, R. equi secretes a functional cholesterol oxidase that is able to build up the cholesterol degradation intermediate cholestenone during macrophage infection and can cause red blood cell hemolysis when either phospholipase C or D is present [55, 59]. Initially, it was believed that cholesterol metabolism was not important for virulence, as gene deletions of cholesterol permeases, supA and supB, did not cause deviation from the parental phenotype during human in vitro monocyte infection [57]. However, deletion of two genes, ipdA and ipdB, necessary for cholesterol metabolism, resulted in decreased R. equi survival in that infection system [58]. While the importance of cholesterol use during R. equi infection is still enigmatic, it is clear that the bacterium produces energy during macrophage infection through the utilization of fatty acids via the glyoxylate shunt [53, 56]. The glyoxylate shunt is a divergent pathway of the tricarboxylic acid cycle (TCA) which uses acetyl-CoA produced by β-oxidation of fatty acids in order to generate products for gluconeogenesis [53, 60]. This alternative pathway is beneficial to the bacterium because it allows the bypass of two rate-limiting steps in the TCA cycle and avoids the loss of two CO<sub>2</sub> molecules. The two critical enzymes for function of this cycle are isocitrate lyase (ICL) and malate synthase (MS) [60, 61]. ICL has been the main focus of study in this pathway and is an enzyme crucial for the in vivo survival of some other pathogenic bacteria, such as Mycobacterium tuberculosis, Salmonella enterica, and Pseudomonas aeruginosa [53, 56, 60]. In murine infection experiments, it was found that an M. tuberculosis mutant lacking ICL

activity was unable to replicate to numbers comparable to that of the wild type bacterium [60]. Similarly, the deletion of aceA, the gene responsible for ICL production in R. equi, compromised the organism's ability to replicate in macrophages and resulted in the attenuation of virulence for both mice and foals. Specifically, pyogranulomatous pulmonary lesions were observed following intrabronchial challenge of foals with wild type R. equi, whereas foals receiving similar numbers of  $\Delta aceA$  R. equi did not develop any clinical symptoms or lesions [56]. These data show that, like other intracellular pathogens, isocitrate lyase is important during R. equi infection.

### Mycolic Acids

Mutational analysis has revealed that mycolic acids also play a role in R. equi virulence. Specifically, deletion of kasA, a  $\beta$ -ketoacyl-acyl carrier protein synthase responsible for elongation of the meromycolate chain in mycolic acids, resulted in a mutant strain less able to replicate in macrophages and thus more likely to end up in a fused phagolysosome. The meromycolate chains of this mutant were shorter by 10 carbons. Interestingly, supplementing  $Escherichia\ coli$  with mycolic acids isolated from wild type R. equi, and not  $\Delta kasA\ R$ . equi, allowed for better avoidance of the phagolysosome thereby linking an intracellular survival phenotype to mycolic acid chain length [39]. The ability of mycolic acids to inhibit phagolysosomal fusion and acidification has been shown previously in studies using trehalose dimycolate (TDM) isolated from M. tuberculosis and therefore suggests that mycolic acids have a natural capacity to alter phagolysosomal fusion [42].

#### Siderophore

Iron is an essential cofactor for enzymes in both eukaryotes and prokaryotes alike.

Bacteria can obtain iron through either direct contact or by secreting scavengers, known as siderophores, into their environment. Three varieties of siderophores have been characterized

based on their iron ligation group; where the coordinating groups are hydroxamate, catecholate, and carboxylate [54, 62]. During intramacrophage growth, the phagosome, in which the *R. equi* resides, is depleted of iron through the activity of an exporter known as Nramp [63]. Previous work demonstrated that *Nramp-/-* macrophages are more susceptible to infection by *Mycobacterium spp.*, *Leishmania spp.*, and *Salmonella spp.*, presumably due to the iron replete phagosome [63, 64]. To combat the iron starved phagosome, bacteria will utilize their siderophores to attain iron from host chelators [62]. Experimentation done by De Voss et al., in 2000, supported this theory, as inhibiting synthesis of the siderophore mycobactin of *M. tuberculosis*, diminished the intramacrophage replication capacity of the bacterium [65].

Specific siderophores that have been described for *R. equi* are the hydroxamate siderophore, Rhequichelin, and a catecholate siderophore, which remains unnamed [54, 66]. Like most siderophores, low iron conditions caused induction of both Rhequichelin, from the *rhbABCDE* gene cluster, and the catecholate siderophore, from gene clusters *iupU* and *iupST* [54, 62, 66]. In agreement with bacteria using siderophores to acquire iron during infection, it was found that deletion of *rhbCD* caused attenuation, not only in intramacrophage replication, but during *in vivo* infection of SCID mice [54]. In contrast, knockout of the catecholate siderophore did not alter *in vivo* infection of mice with *R. equi*, proving that not all siderphores are essential for survival in the host [66].

### **Virulence Plasmid**

#### Rhodococcus equi Associated Virulence Plasmids

Virulent strains of *R. equi*, isolated from animals and humans, are commonly equipped with a single copy of a virulence plasmid [38, 48, 67, 68]. Discussed earlier is the capability of *R. equi* to infect a variety of different hosts, wherein the type of virulence plasmid carried by the

bacteria generally correlates with a specific host species. Three types of virulence plasmids have been described to date, specifically pVapA, pVapB, and pVapN, wherein *R. equi* possessing pVapA infect foals, strains carrying pVapB generally infect swine, and those with pVapN will infect cattle [23, 69-74]. This trend is not absolute, and recent experimentation has shown that species specific intramacrophage replication is not dependent upon the type of virulence plasmid carried by the bacterium. Instead, *R. equi* strains equipped with either pVapA or pVapB could replicate within swine and equine macrophages *in vitro*, suggesting that plasmid:host association is more complex than intracellular replication [75]. Support of this theory comes from isolation of pVapB-carrying *R. equi* strains from cattle and the lack of plasmid type specificity in human isolates. Environmental isolates, such as those from soil often lack a virulence-associated plasmid entirely, indicating its dispensability in this setting [71].

All the virulence plasmids discussed have been fully sequenced. Sequencing revealed that pVapA is 80.1 kb in size with 73 coding sequences, pVapB is nearly identical in size (80kb) with 72 coding sequences, and pVapN is 119kb with 148 coding sequences [69, 73, 76]. Notably, the pVapA and pVapB plasmids are circular in nature and share a common ancestor for their housekeeping backbones, whereas the pVapN plasmid is linear and differs in backbone ancestry [73, 76, 77]. Characterization of the coding sequence homologs of pVapA and pVapB has given rise to four plasmid regions, specifically, the conjugation, replication/partitioning, pathogenicity, and unknown regions; where the unknown region is suggested to encode membrane proteins [76, 77]. Other species of *Rhodococcus* carry different plasmids and through alignments between these and the circular *R. equi* virulence plasmids, along with plasmids of other actinobacterial ancestry, it could be determined that there is plasmid synteny, or positioning, of these regions. Specifically, the synteny described is referred to as the CURV motif where the plasmid regions

are arranged in the following order: conjugation-unknown-replication-variable (pathogenicity) [76]. The conjugation, unknown, and replication/partitioning regions of the plasmids make up the housekeeping backbone and are 95% identical between pVapA and pVapB [76, 77]. It has been proposed that the replication region of pVapA and pVapB contains a hot spot for horizontal gene transfer and that these plasmids have acquired variable pathogenicity islands equipped with niche adaptive genes that are important for infection of their respective host species [76]. Comparatively, study of the pVapN plasmid has shown that it too has regions corresponding to conjugation, replication, and pathogenicity [73].

#### Pathogenicity Island

While the housekeeping region of the virulence-associated plasmids was defined on the basis of homologous genes, the pathogenicity island was delineated based on genetic composition and functional characterization [76-78]. Pathogenicity islands (PAI) are well studied genomic elements from 10-100kb in size that are obtained from a foreign source and allow the recipient to gain pathological function [79, 80]. The *R. equi* PAI was discovered by identifying an altered GC content (60.8% in the PAI and 66.6% in the rest of the plasmid), the presence of resolvase mobility genes, virulence genes, as well as a foreign tRNA [76, 77, 79-82].

Comparison between the pVapA, pVapB, and pVapN PAI regions has shown that the pVapA PAI is larger than the pVapB and pVapN PAIs at 21.5, 15.9, and 15.1 kb respectively, as determined by the *cgf* and *invA* or *cgf* and *tniQ* gene boundaries [73]. Unlike the plasmid backbone, the PAI regions of pVapA and pVapB are only 43% identical. Much of the likeness between these two PAI regions is due to the 6.2kb sequence from *lsr2* to *orf8*. Presumably, this region of the PAI was evolutionarily conserved because of the essentiality of virulence determinants residing in this area of the plasmid [76].

Importantly the virR operon, comprised of five separate genes, including two transcriptional regulators, is located within this conserved 6.2kb region [73, 76, 83-87]. The first gene in this operon, virR (orf4), is a homolog to the Lys-R type transcriptional regulators and controls transcription of the virR operon as well as influence the vapAICD operon, to be discussed later [83, 84]. Two promoters exist to control the transcription of the virR operon,  $P_{virR}$ and  $P_{icgA}$ , where VirR plays a role in transcriptional regulation at both promoters [83, 87].  $P_{virR}$  is upstream from virR and is constitutively active in R. equi; however, the produced VirR is able to bind the transcription start site of virR and negatively alter  $P_{virR}$  transcription. In contrast, VirR has a positive, but not sufficient, effect on transcription at the P<sub>icgA</sub> promoter during growth at lower pH (6.5) and higher temperature (37°C) conditions [83, 84]. The other transcriptional regulator present in the virR operon is the orphan two-component response-type regulator, virS (orf8), which is present at the end of the virR operon [77, 83, 84]. VirS does not play a role in transcriptional regulation at either  $P_{virR}$  or  $P_{icgA}$ , but does alter transcription of other PAI genes, including the vapAICD operon [83-85, 88]. Individual deletions of virR and virS show that the generated proteins cooperate to regulate transcription of PAI genes and their absence compromises bacterial survival in vivo [85].

icgA (orf5) is the second genomic element in the virR operon and is related to the major facilitator superfamily transporters [76, 87]. Wang and coworkers were able to demonstrate that deletion of icgA leads to a hypervirulent strain of R. equi that replicates to higher intracellular levels than wild type resulting in destruction of the infected monolayer; suggesting that IcgA may sense the phagosomal environment and allow R. equi to adjust its growth when it is inside of the host cell. In this way, IcgA may be a negative regulator of certain virulence factors so that R. equi does not kill the host macrophage, destroying its in vivo niche. It has been shown that

IcgA does not play a role in *virS* or *vapAICD* transcription but that it is upregulated two hours post macrophage infection. Alternatively, deletion of either *vapH* or *orf7*, genes three and four in the *virR* operon, was found not to affect the intracellular replication of *R. equi* and it is therefore presumed that these elements do not play a major role during macrophage infection [87].

Besides the conserved 6.2kb *virR* operon expanse, the remainder of the PAI is divergent in gene composition including the *vap* genes. It is believed that much of the genetic alterations occurring in the PAI were driven by direct repeats associated with the *vap* genetic elements [76]. Other genes residing in the PAI include *scm2* (*orf21*) and *orf10* [76, 85]. *Scm2* is homologous to other chorismate mutase genes that play a role in generation of aromatic amino acids, which are depleted in the phagosome. It has not been proven whether or not this gene is beneficial during *R. equi* infection of macrophages but it has been stated that the mammalian cell does not contain any of the known substrates of chorismate mutase [76]. Lastly, *orf10* deletion resulted in delayed clearance of *R. equi* from mouse livers; yet the significance of that finding is unclear, and it is not known how this gene alters infection [85].

Of note, it has been shown that pathogenicity island genes *virR* and *virS* can regulate genes residing on the chromosome of *R. equi*, supporting the idea of cooptive evolution.

Cooptive evolution is the process by which genes become adapted for processes other than those originally intended, allowing for new bacterial traits, like virulence. Specifically, the chromosomal genes regulated by the two transcriptional regulators present in the PAI deal with metabolism, regulation, and macromolecular transportation [48, 89]. The most heavily influenced chromosomal genes are a chorismate mutase, like *scm2*, and an anthranilate synthase. Anthranilate synthase is another enzyme that assists in aromatic amino acid synthesis.

Concordantly, deletion of either of these genes leads to an attenuated strain of *R. equi* [48].

## Virulence Associated Protein (Vap) Family

As discussed earlier, the *R. equi* PAI was partially characterized based on the presence of virulence genes that do not have homologs in any other species. Specifically, there is the virulence associated protein, or *vap*, gene family that is found within the pathogenicity islands of *R. equi* [76, 77]. It has been determined, that the PAI of the pVapA type plasmid is comprised of nine *vaps*, six full length and three pseudogenes, and that the PAIs of pVapB and pVapN type plasmids are comprised of six *vaps*, all full length [73, 76]. The *vaps* that make up the pVapA PAI are *vapG*, *vapH*, *vapX*, *vapA*, *vapI*, *vapC*, *vapD*, *vapE*, and *vapF* [76]. *vapF*, *vapI*, and *vapX* are the *vap* pseudogenes present on pVapA, arising through gene truncations and frameshifts [76, 90]. In contrast, the pVapB PAI consists of *vaps J*, *K1*, *L*, *K2*, *M*, and *B* and the pVapN PAI consists of *vaps O*, *P*, *N*, *Q*, *R*, and *S* [73, 76].

Comparison between the *vaps* on pVapA and pVapB shows 41-99% identity; *vap* comparison between pVapN and pVapA/B shows 20-81% identity. Sequence identity can help provide a map of evolutionary progression, wherein it is believed that *vapG/L/O*, *vapH/J/P*, *vapX/M/Q*, *vapA/B/N*, *vapI/R*, *vapC/S*, and *vapD* represent the initial *vap* genes before evolutionary divergence [73, 76]. Interestingly, only a single *vap* for each PAI is in the negative direction, genes *vapL*, *vapG*, and *vapO*, where these genes are evolutionarily paired [73, 76, 77]. *Vaps* not mentioned previously, *vapE* and *vapF* from pVapA and *vapK1* and *vapK2* from pVapB, are suggested to have arisen via gene duplications after PAI acquisition. These alterations may lend to the species tropism observed with *R. equi* isolates containing the pVapA or pVapB virulence-associated plasmids [73]. Due to the nature of my research project, and the paucity of information on the pVapB and pVapN type *R. equi* plasmids, this review will focus on the *vaps* present in the pVapA type plasmid.

Most transcriptional studies have focused on the control of the *vapAICD* operon, composed of vapA, vapI, vapC, orfA, orfB, and vapD [88, 90]. As mentioned earlier, both VirR and VirS play a positive role in transcriptional regulation of the *vapAICD* operon [86, 91]. Experiments have revealed that a single promoter is responsible for transcription of this operon, where transcription is active in acidic conditions (pH5.5), at higher temperatures (37°C), in magnesium and calcium depleted environments, or upon hydrogen peroxide exposure [85, 86, 90, 92, 93]. However, it is unknown whether this induction is due to specific control at the *vapAICD* operon or production of its regulators, VirR and VirS, under these conditions [84]. Once *vapAICD* transcription has occurred, the portion of the transcript that contains *vapA* is cleaved, generating a 700bp mRNA fragment containing vapA. The generated vap transcripts have differing half-lives; where vapA has the longest half-life at 7.2 min and vapC and vapI have the shortest half-life at ~1.5 min. vapA's half-life is presumed to be longer due to a 226bp 5' UTR and a hairpin loop structure at the 3' UTR [90]. The remaining functional vaps, located outside of the vapAICD operon, have been shown to rely on the presence of VirR and VirS as well. Specifically, transcription of vapG and vap E also increases when the temperature is 37°C and the pH is 6.5 [88]. Importantly, a study of the pVapA type vap transcripts produced during foal infection with R. equi has shown that vaps G, A, and D have the highest number of transcripts present [94].

Translation of these *vap* transcripts will give rise to proteins comprised of 150-206 amino acids [77]. Alignment of the predicted Vap proteins shows an overall sequence similarity of 50%, which increases to 70-80% when comparing the Vap's C-termini [92]. *In silico* studies of the translated proteins would suggest that the N-terminus contains a signal sequence that can be cleaved by signal peptidase I [76, 77, 92]. Data that supports the presence of the signal sequence

includes mature VapA beginning with amino acid 32 (threonine), secretion of Vaps C, D, and E, and surface localization of VapA [49, 92, 93]. Following the putative signal sequence, there is a disordered non-conserved region and a conserved structured C-terminus that make up the remainder of the protein [76]. Interestingly, of the Vap proteins studied, both VapA and VapE present themselves as doublets during western blot analysis, implying either post-translational modification or protein interaction [92].

Initial characterization of whole cell lysates of *R. equi* probed with immune foal serum revealed the presence of a 15- and 17-kDa band pair to be associated virulent isolates [38, 67, 70]. As mentioned previously both Vaps A and E present as a doublet during western blot analysis, but this major immunogenic protein was found to be VapA [92, 93]. To study if the Vap proteins aided in virulence, deletion analysis of all the *vap* genes was done and it was determined that deletion of *vapA* alone could attenuate *R. equi*'s virulence [81, 82, 87, 89]. Later experimentation would prove that VapA alone is not sufficient for *R. equi* virulence and that both VirR and VirS must be present in order to modulate the expression of chromosomally encoded genes [81, 89, 95]. Of note, the correct localization of VapA during these assays would support the contention that the genes coordinating the secretion of VapA are carried on the chromosome [81, 93, 95]. It has yet to be determined if the other *vaps* play a more modest role during host infection with *R. equi* but characterization of VapA's function during altered phagosomal maturation is underway and will be considered later in this review.

#### Vap Structures

In 2014, structures for Vaps B, D, and G were solved using X-ray crystallography [96-98]. X-ray crystallography is an important technique that has been used since the early 1900s to better understand protein structure where it is widely viewed that structural insight will help

better inform molecular function [99]. The basis of this technique comes from crystalizing a macromolecule of interest in a homogeneous structure and bombarding this structure with a certain wavelength of x-rays [99, 100]. During exposure, some of the x-ray beams will end up diffracting due to interaction with the sample; where this diffraction can be read by either exposure of a film or, nowadays, by radiation counters placed behind the crystal [100].

Afterwards, the spots generated can be mathematically resolved into a protein structure using Bragg's law [100]. This technique is not without limitations as crystallization is a very tedious task; even after crystallization, the crystals can be very sensitive to destruction by the x-rays used and disordered domains are not prone to structure solving [99, 100]. However, these challenges have not prevented the field from pushing forward, as x-ray crystallography has advanced our general knowledge of virion structure, protein motifs, macromolecular complexes, and cell signaling mechanisms [99].

In the case of Vaps B, D, and G, the stable core of the proteins was found at the C-terminal end, the area of highest similarity between Vap proteins. The N-terminus, the first 20-50 amino acids, was found to be disordered and has therefore been left unresolved. As determined by x-ray crystallography, the structure of the C-terminus in each of these Vaps contains an eight stranded anti-parallel  $\beta$ -barrel with an  $\alpha$ -helix present at the bottom of the structure, where the  $\alpha$ -helix links the fourth and fifth  $\beta$  strands. Of note, the topology of the  $\beta$ -strands in these solved structures is unique as  $\beta$ -barrel strand order is typically  $\beta$ 1-  $\beta$ 2-  $\beta$ 3-  $\beta$ 4-  $\beta$ 5-  $\beta$ 6-  $\beta$ 7-  $\beta$ 8 and the  $\beta$ -barrel strand order in the Vaps is  $\beta$ 1-  $\beta$ 2-  $\beta$ 3-  $\beta$ 8-  $\beta$ 5-  $\beta$ 6-  $\beta$ 7-  $\beta$ 4 [96-98]. This alternate order of the  $\beta$ -strands lends to two Greek key motifs in the Vap  $\beta$ -barrel and a possible capping of the structure at its two ends by the  $\alpha$ -helix at the bottom of the structure and the loops between  $\beta$ -strands 3-4 and 7-8 at the top of the structure [96, 98]. Even though the

arrangement of the  $\beta$ -barrel is distinctive, there were some similar structures, with less than fifteen percent identity, found in databases. These structures included some bacterial outer membrane proteins, cytoplasmic fatty-acid-binding proteins, avidin superfamily proteins, and lysozyme inhibitors [97].

Characteristically, the core of the  $\beta$ -barrel is compact, with the lower region of the structure containing a tryptophan that coordinates with multiple other aromatic side chains and the upper region containing amino acids with polar side chains, lending to hydrogen bonding [96, 98]. The opposite can be said for the surface of the proteins, as the top third is comprised of a very flattened and hydrophobic surface and the bottom two-thirds has a more polar atmosphere with both positive and negative residues [96, 97]. The proteins are also glycine rich in certain  $\beta$ -strands giving rise to a possible hydrophobic face of the Vap proteins, as has been found to occur in VapD [98].

During *in silico* overlay of these solved Vap structures it could be seen that the  $\beta$ -barrels almost superimposed with the major differences being the loops between  $\beta$ -strands 2-3 and 7-8 in VapD [96, 98]. However, it was also mentioned that VapB may have longer loops at the top of the  $\beta$ -barrel, which was not seen in the structural overlay [96, 97]. As mentioned earlier, VapA is the major Vap protein needed for virulence of *R. equi*. Nonetheless, difficulty crystalizing this protein has led to work being done on the homologous family members of VapA; where it is presumed that VapA's structure is similar to the aforementioned proteins [98].

### Pathogenesis of Rhodococcus equi

#### Recognition and Phagocytosis

As *Rhodococcus equi* is inhaled into the lower airway, the bacterium will come into contact with professional phagocytes known as alveolar macrophages. These macrophages are

specific to the lower airway and are kept in a steady state to allow clearance of invading pathogens or particles that have been respired [78]. Macrophages are able to encapsulate material using receptor-mediated endocytosis, pinocytosis, or phagocytosis. Phagocytosis is mediated by recognition of macromolecules with cell-surface receptors and is the major mechanism by which macrophages take up bacteria [101]. The majority of respired R. equi is phagocytosed after recognition by the CR3, or Mac-1, receptor. In order for R. equi to be recognized by the CR3 receptor, iC3b deposition on the bacterial surface must occur via activation of the alternative complement pathway (ACP) [102]. The ACP is constitutively active in the host due to random thioester hydrolysis of the C3 protein, present in both the serum and lung [103-105]. This thioester hydrolysis allows C3 to interact with downstream Factors B and D in order to generate the amplifying agent C3 convertase, made up of C3(H<sub>2</sub>0)Bb [103]. Factor B exists at lower levels in the lung compared to the serum, in order to avoid lung injury, but can be synthesized upon pathogenic stimulation [104]. Thereafter, generated C3 convertase can cleave inactive C3 to produce C3a and C3b; where C3a will be integral in mast cell stimulation and C3b will become surface bound to bacteria through cooperation of its activated acyl group with a hydroxyl group present on the bacterial surface. The interaction between C3b and the bacterial hydroxyl group leads to a covalent bond between the two, allowing for the initial opsonization of the bacterium [103, 106]. Thereafter, amplification of the ACP can occur through subsequent rounds of C3 convertase generation; where C3 convertase is kept stable through interaction with Properdin, P. As mentioned earlier, Factor B is present in lower levels in the lung to prevent host cell damage. However, many other regulators of this system exist in an attempt to keep the ACP from harming the host. One such regulator is known as Factor I and with its cofactor, Factor H, it is able to cleave C3b and generate iC3b, in order to inhibit subsequent amplification of the ACP

[103]. Other complement receptors that exist on macrophages include CR1 and CR4, but these receptors have been shown to play only a minor role in the uptake of *R. equi* [101, 102].

Phagocytosis mediated by the ACP provides a more passive mechanism of uptake than antibody opsonization, therefore, bacteria may utilize the ACP in order to replicate and survive within the macrophage. It has been recognized that complement mediated phagocytosis of microbes leads to a loosely associated membrane with small regions of enriched cytoskeletal components. Comparatively, antibody mediated phagocytosis produces a tightly associated phagosome decorated with effectors. Intracellular pathogens known to exploit the ACP include *Mycobacterium tuberculosis*, *Legionella pneumophila*, and *Listeria monocytogenes* [101, 107]. Specifically, *M. tuberculosis* uses multiple means of C3b deposition on the bacterial surface to allow for CR1 and CR3 receptor mediated phagocytosis; however, not only will the bacterium opsonize itself to interact with the CR3 receptor, but the *M. tuberculosis* capsule can also mediate recognition by the CR3 receptor [108].

Uptake of *R. equi* can also be influenced by recognition through the Fc $\gamma$  receptor, Toll-like receptor 2 (TLR2), and mannose receptor (MR) [109-111]. Alveolar macrophages present three types of Fc $\gamma$ Rs, which include Fc $\gamma$ RI, Fc $\gamma$ RII, and Fc $\gamma$ RIII [112]. Enhanced clearance of invading pathogens following Fc $\gamma$ R stimulation is due to the subsequent activation of the phagosomal maturation pathway [113]. Signaling by the Fc $\gamma$ Rs occurs via the intracytoplasmic immunoreceptor tyrosine-based action motif, more commonly known as ITAM. ITAMs become activated through tyrosine phosphorylation by Src family kinases. Consequently, the phosphorylated tyrosines of ITAM will provide a recognizable domain for SYK family kinases, where the SYK family kinases mediate signaling cascades in order to modify the actin cytoskeleton for bacterial phagocytosis and transcriptional factors for cytokine production [113].

Notably, Hietala and Ardans determined that opsonization of *R. equi* with species specific antibodies led to a higher percentage of bacterial killing by equine alveolar macrophages [114].

Macrophages can also recognize invading pathogens using pathogen recognition receptors (PRRs) which are localized on the cellular surface, contained within cellular organelles, and present in the cytoplasm in order to sense pathogen-associated molecular patterns (PAMPs). Toll-like receptors represent a class of PRRs present on the macrophage that allows for recognition of different PAMPs present on R. equi. The major Toll-like receptor that recognizes R. equi is the TLR2 receptor [109, 115]. TLR2 mediated stimulation can be directed by multiple bacterial components such as lipoproteins, peptidoglycan, lipoarabinomannan and lipoteichoic acid. The different molecular components that activate TLR2 signaling are categorically recognized through TLR2 homodimers or heterodimers of TLR2 with TLR 4 or 6. For instance, TLR2 dimerized with TLR6 is stimulated by diacylated lipopeptides from Grampositive bacteria. Once stimulation of the receptor has occurred, downstream events will activate both the NF-κB and mitogen-activated protein kinase (MAPK) transcription pathways in order to produce inflammatory cytokines [115, 116]. Previously, it has been shown that infection of murine macrophages with both virulent and avirulent R. equi elicited the movement of p65 and c-Rel, two epitopes present on NF-κB, to the nucleus of the infected cell; subsequently the infected macrophage produces TNFα and IL-12p40. Related to this finding was the determination that the major virulence protein VapA has the ability to stimulate the TLR2 without any other bacterial component present [109].

Along with TLR2 altering transcriptional processes, there are other cellular mechanisms modified in order to phagocytose the interacting organism and increase the rate of phagosomal maturation [117]. One such modification occurs through the activation of p38 MAPK, allowing

for the removal of the early endosome marker EEA1 and progression of the phagosome to the lysosome. A bacterium that takes advantage of this cellular process is *M. tuberculosis*; which activates p38 MAPK in order to displace EEA1 prematurely to generate a replicative niche inside of the macrophage [118].

No direct evidence exists to state that R. equi interacts with the macrophage mannose receptor (MR), but it has been recognized that the MR located on human macrophages interacts with the close R. equi relative, M. tuberculosis [50, 119]. MR recognition of M. tuberculosis is presumed to occur through the terminal mannose present in the ManLAM molecule, a cell wall component discussed previously. Therefore, it is suggested that ReqLAM, produced by R. equi, may also interact with the MR present on macrophages [51]. Another innate immune system molecule that recognizes terminal mannose residues is the mannose binding lectin (MBL), a component of a different branch of the alternative complement pathway mentioned earlier [119, 120]. MBL binding to ReqLAM has previously been established by Garton and coworkers, therefore providing a second method for R. equi to activate the complement pathway [51]. Once MBL deposition has occurred on the bacterial surface, MASP proteins, or MBL-associated serine proteases, are able to interact and stimulate C4 and C2. C4 and C2 represent a separate arm of the complement pathway that generates C3 convertase from C3. Subsequently, the alternative complement pathway activation proceeds and iC3b is deposited on the on the bacterial surface as described previously [120]. Together, the aforementioned pathways help macrophages recognize and phagocytose R. equi [121]. The act of phagocytosis does not appear to differ between virulence plasmid-containing and lacking strains of the bacterium. Nonetheless, uptake of virulent R. equi by alveolar macrophages delivers the bacterium to its replicative niche in the host [122, 123].

## Intracellular trafficking of R. equi

Following phagocytosis, the R. equi containing phagosome will undergo fusion events as the macrophage attempts to deliver the bacterium to the lysosome [122, 124-126]. Phagosomal fusion has been well studied in the macrophage, but despite these efforts, it is still unclear whether phagosomal maturation occurs through a kiss and run method, constituting partial fusion, or through full fusion of downstream organelles [125, 127]. Nevertheless, characteristic markers of phagosomal maturation exist, allowing one to follow the developing phagosolysosome through remodeling of its membrane and luminal components [125-127]. Initially, phagocytosed organisms reside in a nascent phagosome containing extracellular constituents in a plasma membrane derived vesicle [125]. From here, the phagosome acquires early endosomal markers Rab5, PI(3)P, and EEA1 [125-128]. Rab5 is the first of these effectors recruited to the phagosome via activation by the appropriate guanine nucleotide exchange factor, leaving Rab5 in its active GTP bound state. Subsequently, downstream signaling by Rab5 will allow PI(3)P deposition on the cytoplasmic face of the phagosome mediated by phosphatidylinositol 3-kinase and, together, these factors will recruit EEA1 [125, 127]. Homotypic fusion between the bacteria containing phagosome and existing early endosomes transpires once recruitment of the early endosomal effectors has occurred [125, 126]. The resulting early endosome has a pH of 6.1-6.5 and may undergo further trafficking events to recycle plasma membrane constituents back to the surface of the cell [125, 127]. Ultimately, bacterial residence in the early endosome lasts from 5-10 minutes, unless bacterial effectors are employed to arrest maturation of the phagosome at this stage [125].

It is well understood that the early trafficking events of the phagosome are not altered in the presence of virulent *R. equi*. This has been demonstrated by two separate research groups via

the localization of early, recycling, and late endosomal markers. Specifically, virulent *R. equi* containing phagosomes gain and displace EEA1, PI(3)P, and Rab5 in a timely manner after uptake by the macrophage, where the transferrin receptor, a marker of the recycling endosome, has not been colocalized with *R. equi*. During early endosomal marker removal, the *R. equi* containing vacuole (RCV) was shown to gain the late endosomal markers lysobisphosphatidic acid (LBPA), LAMP-1, LAMP-2, and Rab7 [122, 124]. The transition between the early and late endosomal stages is not fully understood, but it is believed that the HOPS complex provides a means by which Rab5, on the early endosome, may be replaced by Rab7, on the late endosome [125, 126]. Additionally, formation of multivesicular bodies via phagosomal membrane invagination takes place somewhere between the early and late endosomal stages [125]. This multivesicular body accumulation allows for PI(3)P to be sequestered inside of the maturing phagosome and for targeted degradation of membrane components [125-127]. Simultaneously, PI(3)P is metabolized by kinases to generate PI(3,5)P<sub>2</sub>, thereby labeling the late endosome [110, 127].

Typically, late endosomes obtain a pH of 5.5-6.0 and gain the markers Rab7, LAMP-1, LAMP-2, LBPA, and mannose-6-phosphate receptor [125, 127]. Additionally, there is the acquisition of more vATPase subunits and hydrolytic enzymes [125]. Rab7 has been shown to recruit other effectors to the late endosome, consisting of RILP and ORP1L. Together, Rab7, RILP, and ORP1L are able to use the microtubule network of the macrophage to move the phagosome towards the center of the cell and simultaneously in proximity with lysosomes [125-127]. Fusion of the lysosome with the late endosome not only relies on Rab7 and its recruited effectors but also on a phosphatidylinositol controlled event. Ultimately fusion of the late endosome with the lysosome will generate the microbicidal compartment known as the

phagolysosome, thereby concluding phagosomal maturation [125]. In the phagolysosome, the pH will drop to ~4.5 allowing for the full activation of hydrolytic enzymes. Differentiation between the late endosome and lysosome is difficult as they both possess LAMP-1, LAMP-2, hydrolytic enzymes, and a plethora of vATPase subunits [125, 127]. Therefore, it is important to analyze the absence of LBPA, the mannose-6-phosphate receptor, and PI(3)P in the lysosome to discern it from the late endosome [125].

As mentioned, the RCV gains a portion of late endosomal characteristics. However, divergence from conventional phagosomal maturation by R. equi occurs somewhere between the late endosomal and lysosomal compartments. Notably, virulent R. equi is able to inhibit acidification of its phagosomally derived niche, where this activity depends on the presence of the virulence determinant VapA [122, 124, 129]. Concurrently, Fernandez-Mora et al. suggests that this quality is a failure of the phagosome to recruit the cytoplasmic subunit of the vATPase [124]. Confounding this data is the ability of normal rat kidney cells to colocalize endocytosed recombinant VapA with lysotracker, showing that lysotracker dye may not be the preferred method to study compartment acidification and that there may be differences in using protein alone versus during R. equi infection [124, 130, 131]. Along with studying RCV acidification, both Toyooka et al. and Fernandez-Mora et al. analyzed the RCV for the procurement of the hydrolytic enzyme Cathepsin D. Cathepsin D is predominantly delivered to the late endosome as a pre-pro form of the enzyme. Thereafter, acidification of the phagosomal compartment allows for cleavage of the protein, generating its mature form [132]. Between these two studies came confounding results, where one group found that both avirulent and virulent RCVs lack Cathepsin D and the other group detected Cathepsin D in both RCV types [122, 124]. Unfortunately, this discrepancy is likely due to the difference in primary antibody used, as one

lab may have probed for every form of Cathepsin D where the other lab only probed for one. Other data suggesting that lysosomal fusion is inhibited exists. One piece of evidence, is the lack of electron dense material in the RCV during scanning electron microscopy, where the bacteria reside in a loosely associated phagosome [33]. Additionally, colocalization of lysosomes preloaded with BSA-rhodamine, dextran, or calcein did not occur with phagocytosed *R. equi* [124, 129]. Complicating these results is the belief that phagosomes may behave differently depending on the cargo the vesicle is carrying [117, 127]. In agreement with this, both virulent and avirulent *R. equi* are less able to traffic to preloaded lysosomes compared to the molecule zymosan [124]. Regardless, virulent *R. equi* was better able to avoid preloaded lysosomes as compared to its plasmid-cured avirulent counterpart [124, 129].

More recent work has begun to elucidate some of the later trafficking events that occur during intramacrophage replication of *R. equi* [131, 133]. Specifically, two studies have shown trafficking alterations during bone marrow-derived macrophage infections with *R. equi* at 24-72 hours post inoculation [131, 133]. Within the following data, use of a *vapA* deletion mutant of *R. equi* showed the reliance of the bacterium on VapA in order to derive a spacious phagosome at 48-72 hours post infection, wherein VapA was shown to reside at the limiting membrane of the RCV. Furthermore, 72 hours post infection also showed the upregulation of a heavily stained LAMP1 compartment, which seemed unable to fuse with the wild type, pVapA equipped, *R. equi* containing vacuole [131]. The identity of this generated compartment remains unknown but could indicate lysosomal biogenesis due to the trafficking dysregulation caused by *R. equi* [130, 131, 134]. Separately, Rofe and colleagues studied the response of normal rat kidney cells incubated with recombinant VapA containing medium and saw a corresponding increase in late endosomal/lysosomal swelling and relocation of transcription factor EB (TFEB) to the nucleus of

the cell [130]. TFEB is responsible for transcriptionally activating genes required for lysosomal biogenesis and thereby supports the theory that the densely stained compartment seen within our lab represents newly synthesized lysosomes [130, 131, 134, 135]. Regulation of autophagic genes has also been discerned as a function of TFEB [135]. Autophagic markers Beclin 1, LC3-II, and LC3-I were shown to increase at 24-48 hours post *R. equi* infection as compared to uninfected control macrophages [133]. Autophagy represents a means for a cell to recycle the nutrients present as complex structures or to rescind unfunctional organelles [136]. Proteins involved in autophagy have been recognized as being intertwined with immune system function as well as lysosomal biogenesis [135, 137]. Notably, the *R. equi* containing phagosome is in need of more detailed analysis as it remains unclear precisely where phagosomal maturation is arrested.

The mechanism of action of VapA has yet to be discerned but studies, in the following work as well as in other research labs, have now shown that recombinant VapA supplemented in cellular media can rescue the  $\Delta vapA$  of R. equi during intramacrophage replication, induce hindered endolysosomal progression in normal rat kidney cells, and bind phosphatidic acid containing liposomes [130, 131, 138]. In total, alteration of phagosomal maturation by R. equi produces a replicative niche for the bacterium which ultimately results in necrosis of the macrophage [122-124, 129, 139]. Importantly, it has been discerned that this cytotoxicity is not due to the presence of VapA [129].

#### **Macrophage Microbicidal Tactics**

In the macrophage, *R. equi* will face an arsenal of antimicrobial factors, whose presence is adjusted based on the activation state of the macrophage [121, 125, 140]. Specifically, studies have shown that *R. equi* can only replicate in non-activated macrophages and that activation, via

IFN-γ with LPS, inhibits bacterial growth. A major distinction for *R. equi* infection of activated macrophages is the induction of *iNOS*, allowing for the production of reactive nitrogen species (RNS) [141-143]. Data supporting the importance of RNS to *R. equi* growth restriction includes the block in bacterial replication seen amidst infection of non-activated macrophages with exogenously added RNS. Nevertheless, the replicative niche generated during *R. equi* infection of activated macrophages is similar to that of resting macrophages, wherein the RCV does not acidify and the bacteria aren't delivered to preloaded lysosomes [141].

Shared bactericidal actions between activated and non-activated macrophages include acidification of the phagosome, formation of reactive oxygen species (ROS), delivery of antimicrobial peptides, and removal of nutrients. The multisubunit protein vATPase is responsible for phagosomal acidification and uses cytoplasmic ATP to move protons into the phagosomal lumen. Along with lowering the pH, the produced proton gradient facilitates other antimicrobial properties of the phagosome. One such instance is the removal of nutrients, specifically divalent cations, by NRAMP1. Additionally hydrolytic enzymes, constituting a portion of the delivered antimicrobial peptides, become activated under acidic pH, leading to improved degradation of the invading bacterium. Finally, the positive charge provided by the protons also allows for the increased transfer of the ROS superoxide [O<sub>2</sub>-], via NADPH oxidase. Afterwards, interaction between H<sup>+</sup> and O<sub>2</sub> aids in the formation of additional ROS. Translation of the NADPH oxidase is constitutive, with three cytoplasmic subunits and two subunits present in the membrane, but it is only under macrophage stimulation that the multisubunit complex assembles on the phagosomal surface to produce ROS [125]. Darrah et al. has shown that in vitro incubation of R. equi with ROS or RNS does not alter bacterial viability, but that the combinational molecule peroxynitrite does [125, 142]. This suggests that R. equi replication in

macrophages is inhibited by the production of peroxynitrite [121, 142]. Discordantly, activated macrophages lacking in a membrane subunit of NADPH oxidase were still able to inhibit *R. equi* growth during infection, implying that RNS may have a separate function aiding in bactericidal activity [141, 142].

Even with the plethora of antibacterial effectors employed by the macrophage, R. equi has still managed to generate a replicative niche. Known mechanisms exploited by R. equi were mentioned earlier and therefore will not be discussed again. Besides the intracellular mechanisms used by the macrophage to destroy invading bacteria, there are also ways in which the macrophage alerts surrounding host cells. Briefly, stimulation of macrophages via PRRs causes secretion of small molecules known as cytokines. Thereafter, cytokines promote an adaptive immune response and positive feedback for the innate immune system. Proinflammatory cytokines consist of IL-1β, TNF-α, IL-6, IL-8, IL-12, and IL-23. Generally, these cytokines encourage migration of neutrophils, lymphocytes, and monocytes to the site of infection and activation of T and B -cells. T-cell activation by proinflammatory cytokines supports a Th1 polarization, allowing for IFN- $\gamma$  secretion [143]. Together, both IFN $\gamma$  and bacterial stimulation support the M1 macrophage phenotype [113, 143]. In the M1 activated state the macrophage is primed to fight intracellular pathogens, where transcriptional regulators NF-κB, AP-1, and STAT-1 are able to enhance the antimicrobial capabilities of the host cell [144]. Alternatively the anti-inflammatory cytokines are IL-10, IL-4, IL-13, and TGF-β. In contrast to the proinflammatory cytokines, these molecules elicit a Th2 polarized T-cell response and evoke the M2 activated macrophage [113, 143]. M2 macrophages are responsible for tissue repair and dampening of the immune response and therefore are not advantageous during host infection with an intracellular bacterium [143].

Importantly, examination of cytokines following *R. equi* infection of murine macrophages has demonstrated that both virulent and avirulent bacteria cause a proinflammatory response, where the macrophage induces transcription of IL-1β, TNF-α, IL-10, and IL-12p40 mRNAs [145]. Furthermore, during investigation of cytokine protein levels, it was found that infection with *R. equi* causes secretion of IL-6, TNF-α, IL-1β, IL-10 and IL-12p40 [109, 145]. This response is mediated through TLR2 stimulation and consequent migration of active NF-κB to the nucleus of the cell. Notably, VapA also triggers TLR2 mediated signaling [109].

In contrast, *R. equi* infection of equine macrophages through *in vivo* intrabronchial means elicited an alternate cytokine profile [145, 146]. Of specific interest is the marked increase in cytokines IL-10 and IL-1β by virulent *R. equi* throughout day 14 of infection compared to plasmid cured *R. equi*, wherein murine macrophage infection alternatively showed that infection with avirulent *R. equi* produced higher amounts of these cytokines [145, 146]. Notably, IFN-γ and TNF-α were still produced during foal infection with virulent *R. equi* [146]. Intriguingly, more recent experimentation of equine macrophages *in vitro* has shown that polarizing a monocyte derived macrophage with IL-10 can support virulent bacterial replication within the monolayer while TNF-α and IFN-γ individually can prohibit bacterial replication. Furthermore, equine macrophage infection done after polarizing the cell with these two cytokines, showed that the presence of IL-10 in combination with either IFN-γ or TNF-α allowed for better intramacrophage replication [147]. Taken together, these experiments show the importance of IL-10 levels during *R. equi* infection of equine macrophages or foals and how its presence could tip the infection outcome in favor of the virulent bacterium.

#### **Host Response**

Foals infected with virulent *R. equi* can either progress to a diseased state or undergo spontaneous recovery. Clearance of the bacterium is enigmatic and may result from a lower infective dose or through achievement of the appropriate immune response. Studies attempting to elicit a protective immune response in the foal are currently underway, where it is likely that *R. equi* elimination involves complex interactions between the differing arms of the immune system [72, 148, 149]. Characterization of an effective immune response against *R. equi* was predominantly done using a mouse model. In this model, virulent bacterium typically replicate during the first few days and are thereafter progressively cleared by ~21 days post infection following specific immune induction [150].

# **Humoral Mediated Immunity**

The humoral arm of the immune system is composed of complement and antibody mediated defenses. Complement levels in the foal are comparable to that of adult horses, where the involvement of complement in the phagocytosis of *R. equi* was discussed previously [102, 151]. Despite complement's role in bacterial uptake, the arm of complement responsible for the membrane attack complex does not appear to be necessary in the immune response against *R. equi*, as demonstrated by the ability of C5-deficient (A/J) mice to successfully clear infection [152].

Alternatively, antibody opsonization of R. equi yields promising results with partial protection during foal infection. In vitro analysis using equine macrophages and neutrophils has shown that the bacterium is more readily phagocytosed and killed in the presence of opsonizing antibodies [110, 151, 153]. Concordantly, an increase in macrophage oxidative burst, TNF- $\alpha$  secretion, and lysosomal fusion were also observed [110, 114]. Studies examining passive

immunization of foals with hyperimmune anti-R. equi serum has yielded disparate results wherein both protection and lack of efficacy were demonstrated [4, 148, 149, 154]. This is presumably due to the variations between applied serums, where both antibody quantity and epitope recognition could differ [149]. Experimental analysis of the passive transfer of antibodies specific for VapA and VapC demonstrated protection of foals against R. equi challenge, suggesting that the immune response to these antigens should be further studied [72]. A more recent study with hyperimmune plasma (HIP) has aimed at lowering variation between both the foals being challenged and the plasma being given to better assess the treatment's affects. The power during this study was not high enough to show overall disease protection during HIP administration, but there was a decrease in the severity of lung lesions and in the length of time before lesion regression between control and HIP treated foals. Lastly, Sanz and colleagues were able to determine effective delivery of HIP derived antibodies into the bronchoalveolar space [155]. Foal antibodies wane between 4 and 12 weeks of age, the time in which disease is most prevalent, where their absence may allow for progressive infection [151]. Even with the promising results during treatment with hyperimmune serum, vaccine studies should continue as serum administration is not only expensive but efficacy is inconsistent [72, 149].

# Cellular Mediated Immunity

Innate immune cells are the first line of defense after *R. equi* is inhaled from the environment, where pathological examination has determined that macrophages and neutrophils predominate the innate immune response [153]. It is well known that macrophages are not able to destroy the bacterium and are responsible for providing the *R. equi* replicative niche [123]. In contrast, analysis of foal neutrophils demonstrated that these cells are fully capable of

phagocytosing and killing the bacterium [151]. However, the innate immune response alone cannot clear infection and cooperation with the adaptive immune response is required.

As a facultative intracellular pathogen, it is believed that R. equi clearance relies on the development of an adaptive immune response [72, 148]. Mouse studies using either transgenic or congenital depletion of cellular subsets have resolved the important mediators of infection and support the significance of an adaptive response. Initial experiments tested the consequences of B and T-cell deficiency through the use of nude (T-cell impaired) and SCID (T and B-cell impaired) mice [150, 152, 156]. These studies showed that T-cells are critical in the response against R. equi. Two separate subsets of T-cells exist, wherein CD4+ T-cells control cellular reactions by cytokine secretion and CD8+ T-cells cause death of infected host cells by receptor mediated apoptosis [148, 149]. Resolution of the important T-cell subset implicated CD4+ Tcells as the major contributor in bacterial clearance, where CD8+ T-cells may still play a minor role [150, 157, 158]. As mentioned previously, R. equi is capable of infecting immunocompromised humans, specifically those with AIDS. This further implicates the importance of CD4+ T-cells, as AIDS patients have greatly reduced numbers of this cell type [150, 157, 159]. CD4+ T-cells generate variant immune responses based on the cytokines secreted. Th1 and Th2 represent two polarizations of CD4+ T-cells, where there are a total of four subsets known to date. In order to pressure one CD4+ polarization over another, Kanaly et al. used monoclonal antibodies that neutralized IFN- $\gamma$  or IL-4. The presence of anti-IFN- $\gamma$ antibodies induced a Th2 type response and anti-IL-4 antibodies lead to a Th1 type response. With the depletion of INF- $\gamma$  and the production of a Th2 response came the inherent inability of the mouse to clear R. equi infection. Together these data suggest that resolution of an R. equi

infection comes from the ability of the host to generate a Th1 response, which activates macrophages and opposes intracellular bacterial survival [159].

To study the consistency of this reaction in the equine host, adult horses were infected with *R. equi* and the cellular infiltrate studied. Between 7 and 14 days post infection there was a cellular efflux predominating in both macrophages and lymphocytes. Infiltrating lymphocytes consisted of CD8+ and CD4+ T-cell subsets which proliferated in response to both *R. equi* and rVapA antigens [160]. Disagreement over the ability of foals to mount a protective immune response exists [72, 161]. Separate groups examining foal immune responses have shown that they are either deficient or capable in mounting a Th1 response [72, 94, 161]. This disparity may result from differing maturities of antigen presenting cells, as foals have lower CD1 and MHCII markers [148, 149]. Nonetheless, evidence of protection after oral administration of virulent *R. equi* and existence of spontaneous recovery suggest that foals can mediate clearance of *R. equi* [72].

# **Clinical Disease and Pathology**

*R. equi* is primarily acquired in foals between one and six months in age via inhalation of aerosolized bacteria [72, 148]. Depending on the inoculation size, disease can either result in a subacute infection or in chronic suppurative bronchopneumonia [21, 72, 153, 162]. With the subacute form, foals will rapidly develop respiratory symptoms and typically succumb to infection overnight [161]. In opposition with this, chronic infection progresses gradually, presumably over a period of weeks [148, 153]. The most common signs during the initial stages of disease include mild fever (68%), cough (71%), lethargy (53%), and increased respiratory rate (43%) [72, 148]. Although these clinical signs are common, they may be overlooked due to the

variable spectrum of presentation [72]. Once the subclinical portion of disease has passed, one may expect to see anorexia, tachycardia, tachypnea, and increased abdominal movement during respiration [95, 148].

Gross examination of post mortem lung tissue will generally reveal abscesses in the cranial ventral region of the lung [20]. These abscesses begin in the alveolar space and will contain not only *R. equi*, but a massive influx of both macrophages and neutrophils [20, 21, 95, 153]. Frequently, necrotic tissue made up of macrophage and neutrophil debris is found at the center of the lesion, where encapsulation is achieved through additional macrophage and neutrophil influx [20]. Discrepancy remains as to whether or not fibrous tissue is also present encapsulating the necrotic cellular region [20, 153]. It is speculated that the necrosis seen during infection is not due to bacterial toxins, but to the release of lysosomal constituents during host cell death [153]. Pneumonia caused by *R. equi* is considered granulomatous and is therefore predominated by macrophage cellular influx, commonly forming multi-nucleated cells [20, 95]. Immune cell infiltration of bronchial lymph nodes can also be seen, as with the lung parenchyma, the majority is comprised of macrophages [20].

R. equi infection is not limited to lung tissue as ~74% of cases will include extrapulmonary disease (EPD) [72]. The most common of these diseases is multi-focal ulcerative colitis [20, 72, 148, 153, 161]. It is speculated that colonizing R. equi will be delivered to the gastrointestinal tract through ingestion of contaminated mucus [20, 72, 148, 153, 161]. In the gut, foci remain localized to Peyer's patches, where bacterial migration may allow infection of the mesenteric or colonic lymph nodes [72, 148, 153]. Other well-established EPDs include septic polysynovitis and abdominal abscesses [72, 148, 161, 163]. Although abdominal abscesses are difficult to diagnose antemortem, polysynovitis is readily visible when cellular effusion occurs in

one or more limb joints [72, 95, 148, 161]. The ability of *R. equi* to metastasize to regions other than the lungs comes from its capacity to employ the host lymphatic system [153]. EPDs do not always develop alongside pneumonia, but if both pneumonia and an EPD are present concomitantly, there is a decrease in the probability that the foal will survive [72, 148, 161].

# **Diagnosis and Treatment**

A simple means to identify lung consolidation or abscesses caused by R. equi, or other bacterial colonization, is ultrasonographic screening [161]. Recently, it was found that ~80% of animals with abscesses identified by ultrasound did not progress to active clinical disease, and prior premature treatment of similar such foals may have led to the development of antibiotic resistance [72, 148, 161]. Therefore, along with ultrasonographic evidence, there needs to be other supportive information indicating that the foal's infection will advance. Standard verification includes culture of R. equi from a tracheobronchial aspirate (TBA), where PCR for vapA should yield an amplicon [161, 164]. PCR has most commonly been done by nested PCR or quantitative real-time PCR; however, testing of a loop-mediated isothermal amplification technology is underway and has shown that this protocol can still assess for vapA while providing easier and cheaper methods of diagnosis [165]. Presence of the *vapA* gene is important as R. equi without VapA expressed is avirulent [82, 161]. Monoclonal antibodies against VapA are also available and may be used as a diagnostic tool [166]. Even with this evidence, there is not 100% certainty that the foal will develop chronic bronchopneumonia. Initially, it was believed that white blood cell count as well as fibrinogen levels might be used as an indicator of disease; however, monitoring of these parameters yielded coinciding values between healthy and infected foals [161, 164]. As of now, it is difficult to predict which foals will develop clinical

disease or clear the infection [161]. It is suggested that farms begin screening their foals at three weeks of age in order to determine if they are at risk but antibiotic therapy should not be initiated until foals show signs of clinical disease [164].

Foals at risk for chronic infection will typically undergo combinational treatment of a macrolide with rifampin. As mentioned previously, *R. equi* antimicrobial resistance is a concern, and resistance to both drug types has been documented [161, 164, 167]. Identification of the genome alterations responsible for both macrolide and rifampin resistance have been identified and include acquisition of a Erythromycin-resistant methylase (*erm*(46)) and mutation within the *rpoB* gene respectively. Importantly, *erm*(46) was shown to be transferable between bacterial colonies allowing for resistance to spread while resistance to rifampin arises through a single amino acid mutation within *rpoB* that can occur sporadically when the bacterium is incubated with antibiotic [167, 168]. Available macrolides consist of erythromycin, azithromycin, and clarithromycin [161, 164]. Importantly, these drugs are bacteriostatic and not bactericidal, meaning that the immune system will need time to clear the infection before treatment is discontinued. Drug treatment will typically last between three to twelve weeks. When *R. equi* is resistant to both macrolides and rifampin, either a fluoroquinolone, aminoglycoside, oxazolidinone, or glycopeptide antimicrobials are used.

Preventative measures also exist and include environmental management, active immunization, and passive immunization. Methodology for environmental control was covered previously in epidemiology and while application still remains plausible, there have not been any studies to indicate effectiveness [164]. Passive immunization with hyperimmune plasma (HIP) from exposed horses has shown some promise, but needs to be administered before *R. equi* infection, and therefore, very early in life [161, 164]. Also difficult is active immunization of the

foals, as they are newborn and have not acquired full function of their immune system. As such, there is not an adequate vaccine available for foal immunization [161].

#### **Bacterial Effectors**

Bacteria that are collectively able to replicate in host cells are known as professional intracellular pathogens [125]. Like *R. equi*, there are other bacterial species that are capable of intramacrophage survival and replication. In order to exploit the macrophage as a replicative niche, bacteria need to be equipped with effectors that are able to alter the killing capacity of the host cell. Typically, bacteria will use one of three mechanisms to hinder delivery to the macrophage lysosome, thereby modifying phagosomal maturation. These methods include bacterial escape into the cytoplasm, niche generation from the phagosome, and resistance to lysosomal antimicrobials [125, 128, 169].

Listeria monocytogenes is an iconic bacterium known to replicate in the cytoplasm of host cells. In order to escape from the phagosome, *L. monocytogenes* uses a variety of lipases, where the most studied lipase is Listeriolysin O. After degrading the phagosomal membrane, *L. monocytogenes* takes advantage of host actin polymerization to facilitate spread to other host cells. Contrastingly, *Coxiella burnetti* requires the acidified environment of the lysosome to replicate. Although *C. burnetti* resides in a phagolysosomal like compartment, the bacterium will use other effectors to slow the process of maturation via use of autophagic vesicles [125].

Important for *R. equi* infection is the capacity of the bacterium to generate a replicative niche from the phagosome. Sufficient mechanisms to produce a phagosome compatible for bacterial growth are utilizing host GTPases, altering phagosome lipids, inhibiting signal cascades, and constraining vesicular movement [128]. Numerous studies have focused on the modification of phagosomal maturation done by *M. tuberculosis*, where the phagosome

containing the bacterium will arrest during the early endosome phase due to phosphatidylinositol remodeling and obstruction of membrane organization [125, 170, 171]. As discussed previously, early endosomal markers consist of Rab5, EEA1, and PI(3)P [125, 126, 128]. Notably, the M. tuberculosis phagosome will enrich only in the Rab5 GTPase, causing inhibition of future fusion events [121, 125]. PI(3)P is a phosphatidylinositol derivative that delineates the early endosome and is required for the association of certain phagosomal effectors. Therefore, without PI(3)P, effectors mediating fusion with the late endosome are not present and the phagolysosome is not formed [125, 126, 128]. Depletion of PI(3)P by M. tuberculosis is accomplished by both LAM and SapM [121, 125, 128, 171]. SapM directly alters the amount of PI(3)P on the early endosome, as it is a PI(3)P phosphatase [125, 128, 171]. Alternatively, LAM, an M. tuberculosis surface glycolipid, is able to inhibit the sphingosine kinase responsible for phosphatidylinositol 3-kinase activation [125, 170]. LAM is also able to intercalate into the phagosomal membrane encapsulating the bacterium, thereby obstructing the membrane fluidity needed for fusion [170]. SapM and LAM are not the only two effectors involved in M. tuberculosis pathogenesis, but they participate in developing a niche that lacks hydrolytic enzymes and is neutral in pH [170, 171].

Markers present on the replicative niche containing virulent *R. equi* suggest that the phagosome progresses to the late endosomal stage. Similar to this is the Salmonella containing vacuole (SCV), which is enriched in the late endosomal markers LAMP-1, vATPase, and Rab7 [128, 172, 173]. *Salmonella typhimuirium* is equipped with two type three secretion systems that are regulated by infection stage, where the T3SS-1 is important in cellular invasion and the T3SS-2 in SCV generation [121, 172, 173]. Constant LAMP-1 deposition and stabilization of the SCV is mediated by the cooperation of bacterial effectors SseJ and SifA [172]. Importantly, this combination of bacterial effectors will produce membranous tubules known as Salmonella-

induced filaments (SIF) [121, 128, 172, 173]. The specific role of these tubules has yet to be elucidated but it has been suggested that their presence is either to provide space for bacterial replication, dilute hydrolytic enzymes that may have been delivered, or transport nutrients [172]. The direct mechanism of SseJ is unknown, but it has been determined that its enzymatic function is as a broad substrate deacylase [172, 173]. Furthermore, SifA binds microtubules to provide a network for the SIF to expand on [121, 172]. Overall, there are many deficiencies in information regarding the replication of Salmonella in the host cell, but when either *sifA* or sseJ are deleted, the SCV releases the bacteria into the cytoplasm allowing for its destruction by autophagy [172].

Lastly, bacteria may create an intracellular niche through the use of other cellular organelles, including the endoplasmic reticulum, autophagosome, and golgi [121, 125, 174]. Legionella pneumophila is one such bacterium that elicits ER derived vesicles to conceal its replicative niche from the host cell [125, 174]. Recruitment of ER membranes occurs via a multitude of effectors comprised of SidC, SdcA, SidM, RalF, and DrrA [125, 128]. Focusing on DrrA, there are three domains which elicit the protein's function, composed of an adenylyltransferase, a guanine nucleotide exchange factor (GEF) for Rab1, and a PI(4)P binding site [174]. Initially, DrrA will localize to the Legionella containing vacuole (LCV) through the use of its PI(4)P binding domain [174]. Thereafter, the plasma membrane protein Syntaxin 3 can interact with DrrA, where this interaction is enhanced when DrrA is able to bind Rab1 [125, 174]. Simultaneous interaction of DrrA with Rab1 and Syntaxin 3 allows Legionella to bring the phagosome containing the bacterium in close proximity with ER vesicles. Successful tethering of the early phagosome to ER vesicles via DrrA allows for subsequent fusion of the two compartments, producing a LCV that is concealed by a membrane with ER components. L. pneumophila encodes a plethora of bacterial effectors, which allows for redundancy in effector

function; therefore, deletion of one bacterial effector typically does not impair LCV production [174]. Additional bacteria that exploit other cellular organelles include *Chlamydia* and *Porphyromonas gingivalis* [121, 128].

# Saccharomyces cerevisiae as a Model Organism

Saccharomyces cerevisiae was first recognized as a plausible eukaryotic model organism in the late 1980's by Botstein and Fink [175]. Since then, research using the budding yeast model has grown exponentially due to the fundamental knowledge of cellular processes and the ease of working with the yeast system. Yeast is not only fast growing and genetically tractable compared to other organisms but has ~85% of its genome functionally mapped. The tools supplied by the yeast community assisted in gaining this knowledge due to the creation of yeast libraries not only tagging each open reading frame but also deleting each non-lethal gene; where importantly, it has been found that mammalian gene homologs can complement these yeast mutants [176]. Not only were homologues found between yeast and higher eukaryotes but cellular processes were also found to be conserved between eukaryotic organisms.

Because of the conservation of cellular processes between yeast and higher eukaryotes it is reasonable to study the effects of bacterial virulence determinants in host systems, through the use of *S. cerevisiae*. During the expression of bacterial effectors in the yeast system one is able to identify yeast growth defects, alterations in cellular morphology, and effector localization [177]. This is critically important for determining the function of effector proteins of obligate intracellular pathogens, as they may be difficult to genetically manipulate and grow in culture, and studying effector proteins that produce cytotoxic effects of eukaryotic cells can be challenging [178, 179]. Specifically, *S. cerevisiae* was employed to express about 230 open reading frames of *Chlamydia* in order to determine which genes are important during

pathogenesis [179]. Once a foundation of knowledge of a certain effector protein has been achieved, different functional assays done in yeast can be utilized to gain further understanding of the mechanism used by the bacterial effector to cause an abnormal yeast phenotype. Such assays include the pathogenic genetic array (PGA), pathogen effector protein screening in yeast (PEPSY), reporter gene expression, and dye localization [177, 180]. A more detailed experiment with ExoU, produced by *Pseudomonas aeruginosa*, was completed in order to determine this effector's function as a lipase. Importantly ExoU is cytotoxic when the protein is expressed in mammalian cells. However, through the use of the Gal1 promoter, differential expression of ExoU was achieved and thereafter the cause of yeast cell cytotoxicity better explored [178]. There are still many other breakthroughs in characterizing bacterial effectors through the use of the yeast system which include, but are not limited to, studies of proteins from *Shigella flexneri*, *Legionella pneumophila*, and Enteropathogenic *Escherichia coli*.

### **Mammalian Membranes**

#### <u>Lipid composition</u>

Cellular boundaries are delineated by a flexible and dynamic lipid bilayer [181]. These boundaries exist not only to encompass the cell, but to allow for the compartmentalization of intracellular events [182, 183]. Formation of these lipid bilayers relies on the amphipathic nature of lipid molecules. This distinguishing feature of lipids is generated through opposing ends of the molecule being respectively hydrophilic and hydrophobic [181, 182, 184]. In an attempt to escape the hydrophilic environment, the hydrophobic ends will pack together, leaving only the hydrophilic region of the lipid exposed [181, 182]. Characterization of the lipid bilayers present in differing cell types and organelles has revealed that lipid composition can vary immensely [181, 182, 185]. An example of this is the mitochondrial lipid bilayer, which has a lipid

architecture similar to that of bacteria due to the presence of cardiolipin. Cardiolipin is absent from the remaining mammalian membranes present in the cell [182]. Experimentation has also determined that the lipid composition of the macrophage can be drastically altered depending on the polarization of the cell towards the M1 or M2 phenotype [186]. Analysis using fluorescent probes has shown that lateral movement of membrane lipids is extremely active, where a freely diffusing lipid can travel up to  $1\mu$ m/s. However, it is presumed that not all lipids are freely moving. Instead, it is believed that certain lipids interact for longer periods of time producing what are known as lipid rafts [181, 182].

In general, mammalian membranes are composed of a mixture of glycerophospholipids, sphingolipids, and sterols [181, 182]. Glycerophospholipids predominate the eukaryotic membrane and consist of a backbone made up of a glycerol molecule conjugated to two fatty acyl chains, in the C1 and C2 position, and a phosphate group, at the C3 position [181, 182, 184]. This backbone provides the basis of all other lipids in the glycerophospholipid class and is known as phosphatidic acid (PA) [181, 183, 184]. At a neutral pH, phosphatidic acid has a net charge of -1, where addition of alternate head groups at the C3 position of glycerol can alter this charge [181]. The environmental conditions surrounding PA can also affect the aforementioned charge; specifically, phosphatidylethanolamine may interact with PA's headgroup causing a more pronounced negative charge to occur [187]. Other glycerophospholipids of note are phosphatidylcholine (PC), phosphatidylethanolamine (PE), phosphatidylinositol (PI), and phosphatidylserine (PS) [182]. PC and PE make up the majority of all mammalian membranes, where PC represents greater than 50% of the glycerophospholipids and both PC and PE contain a net neutral charge [181, 182]. Additionally, PI is a unique lipid as it is able to undergo

phosphorylation on the inositol head group at positions 3, 4, and 5. Therefore PI modification can produce a plethora of different lipids, where PI plays a role in organelle designation [183].

Sphingolipids have a similar structure to that of glycerophospholipids but differ in their backbone composition [181]. Rather than having a glycerol molecule bound to two fatty acyl chains, sphingolipids have a sphingosine molecule with one fatty acyl chain attached [181, 184]. The secondary fatty acyl chain present in glycerophopholipids is mimicked in sphingolipids by an extended hydrophobic region present in the sphingosine backbone [181]. When the remaining carbon, C1, of the sphingosine backbone is unaltered, the compound is ceramide [181, 182, 184]. As with glycerophospholipids, sphingolipids can have differing head groups attached to their C1 carbon [181]. Two important subclasses of sphingolipids in the mammalian membrane are sphingomyelin and glycosphingolipids [181, 182, 184]. Sphingomyelins are comparable to PC and PE as they respectively share the same phosphocholine or phosphoethanolamine head groups. In contrast, glycosphingolipids have sugar moieties bound to the C1 of sphingosine; and these lipids are predominantly found in the outer leaflet of the plasma membrane and are responsible for blood group identification [181, 184].

The remaining lipid type is the sterol group, which is distinct from the glycerophospholipids and sphingolipids. Sterol lipid backbones are composed of four fused rings, known as the steroid nucleus, and an alkyl side chain. The steroid nucleus contains three rings with six carbons and one ring with five carbons, wherein the ring containing five carbons attaches to the alkyl side chain. This base structure is responsible for the hydrophobic portion of the sterol lipid [181]. The hydrophilic portion of this lipid can be as simple as a hydroxyl group, producing the most recognized sterol, cholesterol [181, 182, 184].

# Lipid metabolism and trafficking

The generation of lipids occurs almost exclusively in the endoplasmic reticulum (ER). The ER lipid bilayer is symmetrically distributed, meaning that the lipid composition of the two leaflets of the bilayer are analogous to one another [182]. Despite producing the bulk of the cellular lipid bilayer, the sterol and sphingolipid composition of the ER is rather low. Lipid progression from the ER to other organelles may occur through continuous lipid surfaces, use of lipid transport proteins, or vesicular mediated trafficking, where lipid exchange between the ER and Golgi takes place using both continuous lipid surfaces and vesicular trafficking mechanisms [182, 183]. Once in the Golgi, lipids are sorted for their targeted organelle and become asymmetrically distributed [182]. Targeted lipid delivery presumably arises due to the Golgi's ability to generate sphingolipids, which are known to interact with sterols and produce the lipid rafts mentioned previously [181, 182]. Furthermore, the cytoplasmic leaflet of the Golgi will become enriched in PS and PE while the luminal leaflet, or the extracellular leaflet at the plasma membrane, contains more sphingomyelin, sterols, and PC [181, 182]. Enrichment of sphingomyelin and sterol in the outer leaflet of the plasma membrane is critical, as these lipids are responsible for the cell's ability to withstand mechanical stress [182]. Notably, 5% of the inner leaflet at the plasma membrane is made up of PA, where PI derivatives make up another 15% [181]. It should be mentioned that many mammalian membrane studies have been done with red blood cells and therefore much of our lipid bilayer knowledge is derived from analyses of this cell type.

Certain lipids mediate signaling events, wherein both soluble and membrane associated lipid signaling has been described. Particularly important in lipid driven intracellular signaling is the glycerophospholipid class [182, 183]. PA, PI, and PS represent the minority of the

glycerophospholipids previously mentioned and compose the anionic lipid group [182, 183, 188]. The negative charge of these lipids is particularly important as it allows for the recruitment of proteins containing polybasic residues, or a positive charge. However, this is not the only means by which proteins may interact with the lipid bilayer as interactions can be quite lipid specific and not solely charge driven. Twelve identified lipid binding domains have been described to date, but it is likely that this number will continue to increase as more lipid:protein interactions are characterized. One lipid binding domain that distinctly recognizes PI(3)P is FYVE, which associates with PI(3)P via a conserved basic binding pocket and simultaneous membrane insertion [188]. Importantly, dimerization of proteins containing FYVE domains markedly increases the ability to bind PI(3)P, as is the case for the early endosomal protein EEA1 [125, 188].

My data suggests that lipid binding plays a role in the mechanism of action of VapA [131]. Specifically, VapA was able to bind PA, a lipid which makes up only 1-2% of the total cellular lipid content [131, 183]. There has yet to be a clearly defined protein domain known to mediate interaction with PA, but proteins known to interact typically contain an amino acid region rich in basic residues [188]. The increase in identified PA binding proteins has helped determine that the regions responsible for PA binding are specifically enriched in tryptophan, lysine, arginine, and histidine residues [187]. Previous studies analyzing lipid dynamics during phagocytosis have implicated PA in cellular signaling events [183, 185, 189]. More precisely, PA generators PLD1 and PLD2 are stimulated and localized to the phagocytic cup during phagocytosis of IgG coated particles [189]. At the phagocytic cup, PA activates the enzyme phosphatidylinositol 4-phosphate 5-kinase (PtdInsP5K) permitting enhanced PI(4,5)P2 production and therefore actin remodeling [183, 190, 191]. Similarly, when murine macrophages

were exposed to a TLR4 agonist, Kdo<sub>2</sub>-lipid A, a significant increase in cellular PA could be seen from 8-24 hours post treatment [185]. PA generation during pathogen recognition receptor stimulation may be influential in the provoked inflammatory response. For instance, murine macrophages exposed to PA were able to produce TNF-α, IL-6, IL-1β, iNOS, and COX-2. Together, these effectors encourage a pro-inflammatory response and protection against intracellular pathogens [192]. Further work on the capability of PA to mediate an immune response indicated that Akt was activated, via phosphorylation, when macrophages were treated with PA. Downstream of Akt phosphorylation is the activation of mammalian target of rapamycin (mTOR) which in turn phosphorylates ribosomal subunit S6 kinase (S6K) in order to promote mRNA translation, presumably of the aforementioned immune effectors [191-193]. However, this is not the only study suggesting PA affects S6K signaling, as work by Frondorf et al. suggests that PA contributes to leukocyte chemotaxis through a S6K mediated mechanism [194].

Many of these signaling events begin in proximity to the plasma membrane, but vesicles containing additional PLD1 have been seen fusing with the recently formed phagosome. This allows one to speculate that PA production may continue throughout the process of phagosomal maturation [189]. Unfortunately, PA effects on the later steps of phagosomal maturation have yet to be described, where this subset of PA may be important for VapA's mechanism of action. This speculation is ascribed based on previous studies showing that phagocytosis of *R. equi* does not differ between the virulent wild type and avirulent bacterium (without VapA) [123]. Intriguingly, studies discussed in future chapters are not the only experiments suggesting that altered PA dynamics can affect the macrophage microbicidal properties [195, 196]. Work examining the ability of liposomes carrying PA to alter the outcome of a macrophage infection with

Mycobacterium bovis Bacille Calmette-Guerin (BCG) has shown increased killing capacity in the presence of PA apoptotic body-like liposomes. Not only did PA liposomes impact the killing of BCG, but there was increased killing of *Pseudomonas aeruginosa* and *Escherichia coli* by bronchoalveolar lavage derived macrophages. Molecular changes noted within macrophages incubated with PA containing liposomes included increased phagosomal acidification and reactive oxygen species generation [195].

Other proteins found to interact with PA include but are not limited to Arf-1/6, NSF, Kinesin,  $\beta$ -cop coatomer, NADPH oxidase, Raf-1, and SHP-1 [191, 193, 197]. Additionally, the structural properties of PA allow for negative membrane curvature, which is important in fusion between two lipid bilayers. Specifically, Vicogne and colleagues have demonstrated that PA incorporation into acceptor membranes during fusion can promote fusion events [198]. In sum, PA is central in many cellular events making it difficult to speculate exactly which event may be altered in the presence of VapA.

# CHAPTER 3

# VAPA OF $RHODOCOCCUS\ EQUI\ BINDS\ PHOSPHATIDIC\ ACID^1$

<sup>&</sup>lt;sup>1</sup>Wright LM, Carpinone EM, Bennet TL, Hondalus MK, and Starai VJ. Accepted by Molecular Microbiology. Reprinted here with permission of publisher, Feb 21, 2018.

#### **Abstract**

Rhodococcus equi is a multi-host, facultative intracellular bacterial pathogen that primarily causes pneumonia in foals less than six months in age and immunocompromised people. Previous studies determined that the major virulence determinant of R. equi is the surface bound virulence associated protein A (VapA). The presence of VapA inhibits the maturation of R. equi-containing phagosomes and promotes intracellular bacterial survival, as determined by the inability of vapA deletion mutants to replicate in host macrophages. While the mechanism of action of VapA remains elusive, we show that soluble recombinant VapA<sup>32-189</sup> both rescues the intramacrophage replication defect of a wild type R. equi strain lacking the vapA gene and enhances the persistence of nonpathogenic Escherichia coli in macrophages. During macrophage infection, VapA was observed at both the bacterial surface and at the membrane of the host-derived R. equi containing vacuole, thus providing an opportunity for VapA to interact with host constituents and promote alterations in phagolysosomal function. In support of the observed host membrane binding activity of VapA, we also found that rVapA<sup>32-189</sup> interacted specifically with liposomes containing phosphatidic acid in vitro. Collectively, these data demonstrate a lipid binding property of VapA, which may be required for its function during intracellular infection.

#### **Introduction**

The Gram-positive coccobacillus *Rhodococcus equi* is a causative agent of pyogranulomatous pneumonia in foals less than six months in age and in immunocompromised people [9, 72, 148]. Cattle and swine are also occasional hosts but disease presentation in these species is different and typically manifests as respiratory lymph node abscessation and sub-maxillary lymphadenitis respectively [24, 73, 199]. Delayed type hypersensitivity testing of horses has determined that exposure to *R. equi* is widespread. Disease however, is either sporadic or endemic depending on

the horse farm [11, 12]. While a significant portion of subclinical disease resolves naturally, the unrestrained use of antibiotics on some horse farms has led to the emergence of antimicrobial resistant strains of the bacterium, complicating treatment during disease progression [200]. Additionally, the rise in human immunocompromised populations, whether it be from chemotherapy or HIV, has allowed the bacterium to become a relevant opportunistic pathogen of humans [9].

*R. equi* exposure of foals typically occurs through inhalation of aerosolized bacteria from contaminated soil, wherein the bacterium is introduced to the lower airway [16]. Delivery of the bacterium to the lungs allows alveolar macrophages to recognize and phagocytose the bacterium. Thereafter, the macrophage will attempt to kill the bacterium through a variety of antimicrobial mechanisms, including the production of reactive oxygen and nitrogen species, activation of hydrolytic enzymes, generation of an acidified vacuolar compartment, and depletion of essential nutrients [125]. Despite these tactics, *R. equi* is able to survive and replicate within macrophages of susceptible hosts, designating the bacterium a facultative intracellular pathogen [123].

Initial studies indicated that there are both virulent and avirulent strains of *R. equi*, differing in the possession of a virulence-associated plasmid [95]. Subsequent work has shown that the type of virulence plasmid carried by disease-causing strains of *R. equi* is host specific; wherein pVapA is the plasmid type carried by *R. equi* isolates infecting equine and is the most studied of the virulence plasmid types [71]. pVapB and pVapN comprise the remainder of the sequenced virulence plasmids and are carried by *R. equi* strains infecting swine and bovine species respectively [73]. Human infection can arise from *R. equi* carrying any of the aforementioned virulence associated plasmids, but the most commonly detected pathogen is *R. equi* harboring the pVapB type virulence plasmid [71]. The ability of multiple *R. equi* strains harboring different

virulence plasmids to cause disease in immunocompromised humans confirms the opportunistic capacity of this bacterium. Sequence analysis of these virulence plasmids revealed the presence of four common regions known as the conjugation, replication, unknown function and the virulence or pathogenicity island (PAI) regions [73, 76]. Within the PAI region of these plasmids, members of a novel gene family, the *vap* (virulence associated protein) family reside. Deletion of the plasmid pathogenicity island renders the bacterium incapable of replication in macrophages [81]. Further experimentation on the pVapA type virulence plasmid has shown that, of the twenty open reading frames present in the PAI, only three are required for intramacrophage replication: *virR*, *virS*, and *vapA* [73, 82, 89].

virR and virS encode for transcriptional regulators crucial for the expression of vapA as well as a number of other genes found on both the virulence-associated plasmid and the R. equi chromosome. The vapA gene produces the highly immunogenic protein, virulence associated protein A (VapA) [67, 82, 88, 89]. There are five other open reading frames located in the pVapA PAI encoding for proteins with a high degree of identity to vapA: vapG, vapH, vapC, vapD, and vapE [76]. Targeted deletion studies of each of these vap genes have determined that deletion of vapA alone attenuates the bacterium's ability to replicate within macrophages [81, 82, 87]. Therefore, VapA activity does not appear to be shared among these related Vap homologs even though many of these Vap-family proteins appear to be expressed during R. equi infection [92, 94, 201]. While the mechanism of action of VapA has yet to be discerned, it has been determined that VapA is localized on the surface of R. equi, giving it the capability to directly interact with the host [93]. Studies have shown that virulent R. equi reside within an enlarged neutral compartment in the macrophage and that the presence of vapA inhibits the acidification of the R. equi containing vacuole (RCV), thereby supporting the intracellular survival of the bacterium [122, 124, 129].

Direct visualization of *R. equi* after phagocytic uptake has determined that the recruitment of early trafficking markers to the bacteria-laden phagosome is unaffected. The early endosomal markers Rab5 and early endosomal antigen 1 (EEA1) are gained and lost by the RCV in a timely manner. Late endosomal markers lysobisphosphatidic acid, Rab7, and lysosomal-associated membrane proteins (LAMP) 1 and 2 increase subsequently, suggesting that maturation of these endosomal compartments to late endosomes proceeds unhindered by the presence of the bacterium [124]. The two aberrant phenotypes associated with *R. equi* infection of macrophages are the lack of acidification of, and replication within, an enlarged phagosomal compartment [122, 124, 129]

Sequence characterization of the Vap proteins suggests that they can be broken into three domains, designated as the signal sequence, disordered, and conserved domains [76]. Molecular work on the Vap proteins has determined the protein structure of the conserved domain of VapG, VapD, and VapB; VapB is a virulence associated protein located in the PAI of pVapB [25, 73, 96-98]. Solved structures resolved an eight stranded anti-parallel β-barrel connected by an α-helix for each of the preceding proteins, although the solved structures could not provide much insight into the function of these Vaps [78, 96-98]. Attempts to crystallize VapA have been unsuccessful, but it is presumed that the protein obtains a similar structure to the other Vaps due to high sequence homology. More recent work on endocytosed recombinant VapA has determined that the protein does not directly inhibit acidification but can reduce hydrolytic capacity and cause endolysosomal swelling of normal rat kidney cells; however, a mechanism for how VapA alters cellular trafficking remains to be determined [130].

This study further characterizes VapA, the major virulence determinant of *Rhodococcus* equi isolates carrying pVapA. Experiments focused on localizing the protein during both macrophage infection and *in vitro* expression in yeast show a distinct membrane-binding activity

of VapA, which may be critical for its ability to alter endolysosomal traffic in host cells during infection. Additionally, the ability of rVapA to bind to liposomes of varying lipid composition was analyzed, and provides evidence that membrane phosphatidic acid is a ligand for VapA.

#### **Results**

Recombinant VapA complements the intramacrophage replication defect of an R. equi strain lacking vapA.

In order to survive and replicate intracellularly, R. equi harboring the pVapA-type virulence plasmid requires only the activity of vapA, and two transcriptional regulators, virR and virS, all residing within the plasmid-borne pathogenicity island [89]. Since VapA appears to be the only pVapA-encoded Vap family protein essential for the growth of R. equi in macrophages [82], and considering a recent study that showed that VapA could directly alter lysosomal activity when endocytosed by the normal rat kidney cell line [130], we assessed whether macrophages pretreated with purified recombinant VapA lacking the putative N-terminal signal sequence, rVapA<sup>32</sup>-<sup>189</sup>, could rescue the intramacrophage replication defect of R. equi  $\Delta vap A$ . It is important to note that this fragment of the VapA protein is known to be functional, as mature VapA lacks the first 31 N-terminal amino acids [49]. In these experiments, bacterial intracellular growth in the J774A.1 macrophage cell line was followed over time by traditional lysis and plating of infected monolayer lysates. As anticipated, intracellular bacterial loads of wild type R. equi (103S) increased ~17 fold over 48 hr. This was in contrast to bacteria lacking the pVapA-type virulence plasmid (103<sup>P</sup>-), whose growth was reduced 10-fold over the same time frame (Figures 1A and 1B). Similar to 103<sup>P-</sup> , the wild type R. equi strain lacking vapA ( $\Delta vapA$ ) was unable to replicate intracellularly, although intracellular bacterial loads persisted over the course of the infection (Figures 1A and 1B). Strikingly, the addition of rVapA<sup>32-189</sup> restored the ability of the  $\Delta vapA$  strain to replicate in a dosedependent manner, wherein macrophages pre-treated with 100nM of rVapA<sup>32-189</sup> could replicate to levels comparable to that of the wild type strain (Figures 1A and 1B). Thus, exogenous addition of soluble recombinant VapA could compensate for the loss of the bacterially-encoded VapA protein during *R. equi* intramacrophage growth.

To assess the specificity of rVapA<sup>32-189</sup> activity, other recombinant Vap-family proteins lacking their putative signal sequences were tested in their ability to rescue the intramacrophage replication defect of  $\Delta vapA$ . Of the five other functional vap open reading frames (vapG, vapH, vapE, vapC and vapD) located in the PAI of pVapA, VapG displays the highest sequence identity to VapA at 48%, and is known to have high mRNA expression levels during R. equi infection of foals [73, 76, 94, 96]. Despite these characteristics, purified recombinant VapG<sup>27-172</sup> was unable to rescue the replication defect of  $\Delta vapA$  bacteria (Figures 1C and 1D).

Isolates of *R. equi* that harbor a pVapB-type plasmid contain six distinct *vap* genes (*vapJ*, *vapK1*, *vapL*, *vapK2*, *vapM*, and *vapB*) [73, 76]. Because of the high sequence identity (78%) between the VapB and VapA proteins, it has been proposed that the VapB protein in *R. equi* strains harboring pVapB would be functionally equivalent to VapA during pathogenesis [76]. Despite this, a recent report speculates that VapK1/K2, with 59% identity to VapA, is the functional equivalent of VapA in pVapB-carrying *R. equi* strains [73, 76]. Interestingly, in support of the latter, we found that while the addition of rVapB<sup>35-197</sup> was unable to reverse the intracellular replication defect of  $\Delta vapA$ , rVapK2<sup>32-202</sup> addition resulted in a 10-fold increase of  $\Delta vapA$  bacterial loads 48 hours post-infection (Figures 1C and 1D). Importantly, this increase was in-line with the overall magnitude of intracellular replication displayed by that of the wild type pVapB-carrying *R. equi* strain 33705 (Figures 1C and 1D), although the overall extent of bacterial replication was reduced when compared to the growth displayed by the  $\Delta vapA$  strain in the presence of rVapA<sup>32-102</sup>

<sup>189</sup>. To assess whether the lack of effect of rVapG and rVapB could be explained by improper folding of the recombinant proteins, all of the recombinant Vap proteins used in these studies were subjected to Proteinase K digestion and analyzed by gel electrophoresis, as previously performed by Geerds and coworkers, who described the presence of a properly-folded ~12 kDa core domain of VapA and VapB that was resistant to proteolytic degradation [97]. Upon exposure to Proteinase K digestion, we detected this Proteinase K-resistant core domain in each of the rVaps used in this study; this protease-resistant fragment was lost upon the denaturation of the protein in SDS (Figure 2). These data suggest that each of the Vap proteins tested was appropriately folded and that the inability of rVapB<sup>35-197</sup> or rVapG<sup>27-271</sup> to rescue the intracellular growth defect of a *R. equi*  $\Delta vapA$  strain was likely not due to improperly folded recombinant protein. Taken together, these data show that exogenous addition of either rVapA<sup>32-189</sup> or rVapK2<sup>32-202</sup> can reverse the  $\Delta vapA$  replication defect in macrophages, whereas related Vap-family proteins do not share this property. Surprisingly, VapA does not need to be directly produced by *R. equi* for its activity, likely because this virulence factor directly alters macrophage physiology.

#### rVapA promotes the intramacrophage persistence of nonpathogenic Escherichia coli.

It is known that R. equi expressing vapA has the ability to both neutralize the pH of the RCV during infection and to inhibit the degradative capacity of host macrophages [122, 124, 129]. Because exogenous addition of rVapA<sup>32-189</sup> was able to reverse the intramacrophage replication defect of the  $\Delta vapA$  strain, we hypothesized that rVapA<sup>32-189</sup> could directly alter the killing capacity of macrophages. Thus, we questioned whether the effect was broad in scope, and therefore, we assessed the impact of the presence of rVapA<sup>32-189</sup> on the intracellular survival of a nonpathogenic E. coli strain. As expected, the nonpathogenic E. coli strain was unable to replicate or persist in J774A.1 cells, with intracellular bacterial loads reduced by ~80% at 12 hours post infection

(Figures 3A and 3B). Upon preincubation of macrophages with rVapA<sup>32-189</sup>, however, the survival of *E. coli* was greatly enhanced and bacterial numbers were only reduced by 40% at 12 hours post infection (Figures 3A and 3B). In contrast, macrophages incubated with rVapG<sup>27-271</sup> were not significantly different from untreated macrophages in their ability to kill *E. coli* under these conditions (Figures 3A and 3B). In order to support the intracellular persistence of a nonpathogenic bacterium, it is likely that rVapA<sup>32-189</sup> directly alters host phagolysosomal function.

Localization of VapA during *R. equi* infection shows the protein at the bacterial surface and the RCV membrane.

Because rVapA<sup>32-189</sup> appeared to be able to directly modulate the activity of host phagolysosomal compartments, we sought to localize R. equi-produced VapA over the course of an infection. For these studies, we utilized murine bone marrow-derived macrophages (BMDMs) as the host for R. equi. Both wild type 103S and  $\Delta vapA$  R. equi strains harboring a GFP expression plasmid were utilized to locate bacteria during infection of BMDM monolayers, and intracellular bacterial loads were measured via direct visualization and enumeration. As expected, the 103S-GFP wild type strain was capable of replicating intracellularly over 72 hr, and the  $\Delta vapA$ -GFP strain was cleared from these macrophages over the same timeframe (Figures 4and 4B). As previously observed, supplementation with exogenous rVapA $^{32-189}$  restored the ability of the  $\Delta vapA$ -GFP strain to survive and replicate intracellularly (Figures 4A and 4B). Of note, these results (Figure 4B) likely underestimate the total number of intracellular bacteria because of the clumping nature of R. equi and the fact that macrophages containing more than 10 organisms were quantified as containing only 10 bacteria. Therefore, the number of macrophages containing ten or more bacteria was also followed over time. After 72 hr, 35 of 200 macrophages infected with 103S harbored ≥10 intracellular bacteria, compared to 1 macrophage infected with the  $\Delta vapA$  strain. In the presence

of exogenous rVapA<sup>32-189</sup>, almost 80 of 200 macrophages assessed contained 10 or more  $\Delta vapA$  bacteria, thus directly confirming the ability of rVapA<sup>32-189</sup> to support the intracellular replication of  $\Delta vapA$  *R. equi* (Figure 4C).

Visualization of monolayers infected with 103S R. equi showed the presence of VapA at the bacterial surface throughout the course of infection (Figure 4A). After 48 hours, however, in addition to remaining on the surface of the bacterium, we found that VapA was also observed to accumulate on the membrane of the R. equi-containing vacuole (RCV) (Figure 4A, arrows and insets). In  $\Delta vapA$ -infected monolayers supplemented with rVapA<sup>32-189</sup>, the recombinant protein displayed a highly punctate staining pattern at 1 hour post-infection, reminiscent of vesicular packaging upon endocytic or pinocytotic uptake (Figure 4A, T1). After 48 hr, rVapA<sup>32-189</sup> appears to accumulate around and within RCVs, suggesting that not only is rVapA<sup>32-189</sup> eventually trafficked to bacteria-laden compartments within these cells, but that its activity is needed within (or on) the RCV to support the replication of the R.  $equi \Delta vapA$  strain. Taken together, these images indicate that VapA likely functions in the lumen of the RCV, and that VapA may begin to associate with the membrane of bacteria-laden host vacuoles by 48 hr after infection.

#### VapA localizes to the yeast plasma membrane.

Because of the discovery that VapA appears to localize to the limiting membrane of mature RCVs during *R. equi* infection, we decided to exploit a model eukaryotic system to aid in characterizing the cellular localization of the various Vap-family proteins. The budding yeast *Saccharomyces cerevisiae* is a robust model system for essential eukaryotic processes and has often been used to study the biochemical activities of secreted bacterial effector proteins that alter eukaryotic physiology [176, 177]. N-terminal GFP fusions to full-length VapA, VapA<sup>32-189</sup>, VapG<sup>27-172</sup>, VapB<sup>35-197</sup>, and VapK2<sup>32-202</sup> were constructed in the yeast GFP expression vector pGO35 [202,

203], and protein expression of each of these constructs in yeast was examined via immunoblot (Figure 5A). Each GFP-Vap construct, with the exception of GFP-VapG<sup>27-172</sup>, generated the expected ~44kDa band upon exposure with the polyclonal and cross-reactive anti-VapA antibody. Subsequently, the localization of each GFP-Vap fusion (other than GFP-VapG) within S. cerevisiae was examined. Expression of GFP alone showed a diffuse cytosolic staining, as expected (Figure 5B). However, expression of either GFP-tagged VapA construct (VapA or VapA<sup>32-189</sup>) resulted in a striking localization of GFP to the yeast plasma membrane. In fact, plasma membrane localization of GFP was observed in 100% of the GFP-VapA expressing yeast cells (Figure 5C). In contrast, yeast expressing either GFP-VapK2<sup>32-202</sup> or GFP-VapB<sup>35-197</sup>, showed a marked decrease in the amount of GFP localized to the plasma membrane (Figure 5B). Only ~40% of the GFP-VapK2<sup>32-202</sup> expressing yeast cells showed GFP at the plasma membrane, while ~23% of GFP-VapB<sup>35-197</sup> expressing yeast cells displayed plasma membrane-localized GFP (Figure 5C). Cumulatively, VapA membrane localization in both BMDM infection and upon expression in yeast suggest that VapA can either directly bind to cellular lipids or a conserved membrane-bound receptor. That GFP-VapK232-202 can also moderately localize to membranes in yeast may be relevant in its capacity to rescue the intramacrophage growth impairment of the vapA deletion mutant.

#### rVapA binds liposomes containing phosphatidic acid.

As VapA was seen to interact with both the yeast plasma membrane and the phagosomal membrane containing *R. equi*, we examined the possibility that rVapA<sup>32-189</sup> could interact directly with phospholipid bilayers. Therefore, liposomes of varying lipid concentrations were constructed, and the ability of rVapA<sup>32-189</sup> to bind to these membranes was investigated. We chose to explore rVapA<sup>32-189</sup>'s interaction with four major phospholipid constituents of the eukaryotic plasma

membrane: phoshphatidylcholine (PC), phosphaditylethanolamine (PE), phosphatidylserine (PS), and phosphatidic acid (PA). At a near-physioloigcal pH of 7.4, interactions of rVapA<sup>32-189</sup> with liposomes containing either 100% PC or supplemented with 20% PE, PS, or PA were not detected, as measured by liposome co-floatation (Figure 6A). In contrast, rVapA<sup>32-189</sup> was found to bind to liposomes containing 20% PA when incubations were performed at a pH of 5.5; a minor interaction with PS-containing liposomes was also observed (Figure 6B). Furthermore, rVapA<sup>32-189</sup> bound PA-containing liposomes in a concentration-dependent manner (Figure 6C). Thus, rVapA<sup>32-189</sup> appears to bind to some negatively-charged lipids under acidic conditions, with a preference for membranes containing phosphatidic acid. Finally, we assayed each of the other closely related Vap proteins isolated in this study (VapG<sup>27-172</sup>, VapB<sup>35-197</sup>, and VapK2<sup>32-202</sup>) for their ability to interact with membranes containing phosphatidic acid. Results showed that none of these Vaps could appreciably interact with these liposomes (Figure 6D). Therefore, the interaction of VapA with phosphatidic acid appears to be unique among the Vap-family proteins tested.

#### R. equi resides in LAMP1-negative vesicles in the presence of VapA.

Because the existence of VapA at the phagosomal membrane could impact host phagolysosomal trafficking, we followed the presence of the late endosomal/lysosomal marker LAMP1 (lysosomal-associated membrane protein 1) during the course of macrophage infection [125, 127]. It has been reported that RCVs associate with LAMP1 up to twenty-four hours post infection, and it has been presumed that wild type *R. equi* remain in a late endosome-like compartment by inhibiting the fusion of bacterial-containing vesicles with degradative lysosomes [124]. Using the GFP-expressing 103S and immunofluorescence staining for LAMP1, we similarly found *R. equi*-containing vesicles to be associated with LAMP1 up to twenty-four hours post infection, and noted that the vesicular membranes were closely associated with individual bacteria (Figure 7, 103S,

T24). We extended these observations and at 48h post infection, when bacterial loads were high, we noted that the RCV became enlarged and LAMP1 was no longer associated with *R. equi*containing vacuoles (Figure 7, 103S, T48). Interestingly, LAMP1 appeared to be excluded from VapA-positive membranes (Figure 7, 103S, insets), which continued until at least 72 h post infection (Figure 7B). Furthermore, there was a noticeable increase in LAMP1 staining of macrophages harboring replicating bacteria than the surrounding uninfected cells.

In contrast, RCVs containing  $\Delta vapA$  bacteria were found to be associated with LAMP1 throughout the course of infection, suggesting delivery of these mutant R. equi to the degradative lysosome and a lack of intracellular replication (Figure 7,  $\Delta vapA$ ). Contrastingly, in the presence of 100nM rVapA<sup>32-189</sup>,  $\Delta vapA$  bacteria were found to be located in both LAMP1-positive and negative compartments at 48-72 hours post infection (Figure 7,  $\Delta vapA$ +rVapA, insets). Although the RCV was never found to be enlarged under these conditions, as in the wild type infections, intracellular bacterial loads increased in spite of some overlap with LAMP1-containing vesicles. Taken together, these data suggest that the presence of VapA at the RCV membrane is associated with altered phagolysosomal maturation or altered endolysosomal trafficking pathways in macrophages, and that LAMP1 displacement away from VapA-producing R. equi occurs beyond twenty-four hours post infection.

#### **Discussion**

Herein, we show that exogenous addition of rVapA<sup>32-189</sup> protein to macrophage monolayers both reversed the intracellular growth defect of R.  $equi \Delta vapA$  bacteria and supported the persistence of nonpathogenic E. coli, highlighting the ability of the major virulence determinant of R. equi, VapA, to broadly inhibit the killing capacity of macrophages (Figures 1 and 3). Our work determined that soluble rVapA<sup>32-189</sup> at 100 nm (1.7  $\mu$ g ml<sup>-1</sup>) was sufficient to restore intramacrophage replication

of  $\Delta vapA$  to wild type levels. Our findings are supported by those of another group who very recently described the rescue of  $\Delta vapA$  growth in macrophages in the presence of 100 ug ml<sup>-1</sup> soluble rVapA (Sangkanjanavanich et al., 2017). The group also reported that addition of rVapA allowed for the intracellular growth of an avirulent plasmid-cured strain of R. equi,  $103^{P}$ . The latter was a surprising result, given it is well-established that expression of wild type levels of VapA alone by virulence plasmid-free R. equi is not sufficient to promote intramacrophage replication (Giguere et al., Coulson et al 2015), although Sangkanjanavanich and colleagues used at least 50-fold more rVapA than we found is required to support the intracellular replication of  $\Delta vapA$  R. equi in this study. Interestingly, we also found that a related Vap protein encoded on the pVapB-type plasmid carried by some R. equi strains (e.g. 33705), rVapK2<sup>32-202</sup>, showed a similar capacity to restore the growth of  $\Delta vapA$  bacteria in macrophages, albeit to a lesser degree (Fig. 1). No other recombinant Vap protein tested shared this activity, suggesting that the ability to alter macrophage antimicrobial capabilities is specific for VapA and its functional homologs (like VapK2) across R. equi strains harboring different virulence plasmids.

To better understand VapA's mechanism of action, we sought to observe the localization of VapA during extended *R. equi* macrophage infection. While previous *in vitro* experimentation has determined that VapA is located on the surface of the bacterium (Takai et al., 1992), to our knowledge, this is the first time in which this localization has been confirmed during macrophage infection. Strikingly, at 48 hours post-infection, VapA was no longer solely confined to the bacterial surface, but also appeared at the membrane of the RCV (Figure 4A). The mechanism by which VapA is delivered to the RCV membrane is unknown, but reasoning suggests that active secretion of VapA from intracellular *R. equi*, release of VapA from shedding of the outer cell envelope from intracellularly replicating bacteria, degradation of some bacteria within the RCV,

or delivery via an interaction between the bacterium and phagosomal membrane during initial phagocytic uptake are all viable possibilities. Byrne and coworkers previously described the secretion of VapC, VapD, and VapE into R. equi culture supernatant, but could not detect VapA via immunoblot (Byrne et al., 2001). While this demonstrates that R.equi does not secrete VapA across the outer lipid envelope into the supernatant during routine laboratory culture, it may be that signals within the intramacrophage environment triggers release of the protein from the bacterial surface. Some intracellular pathogens harbor type three (T3SS) and type 4 (T4SS) secretion systems allowing for bacterial effectors to be secreted into the cytoplasm of their host cell (Deng et al., 2017). While genes encoding for a T3SS or classical T4SS are not present in R. equi, the R. equi virulence plasmid harbors genes required for the conjugal transfer of this plasmid (Tripathi et al., 2012). It is unlikely that these genes are responsible for the secretion of VapA during infection, however, as this region is expendable for the proper localization of VapA on the surface of R. equi (Coulson et al 2010). There is genetic evidence in R. equi for the presence of a type seven secretion system (T7SS; ESX) similar to Mycobacterium tuberculosis (Letek et al., 2010). T7SS have been identified in a variety of Gram-positive organisms, where they participate in a wide number of functions including virulence and permitting the transport of substrates across the inner membrane and outer lipid envelope, or mycomembrane; however, these T7SS have not been shown to deliver substrates into the host cytoplasm. What role, if any, the T7SS may play in R. equi pathogenesis remains unknown at present.

This study provides the first experimental evidence showing VapA deposition on the membrane of the RCV during macrophage infection. VapA was not observed outside of the RCV (e.g. in the host cytosol) during macrophage infection with wild type *R. equi*. As a first step to better understand how the presence of VapA at the limiting membrane of the RCV might

potentially affect phagolysosomal trafficking, we assessed the locations of both native VapA and of lysosomal-associated membrane protein 1 (LAMP1), found on late endosomes and lysosomes, over the course of macrophage infection (Figure 7). Previously published work has established that LAMP1 associates with RCVs containing virulent *R. equi* during the 24 hours following uptake (Fernandez-Mora et al., 2005). By extending this assessment further, however, we made a surprising observation: *R. equi*-containing vacuoles appear to exist in a mixed population during infection. Notably, enlarged RCVs with VapA at the limiting membrane were devoid of LAMP1, while RCVs that lacked VapA at the membrane were LAMP1 positive (Figure 7). This finding suggests that VapA's presence at the RCV membrane is important in aiding the bacteria in avoiding destruction by the lysosomal compartment. While LAMP1 is initially gained, the RCV containing actively replicating bacteria can either displace, or avoid further accumulation of, LAMP1-containing endolysosomal vesicles (Figure 7). Thus, there appears to be a late RCV stage that warrants further characterization, but such is beyond the scope of this work.

VapA localization to eukaryotic membranes was not restricted to macrophages, as expression of GFP-VapA in *S. cerevisiae* (VapA or VapA<sup>32-189</sup>) localized strongly to the plasma membrane (Figures 5B and C). Likewise, GFP-VapK2<sup>32-202</sup> displayed plasma membrane localization in yeast, albeit to a lesser extent, and this reduction might account for the decreased ability of exogenous rVapK2<sup>32-202</sup> to rescue the Δ*vapA* mutant and restore its replicative capacity in macrophages, at least as compared to rVapA<sup>32-189</sup> (Figures 5B, 5C, and 1C). GFP-VapB<sup>35-197</sup> showed even less yeast plasma membrane localization than rVapK2<sup>32-202</sup> and was predominantly localized to the cytoplasm. That the two Vap proteins (rVapA<sup>32-189</sup> and rVapK2<sup>32-202</sup>) with the capacity to reverse the intramacrophage replication defect of Δ*vapA* displayed localization to the yeast plasma membrane (Figure 5B and 5C) prompted us to postulate that VapA might possess

lipid binding properties. Thus, we found that rVapA<sup>32-189</sup> bound to synthetic liposomes containing phosphatidic acid (PA) (Figures 6B-6D), and to a much lesser extent, phosphatidylserine (PS) (Figure 6B). Interestingly, membrane PA concentrations in yeast is highest at the outer mitochondrial and plasma membranes, wherein both of these organelles also contain a high percentage of phosphatidylethanolamine (PE). Unique to the plasma membrane, however, is a high amount of PS along with PA and PE (Zinser et al., 1991). Additionally, the more acidic environment (pH 5.5) used in these assays allowed rVapA<sup>32-189</sup> to bind PA as compared to neutral conditions (pH 7.4) (Figures 6A and 6B). This increased interaction at a lower pH could be accounted for because of the lower charge PA holds in this environment (Putta et al., 2016; Shin and Loewen, 2011). The fact that we found GFP-VapA able to bind the yeast plasma membrane in a near-neutral cytosolic pH may identify additional unknown lipid or protein ligands for VapA, which are required to increase the affinity of VapA for PA under these conditions.

PA is an anionic glycerophospholipid that induces the formation of negative curvature in membranes (Kooijman et al., 2005), and can participate in cellular signaling via both electrostatic and hydrophobic interactions with protein ligands (Lemmon, 2008). During phagocytosis, phospholipase D actively generates PA in the phagocytic cup and post-phagocytic vesicles, which is required to properly deform the plasma membrane in order to generate the limiting membrane of the phagocytic vesicle [189]. This phagosomal pool of PA would provide VapA on the bacterial surface its host binding target upon phagocytic uptake. That we observed rVapA<sup>32-189</sup> binding to PA-containing liposomes only in an acidic environment (Figures 6A and 6B) was interesting. Lack of lysosomal acidification has been well documented during *R. equi* infections using Lysotracker dye, which responds to a pH of 6.5 or lower by a shift in fluorescence intensity (Fernandez-Mora et al., 2005; Toyooka et al., 2005; von Bargen et al., 2009). Therefore, the VapA:PA interaction

may occur during an initial acidification step during infection that is later hindered by the replicating bacterium. Support of this theory comes from the ability of *R. equi* to withstand acidic conditions and the upregulation of VapA during the bacterium's acid response (Benoit et al., 2001; Kakuda et al., 2014). Previous measurements of phagosomal acidification during macrophage infections with *R. equi* have shown that while colocalization between the bacterium and Lysotracker dye is low, Lysotracker-positive vesicles are still detected early during the infection (Fernandez-Mora et al., 2005; Toyooka et al., 2005; von Bargen et al., 2009). These acidic vesicles may fuse with the nascent *R. equi*-containing phagosome, thus providing the trigger for VapA binding. Recently, it was discerned that rVapA supplemented normal rat kidney cells had high colocalization between Lysotracker dye and lysosomes but that the lysosomes had a lower hydrolytic capacity (Rofe et al., 2016). Taken together, we can speculate that VapA is not directly altering phagosomal/lysosmal pH, but rather still-undescribed mechanisms downstream of VapA activity are required for *R. equi* to limit RCV acidification.

Signaling mediated by PA is becoming better understood as an important means for cellular communication, and is implicated in the regulation of critical cellular events including vesicular trafficking, actin polymerization, and respiratory burst (Corrotte et al., 2006; Fang et al., 2001; Frondorf et al., 2010; Lim et al., 2003; Schlam et al., 2013; Wang et al., 2006). Phosphatidic acid is able to mediate the Akt-mTOR-S6K signaling cascade at each of the pathway components and may be a way in which the bacterium promotes intramacrophage growth (Fang et al., 2001; Frondorf et al., 2010; Lim et al., 2003; Wang et al., 2006). Macrophages grown in PA-supplemented media activated the Akt-dependent signaling cascade, thus leading to the production of proinflammatory cytokines, nitric oxide, and prostaglandin E2. This response was abrogated in mutant Akt lines, wherein it was presumed that PA indirectly affects Akt localization, and

therefore activity, through its ability to modulate phosphoinositide 3-kinase (Lim et al., 2003). Notably, macrophages infected with either the wild type or plasmid-cured strain of *R. equi* have very similar cytokine production profiles, suggesting that Akt is likely not the primary regulatory target of VapA (Giguere and Prescott, 1998). While PA has an indirect effect on Akt, the lipid has been found to directly interact with mTOR via the FRB domain (Fang et al., 2001; Frondorf et al., 2010). mTOR works in conjunction with the V-type ATPase on lysosomal membranes to sense available nutrients inside the phagosome (Flinn et al., 2010; Zoncu et al., 2011). Thereafter, mTOR mediates downstream signaling events to alter protein synthesis and autophagic pathways (Flinn et al., 2010). Lastly, experiments studying phagocyte chemotaxis have shown that PA stimulates S6K to promote cellular migration through a Transwell plate, and therefore likely promotes the migration of phagocytes into infected tissues (Frondorf et al., 2010). Accordingly, the VapA:PA interaction could have drastic effects on a number of PA-dependent cellular physiologies, wherein modulation of the mTOR or S6K proteins later in the Akt-mTOR-S6K signaling cascade is one such example.

While we found that rVapA<sup>32-189</sup> interacted with PA-containing liposomes, neither of the pVapB encoded Vaps tested, rVapB<sup>35-197</sup> or rVapK2<sup>32-202</sup>, bound PA liposomes to levels observed with rVapA<sup>32-189</sup> (Figure 6D). *R. equi* isolates carrying alternate virulence plasmids differ in their disease presentation and host species tropism; wherein equine isolates, carrying exclusively pVapA, present with pyogranulomatous pneumonia and swine isolates, carrying primarily pVapB, show submaxillary lymphadenitis (Giguere et al., 2011; Komijn et al., 2007; Makrai et al., 2005; Takai et al., 1996). It has been determined, however, that *R. equi* equipped with either the pVapA or pVapB type virulence plasmids can replicate within macrophages of many species; showing that interspecies macrophage differences are not responsible for the plasmid-specific species

tropism observed (Willingham-Lane et al., 2016). It has been presumed that the Vaps responsible for supporting the intramacrophage growth of differing R. equi isolates would employ similar molecular mechanisms during pathogenesis. Here, we have shown that while rVapK2<sup>32-202</sup> supplementation rescues the intramacrophage growth phenotype of  $\Delta vapA$  R. equi and that GFP-VapK2<sup>32-202</sup> to some extent localizes to the yeast plasma membrane, the protein was not detected to interact with PA (Figures 1C, 1D, and 7D). While it is likely that the core structures of the Vap proteins are conserved (Geerds et al., 2014; Okoko et al., 2015; Whittingham et al., 2014), it is possible that rVapK2<sup>32-202</sup> cooperates with a different lipid in the eukaryotic membrane. Alternatively, rVapK2<sup>32-202</sup> may lack the capacity to interact with PA, but contains a shared function with VapA that has yet to be determined. Future work is required to elucidate or eliminate the possibility of lipid binding by rVapK2. It should be noted that the bulk of research on R. equi pathogenesis has focused on pVapA carrying isolates, as these are typical of strains derived from both diseased horses and humans. It is therefore unknown if the R. equi-containing vacuole generated by strains harboring the pVapB-type virulence plasmid follows the same phagolysosomal maturation process as those strains harboring the pVapA-type plasmid (Fernandez-Mora et al., 2005; Toyooka et al., 2005; von Bargen et al., 2009). This represents a gap in the knowledge regarding macrophage infection with R. equi and should be considered when addressing R. equi virulence in the future. In closing, the identification of VapA:host membrane and VapA:PA interactions define a new understanding of VapA:host molecular interactions that should provide insight into the activity of VapA during R. equi pathogenesis. Future work will identify the region of VapA responsible for PA binding, and may help answer the question of why the other highly homologous Vap proteins of R. equi are insufficient to support intramacrophage replication in the absence of the VapA protein.

## **Experimental Procedures**

#### Bacterial and yeast cells.

Bacterial and yeast strains used in these studies are listed in Table 1. *Escherichia coli* was grown in Luria-Bertani (LB) broth at 37°C with antibiotics where appropriate. Selective antibiotics used for *E. coli* were carbenicillin or hygromycin at 50 μg ml<sup>-1</sup> or 180 μg ml<sup>-1</sup>, respectively. *R. equi* was grown in Brain Heart Infusion (BHI) broth at 37°C or 30°C and supplemented with either 80 μg ml<sup>-1</sup> apramycin or 180 μg ml<sup>-1</sup> hygromycin, when appropriate.

Saccharomyces cerevisiae strain BY4742 cells were grown on yeast extract peptone dextrose (YPD) agar or broth at 30°C. BY4742 cells transformed with a plasmid that conferred auxotrophic selection through uracil were grown at 30°C and either plated on or in complete supplemental mixture (CSM) lacking uracil.

## Recombinant Vap purification.

Plasmids utilized and constructed in this study are shown in Table 2. Vap proteins were cloned into the pHis-Parallel1 overexpression plasmid (Sheffield et al., 1999) as follows: Vap open reading frames were amplified from the respective virulence plasmid templates (103S plasmid for *vapA* and *vapG*; 33705 plasmid for *vapB* and *vapK2*) using the primers listed in Table 3. These primers only amplify the part of the *vap* gene that is responsible for the disordered and conserved domains of the proteins, and lack the putative N-terminal signal sequences; accession numbers for proteins are CAQ30407 (VapA), CAQ30394.1 (VapG), CAQ30336.1 (VapK2), and CAQ30339.1 (VapB) (Letek et al., 2008). Amplicons were digested using the appropriate restriction enzymes underlined in Table S2 and cloned into pHis-Parallel1, which had been digested with the same enzymes. Resultant plasmids, pVapALMW, pVapGLMW, pVapBLMW, and pVapK2LMW, were confirmed by sequencing at the Georgia Genomics Facility (University of Georgia).

Plasmids expressing N-terminal hexahistidine fusions to Vap proteins were electroporated into the *E. coli* Tuner<sup>TM</sup> strain (EMD Millipore). Acquired transformants were grown to an OD<sub>600</sub> = 0.8-1.0 at 37 °C in LB supplemented with carbenicillin. His-Vap expression was induced with 1 mM isopropyl β-D-1-thiogalactopyranoside and cells were grown for another 4 hr at 37 °C with shaking. Cells were harvested and suspended in lysis buffer (1 ml 0.5 g<sup>-1</sup> wet weight pellet; 50 mM sodium phosphate pH 7.0, 300 mM NaCl, 10 mM imidazole, 1 mg ml<sup>-1</sup> lysozyme, 1 mM β-mercaptoethanol, and EDTA-free protease inhibitor cocktail (Thermo Scientific)). Cell mixture was incubated for 1 hr at room temperature with gentle agitation, and sonicated to disrupt cells (6 x 30 s).

Lysed cells were clarified via centrifugation (19000 x g, 15 min, 4 °C), and passed over Ni-NTA resin, which had been pre-equilibrated with lysis buffer lacking protease inhibitors, lysozyme, and β-mercaptoethanol. The resin was washed once each with 10 column volumes wash buffer (50 mM sodium phosphate pH 7.0 and 300 mM NaCl) containing increasing amounts of imidazole (20 mM, 40 mM, 60 mM). Protein was eluted with wash buffer containing 500 mM imidazole. Eluted protein was dialyzed into 50 mM potassium phosphate pH 7.4, 150 mM KCl, and 10% (v/v) glycerol, and stored at -80 °C.

# Proteinase K digestion of recombinant Vap proteins.

Vap proteins were digested by Proteinase K (Novagen) in a 500:1 (protein:enzyme) mass ratio as described by Geerds and colleagues (Geerds et al., 2014). Briefly, Proteinase K and Vap proteins were incubated either with or without 1% SDS at 37°C for 75 min. Digestion was halted by addition of 2 mM phenylmethanesulfonyl-fluoride (PMSF) and resulting products were run on an SDS-PAGE gel.

# Construction of yeast expressing GFP tagged Vaps.

To generate GFP-VapA yeast expression constructs, primer pairs GFP-VapA SS F and GFP-VapA R or GFP-VapA NSS F and GFP-VapA R were used to amplify the open reading frames from103S corresponding to VapA or VapA<sup>32-189</sup> respectively. The remaining *vap* genes were amplified using their respective GFP-Vap(X) NSS F and GFP-Vap(X) R primers from either the 103S or 33705S plasmid; wherein a region containing *vapL-M* from 33705 was initially amplified in order to PCR *vapK2*. The resultant PCR products from these primers (Table 3) provided sequence homology to the pGO35 vector, which allows for the constitutive expression of an N-terminally GFP tagged protein of interest (a gift from Alexey Merz, UW Seattle) (Burd and Emr, 1998; Odorizzi et al., 1998). pGO35 was digested with BgIII, and co-transformed with the corresponding amplicons via standard lithium acetate methods (Gietz and Woods, 2002). The resultant plasmids, pGFP-VapA<sup>32-189</sup>, pGFP-VapG<sup>27-172</sup>, pGFP-VapB<sup>35-197</sup>, and pGFP-VapK2<sup>32-202</sup> express GFP-tagged Vap proteins without their N-terminal signal sequences. In contrast, pGFP-VapA will express full length GFP-VapA. Imaging of these strains was completed via fluorescence microscopy.

#### SDS-PAGE and western blotting.

Pure protein samples were boiled for 8 min in 1 X loading dye consisting of 50 mM Tris-Cl (pH6.8), 2 % SDS, 0.1 % (w/v) bromophenol blue, 10% glycerol, and 100 mM DTT. For extracting protein from whole yeast cells, approximately 1 X10 $^9$  cells were suspended in 200  $\mu$ l lysis buffer (0.1 M NaOH, 0.05 M EDTA, 2 % SDS, and 2 %  $\beta$ -mercaptoethanol) before boiling for 10 min. Afterwards, 5  $\mu$ l of 5 M glacial acetic acid was added to the yeast lysates before vortexing for 30 s and boiling samples for an additional 10 min. Yeast samples then had loading dye added to a 1 X concentration.

Prepped samples were run on an SDS-PAGE gel in 1 X Tris-Glycine SDS running buffer (Novex®). Transfer of the samples from the SDS-PAGE gel to a nitrocellulose membrane was done in a 1.4% (w/v) glycine, 0.3% (w/v) Tris Base, and 20% methanol buffer. Thereafter, the nitrocellulose membrane was blocked using the SuperBlock® T20 (TBS) blocking buffer (Thermo Scientific) for either an hour at room temperature or overnight at 4°C with agitation. Primary polyclonal rabbit αVapA was diluted 1:1,000 in blocking buffer. Primary antibodies were then incubated with the membrane for either 1 hour at room temperature or overnight at 4°C with agitation. Afterwards, while rocking, the membrane was washed 4 X for 10 minutes each with a .05% (v/v) Tween 20 and 1X PBS solution. Thereafter, secondary goat αrabbit antibody, conjugated to horseradish peroxidase (HRP), was diluted 1:20,000 in blocking buffer and incubated with the membrane as done with the primary antibody. Next, the membrane was washed as done previously. To expose the western blot, enhanced chemiluminescent HRP substrate and peroxide buffer, both from Thermo Scientific, were mixed and added to the membrane and allowed to incubate at room temperature for 5 minutes.

## Electroporation of *R. equi*.

An overnight 100 ml culture of  $\Delta vapA~R.~equi$  in BHI broth was diluted to an OD<sub>600</sub> of 0.4 with fresh medium, and grown at 30°C until it reached an OD<sub>600</sub> of 0.8-1.0. Bacteria were harvested via centrifugation (3600 x g, 10 min, 4°C), the pellet was washed with 50 ml of cold sterile dH<sub>2</sub>O, and centrifuged for an additional 30 min. This wash step was repeated and additional time, then cells were suspended in 4 ml cold, sterile dH<sub>2</sub>O water containing 5% glycerol. Approximately 200 ng pGFPmut2 DNA was added to 400  $\mu$ l of washed bacteria and mixed by gentle pipetting. The bacteria/DNA mixture was then placed in a pre-chilled 2 mm electroporation cuvette (Bio-Rad) and electroporated (2500 V, 25  $\mu$ F, 1000  $\Omega$ ). Immediately following electroporation, 1 ml of filter

sterilized BHI supplemented with 0.5 M sucrose was added to the cuvette, collected, and incubated for one hour at 30°C. Following incubation, bacteria were harvested via centrifugation, 400µl of the supernatant was discarded, and the bacterial pellet was suspended in the remaining supernatant. Aliquots of the resuspension were then plated to appropriate selective media, and incubated at 30°C for two days.

## Macrophage growth conditions and isolation.

J774A.1 macrophages (ATCC) were grown at 37°C with 5% CO<sub>2</sub> in Dulbecco's Modified Eagle Medium (DMEM) supplemented with 10% heat inactivated Fetal Bovine Serum (FBS) and 2 mM glutamine (complete medium).

Bone marrow-derived macrophages (BMDM) were isolated from femurs and tibias of BALB/c mice (Jackson Laboratories). In order to isolate BMDM precursors, femurs and tibias were dissected from the mouse and flushed with cold cation-deficient 1X PBS containing 100 units ml<sup>-1</sup> penicillin and 10 mg ml<sup>-1</sup> streptomycin (P/S). Cells retrieved from the bone marrow were centrifuged (260 x g, 10 min, 4°C), washed once with complete media containing P/S, then suspended in complete media supplemented with P/S and 10% supernatant from Colony Stimulating Factor-1 (CSF-1) producing L929 cells (24 ml per mouse). These precursor cells were incubated in 6-well non-tissue culture treated plates (37°C, 5% CO<sub>2</sub>; 4ml suspended cells per well) for 3 days. After incubation, 4 ml complete media containing 10% L929 cell supernatant (no P/S) were added to each well and incubation continued. On days five and six, all of the media on the cells was removed and replaced with complete media supplemented with 10% CSF-1 containing L929 cell supernatant. Following a 2 hr incubation with the fresh media on day six, the media was removed from the wells and replaced with cold 1X PBS, incubated at 4 °C for 10 min, and macrophages were harvested. Macrophages obtained were either used immediately in assays, or

suspended in 90% FBS with 10% DMSO at 5X10<sup>6</sup> cells per ml and frozen in liquid nitrogen. For assays, cells were maintained in DMEM supplemented with 10% FBS, 2 mM glutamine, and 10% L929 cell supernatant containing CSF-1.

# Macrophage infection assays.

1 x 10<sup>5</sup> macrophages were placed on 13 mm-diameter glass coverslips or in 24-well tissue culture plates. When applicable, filter sterilized recombinant protein was suspended in macrophage media at a concentration of 50-150 nM and incubated with the monolayer overnight. The next morning, monolayers were washed with complete media. Bacteria, suspended in PBS, were added to the monolayer at a multiplicity of infection of 5:1 (J774A.1) or 7:1 (BMDM) during *R. equi* infections or 10:1 during *E. coli* infections. After 1 hr, the monolayer was washed three times with warm DMEM without supplementation. The monolayers were maintained in complete media supplemented with 20-40 μg ml<sup>-1</sup> amikacin in order to kill any remaining extracellular bacteria; while one plate was lysed for bacterial quantification at T1.

To quantify *R. equi* loads in macrophages, cells were lysed (37 °C, 5% CO<sub>2</sub>, 20 min) with 500µl of sterile dH<sub>2</sub>O. For *E. coli* infections, 500 µl 0.5% (v/v) Triton X-100 was added to macrophages, and the incubation time was reduced to 5 min. The resultant lysates containing bacteria were collected, serially diluted in PBS, and plated on BHI (*R. equi*) or LB (*E. coli*) agar and incubated at 37°C for 24 to 48 hr. For later time points, the monolayer was washed three times with DMEM, as before, and the lysis procedure was performed.

#### Immunofluorescence assays.

Infected macrophage monolayers on 13mm diameter coverslips in 24-well plates were fixed with 4% (v/v) paraformaldehyde in PBS (22 °C, 20 min, in the dark). Coverslips were washed four times with PBS supplemented with 5% FBS, and fixed cells were permeabilized with 350 µl of

PBS containing 0.1% Triton X-100 (3 min). 250μl anti-VapA polyclonal antibody (diluted 1:1600 in PBS with 5% FBS and 0.1% (v/v) Triton X-100) was incubated on the coverslips for one hour in the dark at 22 °C. Coverslips were washed four times in PBS supplemented with 5% FBS and 0.1% (v/v) Triton X-100. Afterwards, 250 μl goat anti-rabbit antibody conjugated to fluorescein isothiocyanate (FITC) (1:500 in PBS with 5% FBS and 0.1 % (v/v) Triton X-100, Thermo Scientific), was incubated with the fixed monolayer and washed, as above. 250μl of an α-LAMP1 mouse monoclonal conjugated to Alexa Fluor 647 (diluted 1:500 in PBS with 5% FBS and 0.1% (v/v) Triton X-100) was used to stain monolayers for LAMP1 as described for the aforementioned primary and secondary antibodies. Washing was completed as done previously. A final wash with with PBS was immediately performed before the coverslips were mounted on microscope slides using ProLong Gold antifade reagent with 4',6-diamidino-2-phenylindole (DAPI) (ThermoFisher Scientific), and were allowed to dry for 24 hours before visualization via confocal microscopy.

## <u>Liposome production.</u>

Stock 16:0-18:1 phospholipids (Avanti Polar Lipids) were dissolved in chloroform and mixed in glass tubes to provide a final amount of 2 µmol total lipid. For quantitation, 0.5% (mol/mol) rhodamine-phosphatidylethanolamine (Rh-PE) was added to all mixtures. Lipid mixtures were composed of 1-palmitoyl-2-oleoyl-sn-glyceryo-3-phosphocholine (POPC) and either 1-palmitoyl-2-oleoyl-sn-glyceryo-3-phosphoethanolamine (POPE), or 1-palmitoyl-2-oleoyl-sn-glyceryo-3-phosphoethanolamine (POPE), or 1-palmitoyl-2-oleoyl-sn-glyceryo-3-phospho-L-serine (POPS) were added to the indicated percentage. Chloroform was removed via a stream of argon gas, and complete solvent removal was obtained under vacuum for 1 hr. Dried lipids were suspended in 1 ml buffer containing either 20 mM 4-2-hydroxyethyl)-1-piperazineethanesulfonic acid (HEPES) pH 7.4 or 50 mM 2-ethanesulfonic (MES) and 3-(N-morpholino)propanesulfonic (MOPS) acid pH

5.5, depending on the pH desired, 10% (v/v) glycerol, and 150 mM NaCl. The suspended lipids were placed in a 37 °C water bath and intermittently vortexed at high speed for 60 min. After 10 freeze-thaw cycles in liquid nitrogen, suspended lipids were passaged 11 times through a Mini-Extruder (Avanti Polar Lipids) fitted with a 1 µm polycarbonate membrane, which had been previously equilibrated on a heating block set to 37 °C.

Liposome quantification was determined with the use of a Rh-PE standard curve in RB150 (20 mM HEPES pH 7.4 or 50mM MES pH 5.5, 150 mM NaCl, 10% (v/v) glycerol) containing 1% (v/v) Thesit; liposomes of interest were also serially diluted in this same buffer. Fluorescence of the suspensions was determined by loading 20  $\mu$ l each suspension into a 384-well, low-volume, black microplate (Corning) and a computer-controlled multimode plate reader ( $\lambda_{ex} = 540$  nm,  $\lambda_{em} = 585$  nm; BioTek). Liposomes were stored at 4°C until the time of assay.

## Liposome floatation.

50  $\mu$ l reactions containing 500  $\mu$ M total lipids and 1  $\mu$ g of recombinant protein of interest were incubated for 1 hr in a 37°C water bath. Afterwards, 5  $\mu$ l of the reaction was collected as a control before adding 50 $\mu$ l of 80% filter-sterilized Histodenz (Sigma Aldrich) in the appropriate pH RB150 buffer. This mixture was inverted to mix, and placed into a 7 X 20 mm polycarbonate centrifuge tube (Beckman Coulter). Sampled were then overlaid with 75 $\mu$ l of filter sterilized 30% Histodenz in RB150 and 75 $\mu$ l of RB150 media. Samples were centrifuged (96,000 x g for 2 hours at 4°C) before collecting 40 $\mu$ l of the floated liposomes. To analyze the samples, the harvested liposome concentrations were determined via Rh-PE fluorescence, equivalent amounts of liposomes were separated via SDS-PAGE, and immunoblotted for Vap proteins.

# Confocal Microscopy.

Fluorescence images were captured on a Nikon A1R confocal microscope system (UGA College of Veterinary Medicine Cytometry Core Facility) using a 100X 1.45NA (Nikon) objective, equipped with an S-P 50 mW multiline Ar laser for imaging GFP and Alexa 488<sup>TM</sup>, a Coherent Sapphire 561nm 20 mW laser for imaging dsRed, and a Coherent Cube 640nm 40mW laser for imaging Alexa 647<sup>TM</sup>. Images were captured using NIS Elements software and processed with the Fiji (ImageJ v. 1.48) software package (Schindelin et al., 2012; Schneider et al., 2012).

## Statistical Analysis.

Sigma Plot version 11.2.0.5 (Systat Software, San Jose, CA) and GraphPad Prism version 6.0b (GraphPad Software, Inc., La Jolla, CA) were used for statistical analysis. Bacterial quantification was evaluated via a two-way analysis of variation (ANOVA) using the Holm-Sidak method, where a P value of  $\leq 0.05$  was considered significant.

#### **Acknowledgments**

The authors would like to thank Drs. Vihbay Tripathi and Jennifer Willingham-Lane for their input and discussions regarding this work, as well as Dr. Alexey Merz for providing pGO35. We also thank Leanna Ritson for technical expertise and Dr. Amy Medlock for providing the *E. coli* strain harboring pTRCHis-GFP. V.J.S. is supported by a grant from National Institute of Allergy and Infectious Diseases (R01-AI100913). The authors have no conflicts of interest to declare.

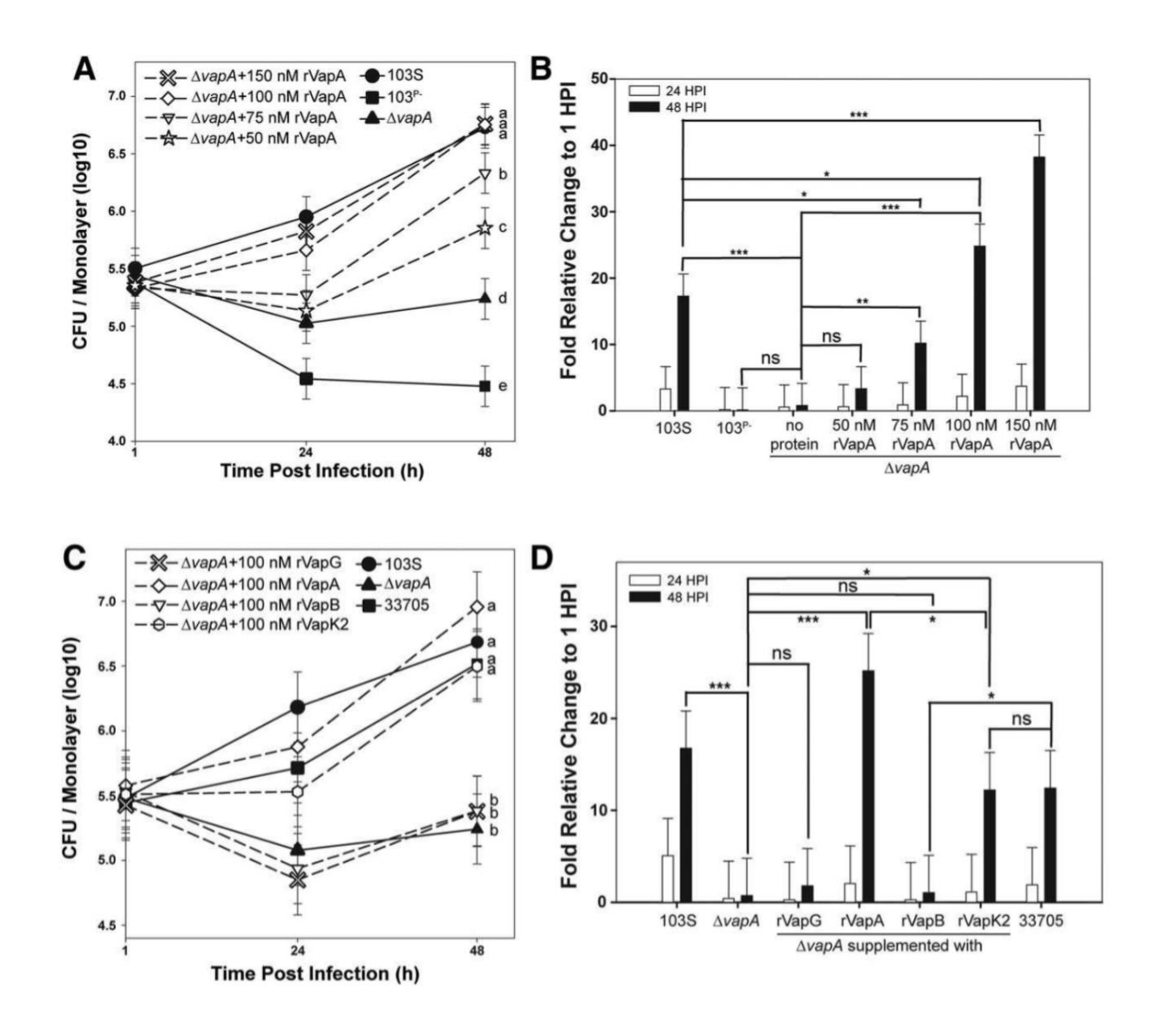


Figure 1. Recombinant VapA<sup>32-189</sup> and VapK2<sup>32-202</sup> complement the replication defect of R. equi  $\triangle vapA$ . Murine J774A.1 macrophage monolayers were incubated overnight with the indicated concentration of recombinant Vap protein (dashed lines and unfilled symbols) or media (solid lines with filled symbols), then infected with the indicated R. equi strain. Each experimental condition was performed in triplicate per infection; n = 3. Symbols denote the mean number of bacteria observed and the bars denote the mean bacterial fold change. Error bars represent the standard deviation using a two-way analysis of variation (ANOVA) by way of the Holm-Sidak test. (A,C) Letters to the right of each curve denote statistical significance; the same letter signifies no statistical difference, while different letters signify statistical difference at  $P \le 0.05$ . (B,D) ns = not significant; (\*) = P < 0.05; (\*\*) = P < 0.01; (\*\*\*) = P < 0.001.

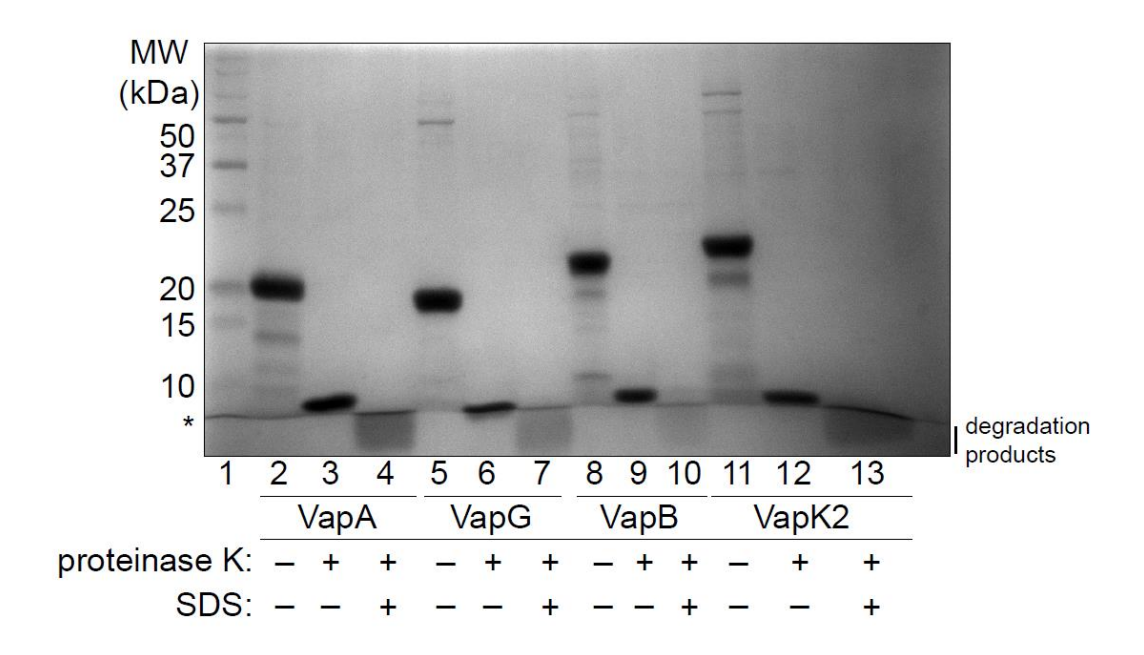


Figure 2. Proteinase K digestion of each recombinant Vap shows a stable protein core.  $3\mu g$  of indicated recombinant Vap protein was incubated with or without Proteinase K (500:1 protein:Proteinase K molar ratio) and, where indicated, 1% SDS for 75 min at  $37^{\circ}$ C. Reactions were separated via SDS-PAGE and stained with Coomassie Brilliant Blue. The asterisk (\*) indicates the dye front of the gel.

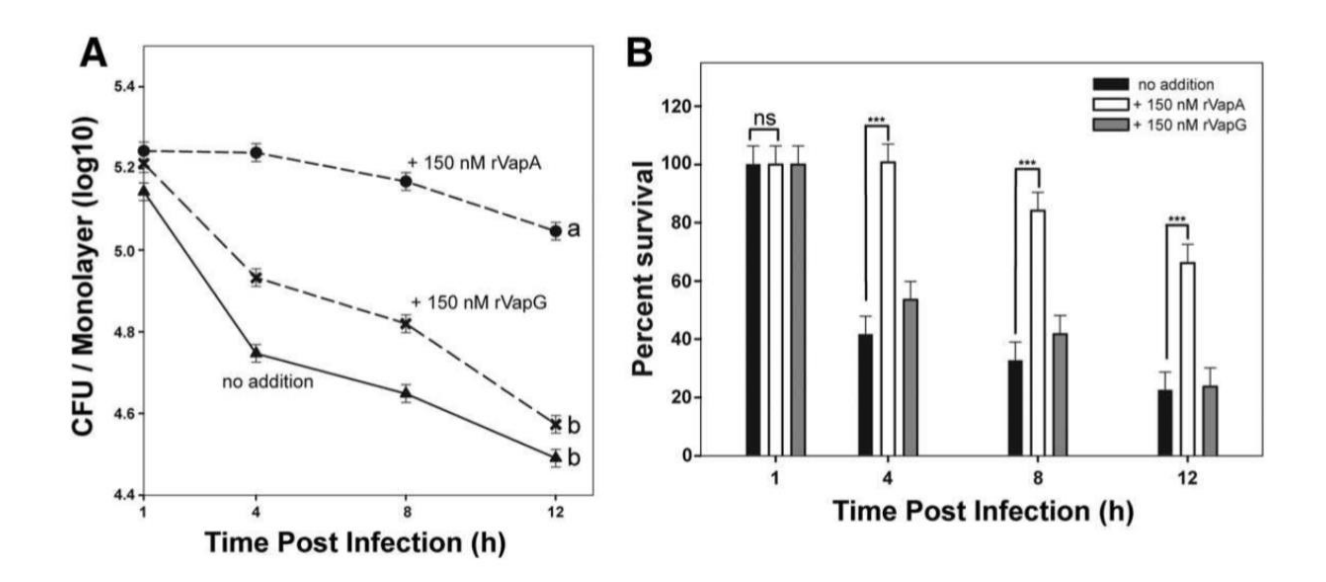
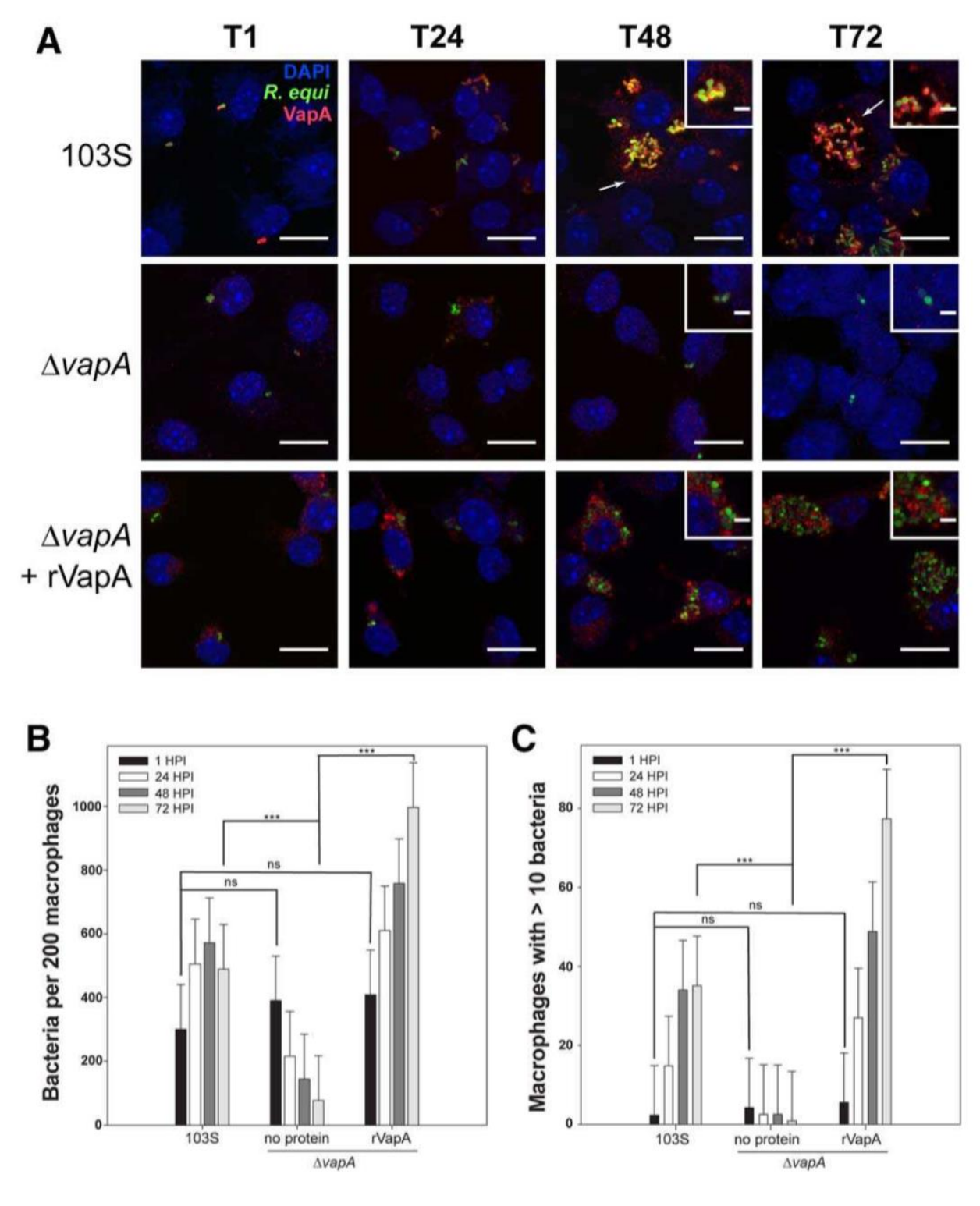
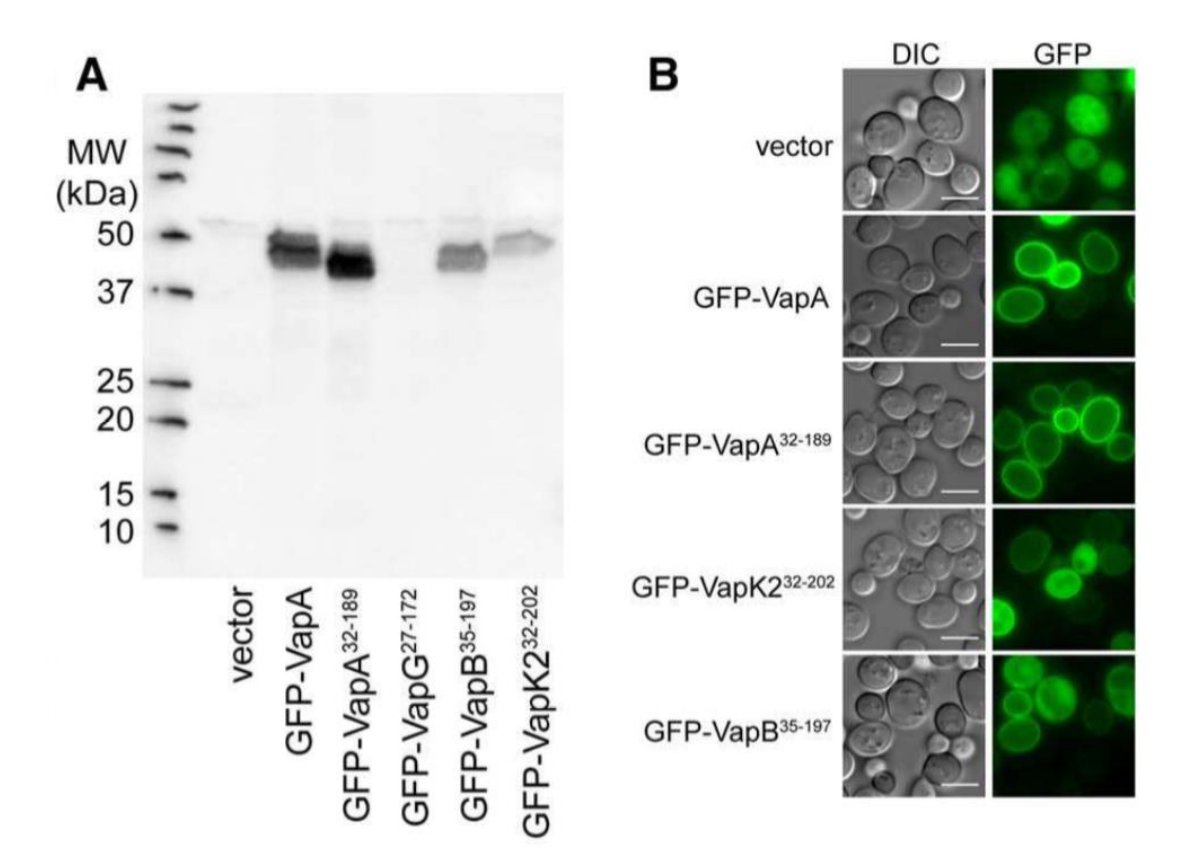


Figure 3. Recombinant VapA<sup>32-189</sup> enhances intracellular persistence of nonpathogenic *E. coli* in J774A.1 cells. J774A.1 macrophage monolayers were incubated overnight with either media (triangles) or 150 nM recombinant Vap protein (VapA, circles; VapG, crosses), and infected with *E. coli*. Symbols delineate the mean bacterial number and bars denote the mean percent survival. The error bars represent the standard deviation calculated using a two-way ANOVA via the Holm-Sidak method. Each experimental condition was performed in triplicate per infection; n = 3. (A) Statistical significance is expressed as letters to the right of the curve, with same letters defining a lack of significant difference, and different letters defining significance with  $P \le 0.05$ . (B) Percent of viable *E. coli* cells detected, as compared to 1 hour post infection (HPI) is shown; ns = not significant; (\*\*\*) = P < 0.001.



**Figure 4. VapA associates with the RCV membrane during infection.** Murine bone marrow-derived macrophages (BMDMs) were infected with R. equi~103S or  $\Delta vapA$  strains harboring the GFP expression plasmid, pGFPmut2. Where indicated, 100~nM rVapA was added to the BMDM monolayer the night before the infection. R. equi~(GFP, green), BMDM nucleus (DAPI, blue), and VapA (anti-VapA, red) were observed. (A) Representative confocal images of infection, bar

= 5  $\mu$ , inset bar = 1  $\mu$ . Arrows indicate VapA detected at the RCV membrane. (**B**) Bacterial numbers per 200 macrophages were quantified by direct visualization at the indicated time points. (**C**) Macrophages containing ten or more bacteria, discerned via direct visualization. (**B,C**) Bars indicate the mean number of quantified bacteria or macrophages, while the error bars represent the standard deviation calculated by a two-way ANOVA using the Holm-Sidak method. n = 3; ns = not significant and (\*\*\*) =  $P \le 0.001$ .



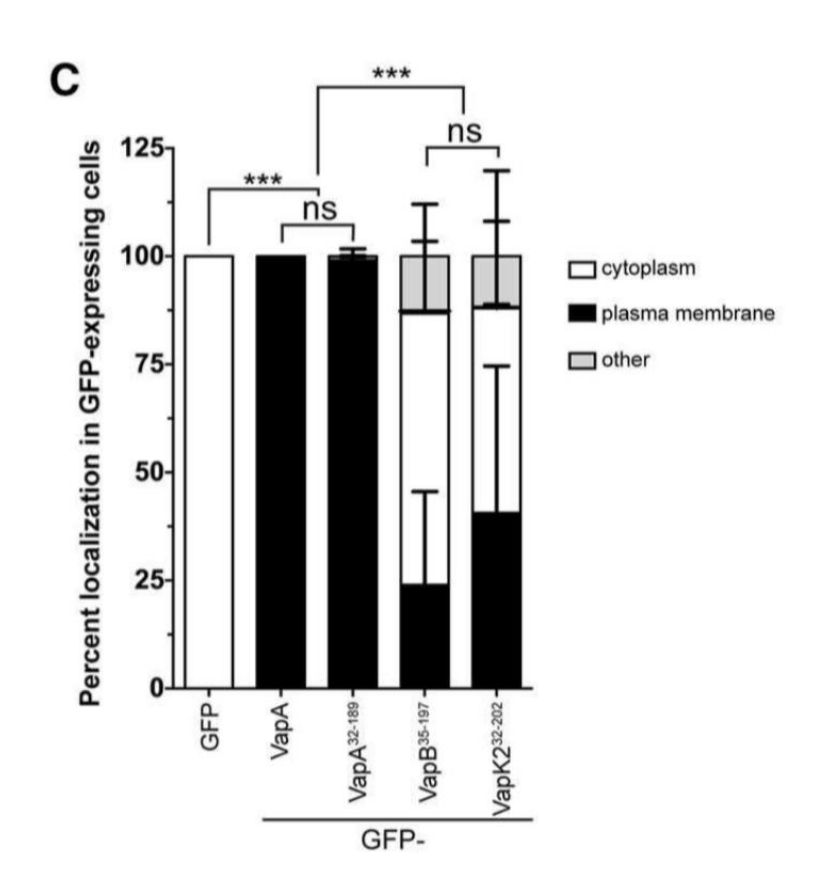


Figure 5. GFP-VapA binds to the yeast plasma membrane upon expression *in vivo*. (A) *Saccharomyces cerevisiae* strain BY4742 harboring either GFP (vector), GFP-VapA, GFP-VapA $^{32-189}$ , GFP-VapG $^{27-172}$ , GFP-VapB $^{35-197}$ , or GFP-VapK2 $^{32-202}$  plasmid constructs were grown overnight and proteins were extracted from equal amounts of cell pellets, separated via SDS-PAGE, and probed with polyclonal anti-VapA antisera. (B) Cells from (A), with the exception of the strain harboring GFP-VapG $^{27-172}$ , were visualized for GFP localization via fluorescence microscopy. Bar = 5  $\mu$ . (C) Quantification of GFP localization from yeast strains imaged in (A); Cells with clear accumulation of GFP-Vap protein at the plasma membrane was counted as "plasma membrane", diffuse GFP staining of the cytoplasm with no plasma membrane localization was counted as "cytoplasm;" all other morphologies were counted as "other." 100 yeast cells were counted per experimental condition, bars denote the mean percent of cells displaying a particular Vap localization pattern. Error bars represent the standard deviation using a two-way analysis of variation (ANOVA) by way of the Holm-Sidak test, and significance pertaining to the difference in plasma membrane localization of GFP-Vap proteins is indicated. n = 3; ns = not significant and (\*\*\*) = P  $\leq 0.001$ .

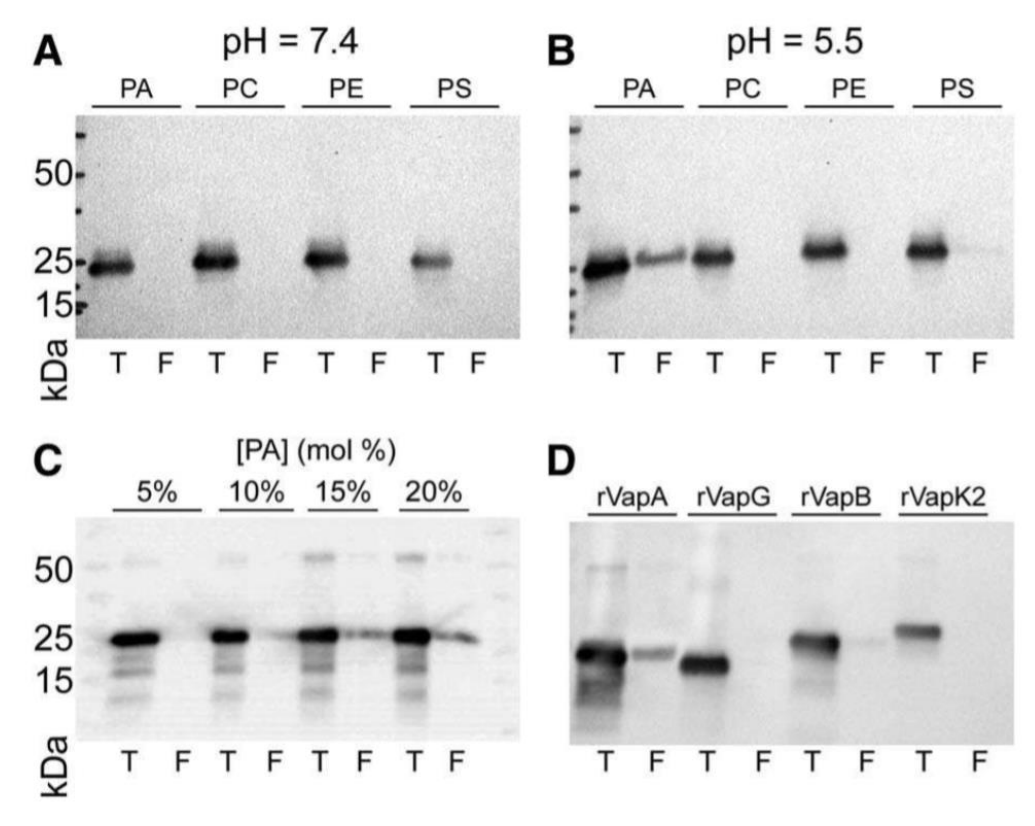
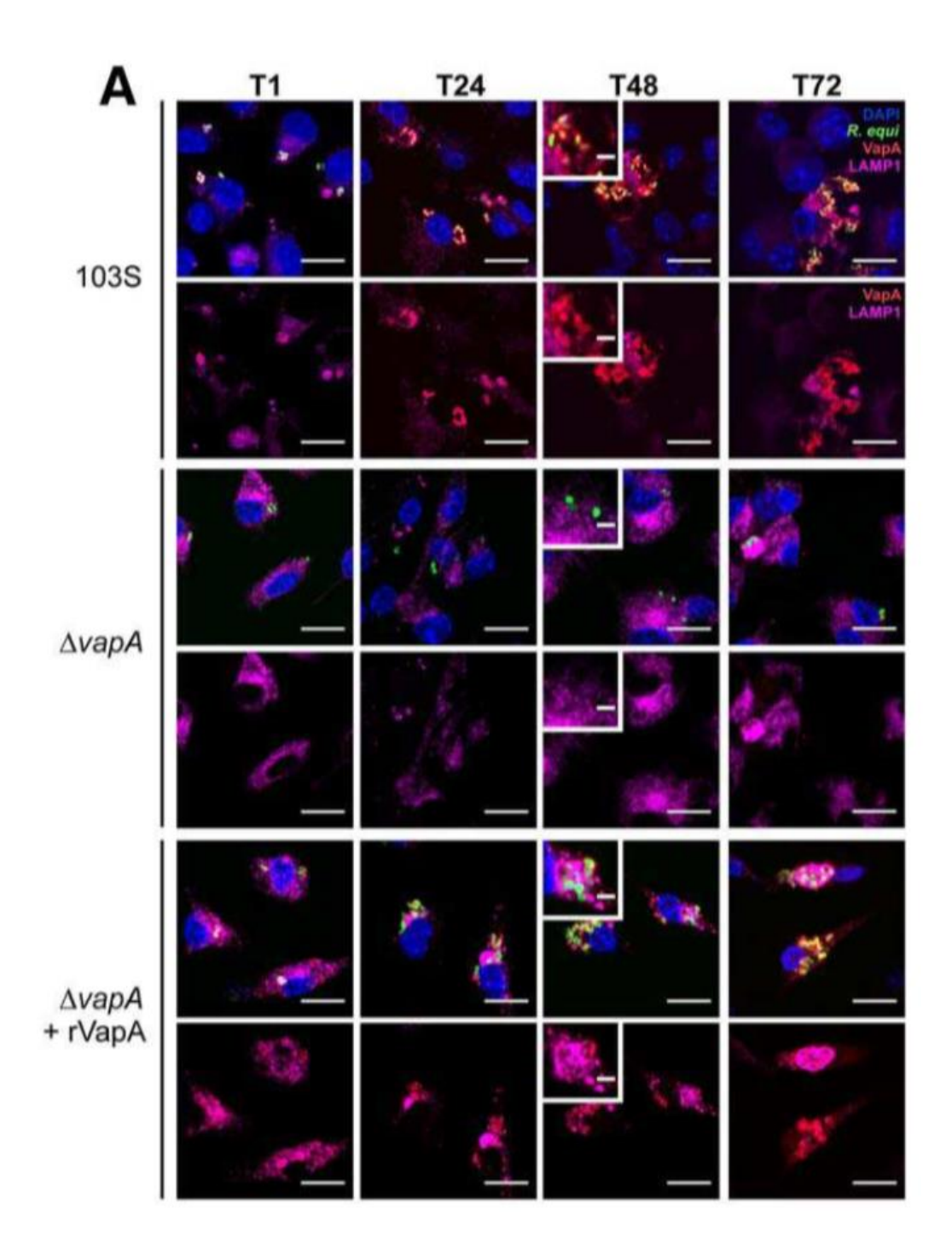


Figure 6. rVapA binds phosphatidic acid containing liposomes. Liposomes of indicated compositions (PA, 20% phosphatidic acid; PC, 100% phosphatidylcholine; PE; 20% phosphatidylethanolamine; PS, 20% phosphatidylserine) were generated as in Experimental Procedures. Liposomes were incubated with recombinant Vap protein at a pH of either (A) 7.4 or (B) 5.5, and liposomes were isolated by flotation (Experimental Procedures). Equal fractions representing 10% of the total reaction (T) and either 900 nmol (A,B) or 1 μmol (C,D) total floated (F) liposomes were separated via SDS-PAGE and immunoblotted for VapA. (C) Liposomes containing increasing amounts of PA were assayed for VapA binding, as above in (6B). (D) Liposomes containing 20% PA were incubated with 1 μg indicated recombinant Vap protein, and assayed for binding, as above in (6B). All recombinant Vap proteins tested cross-react with VapA antiserum.



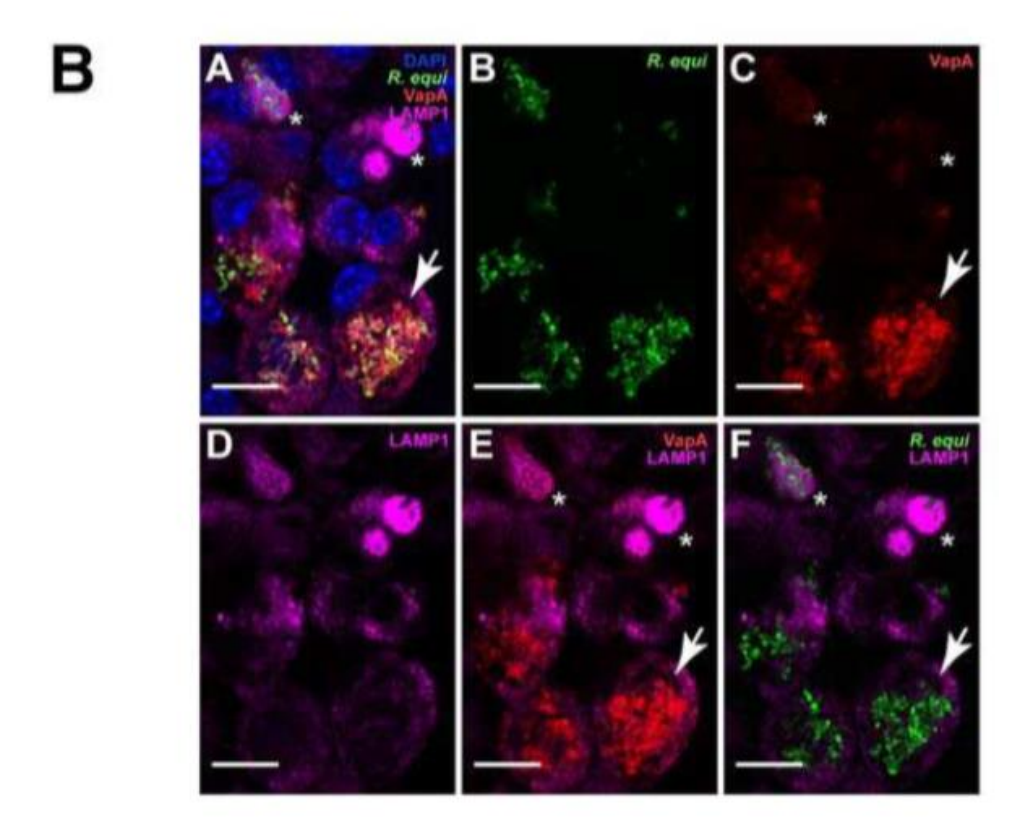


Figure 7. The presence of VapA prevents the accumulation of LAMP1 within the RCV 48 and 72 h post infection. (A) BMDMs were infected with either *R. equi* 103S or  $\Delta vapA$  strains, and 100 nM rVapA<sup>32-189</sup> was added the night before the infection, where indicated. At indicated time points, cells were fixed, immunostained, and visualized via confocal microscopy. *R. equi* (GFP, green), BMDM nucleus (DAPI, blue), VapA (anti-VapA, red), and murine LAMP1 (anti-LAMP1, purple) were observed. n = 3, bar = 5 μ, inset bar = 1 μ. (B) Representative confocal image of 103S infection of BMDMs at T72, performed and stained as in (A). A large RCV containing replicating bacteria and RCV membrane-associated VapA (arrow) is shown in comparison to macrophages containing strongly LAMP1-positive compartments surrounding bacteria that lack detectable VapA at the RCV membrane (asterisks), bar = 5 μ.

Table 1. Bacterial and yeast strains

Bacteria	Description	Source
R. equi		
103S	Wild type strain isolated from pneumonic foal	(Giguere et al.,
1033	(~80kb pVapA type virulence plasmid)	1999)
103 <sup>P-</sup>	Plasmid cured 103+ R. equi variant	(Jain et al.,
		2003)
$\Delta vap A$	103S R. equi variant with vapA deletion; Apr <sup>R</sup>	(Jain et al.,
ΔναρΑ		2003)
103S/pGFPmut2	103S harboring pGFPmut2; Hyg <sup>R</sup>	(Burton et al.,
1035/p011 mac2		2015)
Δ <i>vapA</i> /pGFPmut2	ΔvapA harboring pGFPmut2; Hyg <sup>R</sup> and Apr <sup>R</sup>	This Study
22705	Wild type strain isolated from pig lymph node	(Takai et al.,
33705	(~80kb pVapB type virulence plasmid)	1985)
E. coli		
pTRC His-GFP	Common lab strain of <i>E. coli</i> carrying GFP	A. Medlock
r	expression vector	(UGA)
S. cerevisiae		GE
BY4742	MATα his $3\Delta1$ leu $2\Delta0$ lys $2\Delta0$ ura $3\Delta0$	Dharmacon

Table 2. Plasmids used in this study.

Plasmids	Description	Source
pHis-Parallel1	N-terminal His tag expression vector; Carb <sup>R</sup>	[204]
pGO35	yeast N-terminal GFP fusion expression plasmid	[202, 203]
pVapALMW	vapA(94-567) in pHis-Parallel1; Carb <sup>R</sup>	This Study
pVapGLMW	vapG in pHis-Parallel1; Carb <sup>R</sup>	This Study
pVapBLMW	vapB in pHis-Parallel1; Carb <sup>R</sup>	This Study
pVapK2LMW	vapK2 in pHis-Parallel1; Carb <sup>R</sup>	This Study
pGFP-VapA	vapA in pGO35	This Study
pGFP-VapA <sup>32-189</sup>	vapA(94-567) in pGO35	This Study
pGFP-VapG <sup>27-172</sup>	vapG(79-519) in pGO35	This Study
pGFP-VapB <sup>35-197</sup>	vapB(103-594) in pGO35	This Study
pGFP-VapK2 <sup>32-202</sup>	vapK2(94-609) in pGO35	This Study
pGFPmut2	constitutive GFP expression plasmid; Hyg <sup>R</sup>	[205]

Table 3. Primers used in this study.

Name	Sequence <sup>1</sup>	Plasmid Generated
VapA F (BamHI)	5'-GTA <u>GGATCC</u> GACCGTT CTTGATTCCGGTAG-3'	pVapALMW
VapA R (SalI)	5'-CTAGTCGACCCGGAAGTACGTGCAG-3'	pVapALMW
VapG F (EcoRI)	5'- <u>GAATTC</u> GCGGAAACT TCAATGGTATCCAC-3'	pVapGLMW
VapG R (SpeI)	5'-CTT <u>ACTAGT</u> GTGAGTGCGCCGTCC-3'	pVapGLMW
VapB F (EcoRI)	5'-GTT <u>GAATTC</u> GCGGCTGTGCTGGATTC-3'	pVapBLMW
VapB R (SalI)	5'-CAT <u>GTCGAC</u> CTATGCGTT ATGCAACCTC-3'	pVapBLMW
VapK2 F (EcoRI)	5'-GTT <u>GAATTC</u> CAACCGCTGGACGTTG -3'	pVapK2LMW
VapK2 R (SpeI)	5'-CCT <u>ACTAGT</u> CGAACGTTATGTTCGCC-3'	pVapK2LMW
GFP-VapA NSS F (BgIII)	5'-ATGGATGAACTATACAAGTCCGGA CTC <u>AGATCT</u> ATGACCGTTCTT GATTCCGGTAGC-3'	pGFP-VapA <sup>32-189</sup>
GFP-VapA SS F (BglII)	5'-ATGGATGAACTATACAAGTCCGGA CTC <u>AGATCT</u> ATGGTGAAGACT CTTCACAAGAC-3'	pGFP-VapA
GFP-VapA R (BglII)	5'-GTCGACTGCAGAATTCGAAGCT TGAGCTCG <u>AGATCT</u> CTAGGCGTT GTGCCAGCTAC-3'	pGFP-VapA <sup>32-189</sup> , pGFP-VapA
GFP-VapG NSS F (BgIII)	5'-ATGGATGAACTATACAAGTCCG GACTC <u>AGATCT</u> ATGGGAAACTTC AATGGTATCCAC-3'	pGFP-VapG <sup>27-172</sup>

GFP-VapG R (BglII)	5'-GTCGACTGCAGAATTCGAA GCTTGAGCTCG <u>AGATCT</u> CTATTGC CACCCTCCGGTTC-3'	pGFP-VapG <sup>27-172</sup>
GFP-VapB	5'-ATGGATGAACTATACAAGTCC GGACTCAGATCTATGGCTGTGCT	pGFP-VapB <sup>35-197</sup>
NSS F (BglII)	GGATTCCGGAGGC-3'	
GFP-VapB R	5'-GTCGACTGCAGAATTCGAA	pGFP-VapB <sup>35-197</sup>
(BglII)	GCTTGAGCTCG <u>AGATCT</u> CTATT ATGCAACCTCCCAGTTG-3'	
GFP-VapK2 NSS F (BglII)	5'-ATGGATGAACTATACAAGTCCGGACT CAGATCTATGCAACCGCTGGACGTTG-3'	pGFP-VapK2 <sup>32-202</sup>
· · · · ·		222 202
GFP-VapK2 R (BglII)	5'-GTCGACTGCAGAATTCGAAGCTTGAGC TCG <u>AGATCT</u> CTATTATGACCAGCTGCCG-3'	pGFP-VapK2 <sup>32-202</sup>

<sup>&</sup>lt;sup>1</sup>Underlined sequence represents corresponding restriction site.

# CHAPTER 4

MUTATIONAL ASSESSMENT OF VAPA OF  $RHODOCOCCUS\ EQUI^2$ 

<sup>&</sup>lt;sup>2</sup>Wright LM\*, Carpinone EM\*, Hondalus MK, and Starai VJ To be submitted to Molecular Microbiology.

### Introduction

Rhodococcus equi is a ubiquitous, Gram-positive soil dwelling organism [3, 9]. When in a susceptible host, the bacterium is capable of replicating within macrophages [75, 123]. Foals are the most often affected and widely studied host species, in whom the bacterium causes a pyogranulomatous pneumonia [95]. Infections of numerous other mammalian species has been reported, including humans, wherein a rise in *R. equi* human disease, typically manifesting as pneumonia, has been documented in immunocompromised populations [9, 15].

Replication within host macrophages is determined by the presence of a virulence associated plasmid [67, 95]. To date, three variations or types of the virulence plasmid have been identified, specifically pVapA, pVapB, and pVapN [73, 76]. The type of virulence plasmid carried by R. equi is host specific; the most studied of which is pVapA, the plasmid type carried by R. equi strains infecting equine species [69, 71, 73, 95]. pVapB and pVapN are typically carried by R. equi strains isolated from swine and bovine species respectively, whereas human disease is caused by R. equi possessing any of these plasmid types or R. equi lacking any virulence associated plasmid [9, 23-25, 71, 73, 206]. Each of these plasmid types contain a region with characteristics of a pathogenicity island (PAI), presumed to have arisen from a horizontal gene transfer event [73, 76]. Encoded within the PAI are members of the virulence associated protein (Vap) family along with the virulence associated transcriptional regulators VirR and VirS [73, 76, 79]. Specific vap gene composition varies with plasmid type. VirR and VirS are encoded on a conserved 5 gene operon and are responsible for expression of the vap genes as well as ~18% of chromosomal genes, creating a niche conducive for intracellular survival and replication [86, 88, 89].

As mentioned, the *R. equi* strains derived from foals carry the pVapA type virulence plasmid [71, 73, 95]. The *vap* genes located on the pVapA pathogenicity island include *vapG*, *vapH*, *vapX*, *vapA*, *vapI*, *vapC*, *vapD*, *vapE*, and *vapF* [76]. Deletion studies have shown that *vapA* in particular is required for intramacrophage replication [81, 82, 87, 89]. Further characterization of the *vapA* deletion mutant of *R. equi* has determined that the protein is involved in phagosomal acidification and degradative capacity of the macrophage [82, 129]. The mechanism of action of VapA is still unknown, but newer data analyzing the purified protein suggests that VapA perturbs endolysosomal maturation of Normal Rat Kidney (NRK) cells and can bind phosphatidic acid (PA) [130, 131]. Alteration within the NRK cells mimicked what is seen during natural *R. equi* infection, wherein the endosomal compartment is swollen, Cathepsin B activity is lowered, and lysosomal biogenesis is induced [124, 129, 130].

Phosphatidic acid is the first identified ligand of VapA, and its binding represents a means by which VapA could alter phagosomal maturation [131]. Analysis of proteins that interact with phosphatidic acid have yet to determine a specific PA binding domain, however data suggests that tryptophan, lysine, arginine, and histidine are the amino acids likely to be involved [187, 188]. This study aims to identify the residues of VapA that are essential for interaction with PA and to determine the effect that disruption of VapA:PA binding has on intramacrophage replication of *R. equi*.

#### **Results**

Complementation analysis of  $\Delta$ vap R. equi with mutated vap A.

It is well established that *R. equi* relies on the presence of *vapA* to replicate within macrophages [82]. In addition, we recently showed that the supplementation of soluble rVapA<sup>32-189</sup> to macrophage monolayers reversed the intramacrophage replication defect of an *R. equi* mutant

strain lacking vapA ( $\Delta vapA$ ) and, furthermore, we demonstrated the *in vitro* binding of rVapA to liposomes containing phosphatidic acid [131]. We thus postulated that this lipid binding property of VapA is relevant to the activity of the protein in macrophages. Consequently, a mutational analysis of VapA was performed to gain insight on the roles of specific residues in the function of the protein. Phosphatidic acid has a net negative charge and is likely to interact with positively charged amino acids [187, 188], therefore, we focused our assessment on those residues. There are three regions of VapA, specifically, the signal sequence domain, the disordered domain, and the conserved domain [76]. Our prior experimentation established that the signal sequence is not needed for either rescue of  $\Delta vapA$  R. equi growth during macrophage infection or for phosphatidic acid binding [131]. Thus, mutational analysis was focused within the disordered and conserved domains of the protein, as depicted in Figure 8A, wherein the bolded and underlined amino acids represent those that were altered. Site directed mutagenesis was performed, wherein lysines and arginines were replaced with alanine. VapA(K/R69,75A) has two amino acid residues altered in the disordered domain, VapA(K/R100,109,137,140A) has four amino acid residues substituted in the conserved domain, and VapA(K/R69,75,100,109,137,140A) has all six amino acid residues mutated in the disordered and conserved domains. For simplification,  $VapA^{(K/R68,74A)}$ ,  $VapA^{(K/R99,108,136,139A)}$ , and  $VapA^{(K/R68,74,99,108,136,139A)}$  are designated as VapA.Disordered, VapA.Conserved, and VapA.Full respectively, wherein the annotation pertains to the region mutated.

In the complementation analysis, the wild type and mutated versions of the vapA genes were expressed from the native vapA promoter of plasmid pSJ28 or its derivatives [82] in the attenuated  $\Delta vapA$  strain. Fluorescence cytometry using rabbit polyclonal antisera and Alexa

Fluor 488- labeled goat anti-rabbit IgG as primary and secondary antibodies, respectively, was performed to confirm that the mutated VapA proteins were appropriately localized to the surface of the transformed  $\Delta vapA$  bacteria as it is in wild type R. equi (103S) (Figure 8B). While  $\Delta vapA$ R. equi lacked any positive signal,  $\Delta vapA$  transformed with wild type vapA, vapA. Disordered, vapA.Conserved, or vapA.Full demonstrated that each complemented strain of  $\Delta vapA$  R. equi correctly localized either a mutated or wild type version of VapA on the surface of the bacterium (Figure 8B). In addition, the *in vitro* growth of these strains was assessed to discern if any replication disparity existed among them (Fig. 8C). We noted that R. equi harboring more than one resistance cassette was hindered slightly in replication. For this reason, the control strains 103S and  $\triangle vapA$  R. equi were transformed with an additional plasmid to confer resistance to both apramycin and hygromycin allowing a more appropriate comparison to the complemented strains which also carry each of these resistance markers. Specifically wild type 103S was transformed with pSJ35, a plasmid with both apramycin and hygromycin resistance cassettes, and the apramycin-marked ΔvapA R. equi was transformed with pMV261-H, carrying the hygromycin resistance cassette. As depicted in Figure 8C, the in vitro growth of the vapA complemented strains was mildly reduced in comparison to the wild type 103S/pSJ35 and Δ*vapA*/pMV261H control strains. Nonetheless, the growth profiles of the various complemented strains were similar, thereby allowing for analysis and comparison of the growth of these strains in macrophages.

Mutation within the conserved domain of VapA abolishes the ability of the protein to allow intramacrophage growth

The  $\Delta vapA$  strains expressing wild type and mutated versions of vapA were analyzed for their ability to replicate in macrophages over the course of 72hrs. Strains 103S/pSJ35 and

 $\Delta vapA/pMV261$ -H were used as controls for wild type and  $\Delta vapA$ -attenuated intracellular growth respectively. Typically,  $\Delta vapA R. equi$  persists in macrophages over the course of infection [131]. We noted however, that carriage of pMV261-H compromised persistence such that the  $\triangle vapA$  strain was cleared from the monolayer with time (Fig. 9A). Furthermore, the replication of wild type 103S was hindered when the bacterium carried pSJ35, with the strain demonstrating persistence in the monolayer instead of increasing in number as is characteristic of wild type organisms. It has been shown that in vitro subculturing of 103S can result in loss of the virulence plasmid, resulting in a plasmid-cured strain that does not replicate within macrophages [75, 207]. It is possible that overnight growth of strain 103S/pSJ35 with antibiotic selection to maintain the pSJ35 plasmid resulted in the elimination of the virulence plasmid in a proportion of the 103S/pSJ35 population as a way to increase their fitness within the antibiotic containing environment. Importantly, such a scenario would not occur in the  $\Delta vapA$  strains expressing wild type and mutated versions of vapA since the  $\Delta vapA$  mutation on the virulence plasmid was marked by an apramycin cassette, thus providing pressure to maintain the virulence plasmid during in vitro growth under apramycin selection. In addition, the hygromycin cassette of pSJ28 and its derivatives ensured maintenance of recombinant plasmids possessing wild type or the mutated *vapA* genes during overnight growth in hygromycin containing media.

 $\Delta vapA$  possessing either vapA ( $\Delta vapA$ /pSJ28) or vapA.Disordered ( $\Delta vapA$ /pSJDisordered) began replicating within the macrophage monolayer at 24hrs post infection, wherein the numbers of  $\Delta vapA$ /pSJ28 increased by ~12 fold and  $\Delta vapA$ /pSJDisordered increased by ~25 fold at 72 hours post infection (Fig. 9A/B). In contrast,  $\Delta vapA$  R. equi expressing vapA.Conserved ( $\Delta vapA$ /pSJConserved) or vapA.Full ( $\Delta vapA$ /pSJFull) did not

replicate. Taken together the data suggest that some or all of the lysines and arginines present in the conserved domain of the VapA protein are important for intramacrophage replication (Fig. 8A, Fig. 9A and B).

Expression of GFP-tagged mutated VapA within Saccharomyces cerevisiae depicts GFP-VapA<sup>R99A</sup> mislocalization from the plasma membrane

Saccharomyces cerevisiae provides a model system by which GFP-tagged VapA can be readily expressed and observed. Previous experimentation with GFP-tagged VapA<sup>32-189</sup> showed a distinct plasma membrane localization upon expression in Saccharomyces cerevisiae [131], and for this reason, was employed to assess whether mutating VapA altered its affinity for the plasma membrane. The initial analysis examined VapA<sup>32-189</sup> mutated within the disordered and conserved domains as described for the previous intramacrophage growth experiments. VapA protein expression in S. cerevisiae was confirmed via western blotting using a polyclonal anti-VapA antibody for detection, Figure 10A. While each yeast strain was confirmed to produce a variation of GFP-VapA, it appeared as though GFP-VapA<sup>32-189</sup> and GFP-VapA.Disordered were present in higher amounts than GFP-VapA.Conserved and GFP-VapA.Full; however, an alternative explanation for the reduced signal in the latter two strains might be due to alteration of a major epitope within VapA that decreased antibody binding.

Localization of GFP-VapA. Disordered showed that this protein traffics to the plasma membrane in a similar fashion to GFP-VapA $^{32-189}$  (Fig. 10 B/C). In contrast, analysis of GFP-VapA. Conserved and GFP-VapA. Full revealed a greatly reduced capacity to localize to the plasma membrane with the majority of these protein displaying cytosolic localization. Notably, these are the very same mutations that rendered VapA incapable of rescuing the intramacrophage growth defect of  $\Delta vapA$  and therefore, these findings are of great interest. In order to more

precisely define the relevant residues of conserved domain of VapA necessary for plasma membrane localization we next generated constructs yielding GFP-tagged VapA containing individual mutations at lysine and arginine residues within this domain. Upon visualization of these yeast strains it was observed that GFP-VapA<sup>R99A</sup> failed to localize to the plasma membrane in a comparable fashion to GFP-VapA.Conserved (Figure 11B/C). The other GFP-VapA proteins containing single mutations within the conserved domain were shown to localize at the plasma membrane in a similar manner to GFP-VapA<sup>32-189</sup>. These results suggest that the pertinent residue for plasma membrane interaction within yeast is arginine 99 that resides within the designated conserved domain of VapA.

#### **Discussion**

With the discovery that VapA interacts with eukaryotic membranes and liposomes containing phosphatidic acid, it was critical to understand whether these qualities were important for intramacrophage replication and to identify which residues within the protein are responsible for this interaction [131]. Assessment began by mutating lysine and arginine residues, as these residues have been found to be enriched within domains of other PA binding proteins [187]. Mutation of lysines and arginines within the conserved domain of VapA not only altered the ability of the *vapA* gene to reverse the intramacrophage replication defect of Δ*vapA* but also prohibited GFP-VapA localization to the plasma membrane in *Saccharomyces cerevisiae*. These data are in agreement with Rofe and colleagues who recently discerned that the conserved domain of VapA was responsible for the endolysosomal swelling seen upon protein incubation with NRK cells [130]. Further inquiry into which of the four residues within the conserved domain was responsible for altered plasma membrane localization of GFP suggested that arginine 99 was solely accountable.

Evaluation of the Vap protein alignment, containing Vaps from both the pVapA and pVapB virulence plasmids, provided by Letek and coworkers, suggests that only VapH has this arginine conserved. However, there are Vaps that have positive residues substituted within this region, wherein there is a lysine present in VapB and a histidine present in VapC, VapL, VapG, and VapF. Oddly, neither VapK1 or VapK2 have a positively charged residue present in this position but instead possess a glutamine that has a negative side chain [76]. Interestingly, deletion of VapC, VapL, VapG, VapH, VapF, and VapB has determined that these are not the Vaps responsible for intramacrophage replication, and VapF is known to be a pseudogene [76, 81, 82, 87, 89, 208]. Taken together, these data can support the concept that VapA may have multiple functions, wherein the ability of VapA to bind phosphatidic acid is associated with one of these capacities. Since VapK2 was previously shown to localize to the yeast plasma membrane in low amounts, it may be that this pVapB-encoded virulence protein responsible for intramacrophage replication relies more heavily on the secondary function that has yet to be determined [131]. It is possible, that the R. equi isolates carrying different virulence plasmid types may have divergent steps in their pathogenesis, thereby explaining why VapK1/K2 lack this important amino acid present within VapA.

Future research will need to focus on the role arginine 99 plays during R. equi replication within macrophages and determine whether VapA with this mutation can bind phosphatidic acid like the wild type protein. It is of particular interest to establish the location of arginine 99 mutated VapA when expressed by  $\Delta vapA$  during macrophage infection. Absence of the protein at the R. equi containing vacuole membrane would provide further evidence that this residue is important for VapA protein localization within the host cell. Showing that R. equi can utilize phosphatidic acid within the macrophage would define the first circumstance in which an

intracellular pathogen targets this eukaryotic lipid. It will be important to determine how phosphatidic acid binding affects downstream macrophage signaling events or promotes the secondary function of VapA.

## **Experimental Procedures**

#### Bacterial and yeast cultures.

Bacterial and yeast strains used during this study are listed in Table 4, along with pertinent growth information. *Escherichia coli* was grown in Lysogeny broth (LB) at 37°C with appropriate antibiotics where needed; carbenicillin or ampicillin were used at 50μg/ml and hygromycin was used at 180μg/ml. *R. equi* growth was done at either 37°C or 30°C in Brain Heart Infusion (BHI) medium, supplemented with hygromycin (180μg/ml) and/or apramycin (80μg/ml) when appropriate. Strain BY4742 of *Saccharomyces cerevisiae* was grown in yeast exact peptone dextrose (YPD) at 30°C. Transformation of these cells with a plasmid conferring loss of uracil auxotrophy allowed for growth on complete supplemental medium (CSM) lacking uracil at 30°C.

## Plasmid construction and isolation of mutated recombinant VapA proteins.

Each recombinant VapA expression plasmid was built upon the pVapALMW background used previously [131] and contains *vapA* without its signal sequence. Site directed mutagenesis of *vapA* was performed using primer pairs listed in Table 5. Initially each codon responsible for a lysine or arginine was identified and mutated independently by running a PCR reaction with each mutational primer pair, specifically, VapA K68A F/R, VapA R74A F/R, VapA R99A F/R, VapA K108A F/R, VapA R136A F/R, or VapA K139A F/R. These reactions amplify the entirety of pVapALMW while incorporating the appropriate nucleotide changes, wherein a codon usage table was referenced for alanine substitution. The parental vector was removed by digestion of

methylated DNA using DpnI for 1.5hrs at 37°C. Thereafter, the remaining unmethylated DNA, with the appropriate *vapA* mutations, was used to transform either DH5α or NEB5α *E. coli* and plated on the appropriate selection medium. The resulting constructs contained a single amino acid mutation at the specified VapA residue and are are pVapA K68A, pVapA R74A, pVapA R99A, pVapA K108A, pVapA R136A, and pVapA K139A. Information regarding these constructs is listed within Table 6.

The preceding protocol was followed to build from these initial constructs and add further mutagenic sites. Primers are listed in Table 5, wherein the same primers during the initial mutation were used or, if mutagenic sites were too close to one another, a secondary primer that accounted for previous genetic alterations were employed. End products consist of pVapADis, pVapACons, and pVapAFull. Sequencing via the Georgia Genomics Facility (GGF) was used as a means to confirm correct gene alterations of *vapA* in pVapALMW throughout mutational production.

## SDS-PAGE and western blotting.

Samples were prepped as previously described [131]. Thereafter, samples were loaded in 13% or 15% SDS-Page gels that were run in 1X Tris-Glycine SDS buffer. During western blotting, protein transfer from the SDS-PAGE gel to the nitrocellulose membrane was completed in 1.4% glycine (w/v), .3% Tris Base (w/v), and 20% methanol buffer. The nitrocellulose membrane was then blocked using SuperBlock® (TBS) (Thermo Scientific) supplemented with .05% Tween-20. Blocking was completed for either 3 hrs at room temperature or overnight at 4°C. Thereafter, primary polyclonal rabbit αVapA was antibody incubated with the membrane at a 1:1,000 dilution in blocking buffer; this antibody was either incubated for one hour at room temperature or overnight at 4°C. Afterwards, the nitrocellulose membrane was washed 4X using 1X PBS

containing .05% (v/v) Tween 20, wherein each wash lasted 10 minutes. Secondary goat αrabbit antibody conjugated to horseradish peroxidase (HRP) was next incubated with the nitrocellulose membrane in blocking buffer at a 1:20,000 dilution, as was done previously for the primary antibody. Washing of the membrane was completed as formerly discussed. Gentle agitation was constantly applied throughout this process. Exposure of the western blot used enhanced chemiluminescent HRP substrate and peroxide buffer (Thermo Scientific). Substrate and buffer were mixed at an equal ratio and incubated with the membrane at room temperature for 5 minutes before visualization.

### Generation of $\Delta$ vapA complementation vectors.

pVapADis, pVapACons, or pVapAFull were used as templates in a PCR reaction with primers pSJ28 overlap F and pSJ28 R End (ScaI) to generate a 421bp amplicon whilst pSJ28 was included in a PCR reaction with pSJ28 F End (KpnI) and pSJ28 overlap R to generate a 691bp band. Each amplicon from the PCR reaction with pVapADis, pVapACons, or pVapAFull was mixed in equimolar amounts with the amplicon from pSJ28 and used in an overlap PCR for 15 cycles with a 60°C annealing temperature. Thereafter, primers pSJ28 F End (KpnI) and PSJ28 R End (ScaI) were added to the reaction to amplify DNA products that had combined both PCR amplicons into one product, wherein the PCR was continued for an additional 20 cycles with a 65°C annealing temperature. The latter PCR generated an approximate 1.1kb amplicon that was subsequently digested with ScaI and KpnI. pSJ28 was also digested with ScaI and KpnI and, thereafter, ligated overnight with the digested overlap PCR products at 16°C. Following ligation, plasmids were transformed into Neb5α cells. Sequencing was completed to confirm that the mutated *vapA* genes were correctly fused with the *vapA* gene from pSJ28, producing pSJDisordered, pSJConserved, and pSJFull.

Each of these plasmids, including pSJ28, was electroporated into  $\Delta vapA~R~equi$  using the a standard protocol [131]. R.~equi was electroporated at 2500 V with a capacitance of 25  $\mu$ F and a resistance of 1000 ohm. Recovery was completed at 30°C in filter sterilized BHI supplemented with 0.5M Sucrose. Colonies were grown on selective media at 30°C for three days.

Flow cytometry analysis of *∆vapA* bacteria expressing mutated VapA.

 $R.\ equi$  strains were grown overnight with antibiotic where appropriate. The following morning bacteria were subcultured and allowed to reach an  $OD_{600}$  of 1. Approximately  $1x10^8$  bacteria were harvested per condition tested and washed twice with 1X PBS. Cells were either incubated with polyclonal rabbit  $\alpha$ -VapA or pre-immune serum at a 1:500 dilution or left deprived of antibody for 45min at room temperature in 1X PBS containing 5% FBS. Post incubation, samples were washed three times with 1X PBS supplemented with 5% FBS. Secondary Alexa Fluor 488-labeled goat  $\alpha$ -rabbit IgG was incubated as described for the primary antibody, wherein some samples were left unexposed. Cells were washed as done previously. Fixing occurred by exposing bacteria to 4% Paraformaldehyde in PBS for 20min at room temperature. Bacteria were washed in PBS and then analyzed via a Becton Dickinson LSR II flow cytometer (Becton Dickinson, Franklin Lakes, NJ).

### Growth Curve.

*R.equi* strains were grown overnight in the appropriate selection medium. Bacteria were diluted to an optical density (OD600) of 0.05 in 200 $\mu$ l in media without antibiotic. A 96 well flat bottom plate (Corning) was employed in a computer-controlled multimode plate reader ( $\lambda$ = 600 nm; BioTek) to measure the optical density (OD600) of bacterial strains over the course of 22 hrs.

Bacteria were harvested thereafter and serially diluted in 1X PBS. Diluted bacteria were plated on BHI and BHI containing Apramycin and Hygromycin to determine the percentage of bacteria retaining antibiotic resistance.

## Macrophage growth and infection.

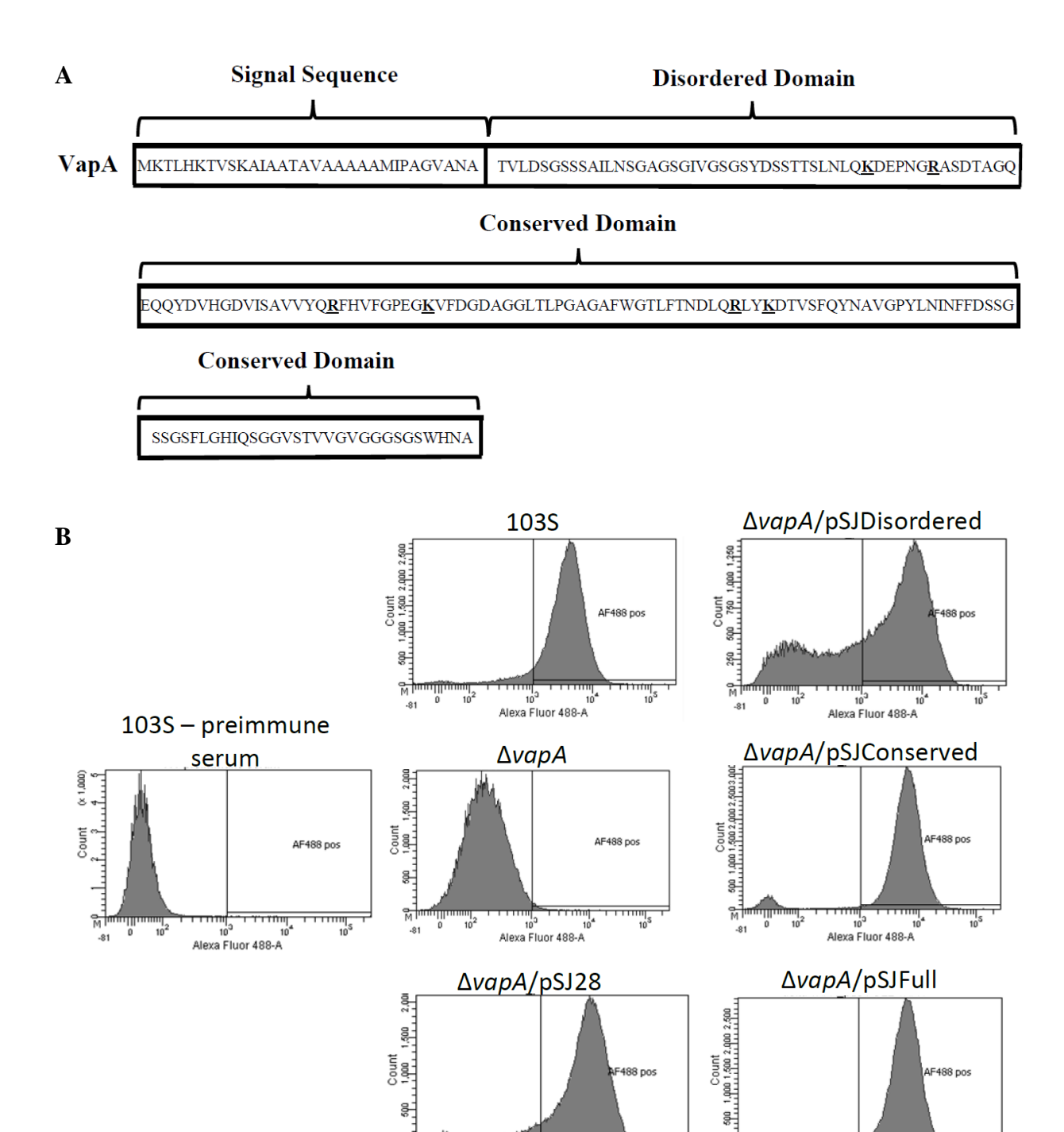
J774A.1 macrophages (ATCC) were maintained in Dulbecco's Modified Eagle Medium (DMEM) supplemented with 2mM L-glutamine and 10% FBS and kept at 37°C with 5% CO<sub>2</sub>. During infections, 1 x 10<sup>5</sup> macrophages were adhered to a 24-well plate. Preceding infection, the monolayers were washed with fresh media to remove any nonadherent cells. Bacteria suspended in 1X PBS were added to the monolayers at an MOI of 5:1 and incubated for an hour at 37°C and 5% CO<sub>2</sub>. Afterwards, monolayers were washed 3X with unsupplemented DMEM and either lysed or incubated in media containing 35µg/ml of Amikacin, to kill any remaining extracellular bacteria. Lysis was obtained by adding 500µl of autoclaved di H<sub>2</sub>O and incubating the plate for 20min at 5% CO<sub>2</sub> and 37°C. Bacterial quantification was accomplished through plating serial dilutions of the lysate in 1X PBS on BHI. Plates were incubated for 48 hrs at 37°C before colony forming units (CFU) were obtained.

## Yeast expression of GFP tagged mutations VapA.

Saccharomyces cerevisiae strain BY4742 carrying either pG035 or pGFP-VapA<sup>32-189</sup> were used as a control strains [131]. Afterwards, primers GFP-VapA NSS F (BgIII) and GFP-VapA R (BgIII), listed in Table 5, were used to amplify *vapA* containing the appropriate mutations from the template plasmids pVapADis, pVapACons, pVapAFull, pVapA R99A, pVapA K108A, pVapA R136A, and pVapA K139A. Amplicons generated were ~550bp in length and were treated as discussed previously to obtain yeast transformants with a specific *vapA* derivative within pG035 [131].

# Statistical analysis.

Sigma Plot version 11.2.0.5 (Systat Software, San Jose, CA) was used for statistical analysis. Bacterial quantification was evaluated via a repeated measures two-way analysis of variance (ANOVA) using the Holm-Sidak method, a P value of  $\leq 0.05$  was considered significant.



10<sup>3</sup> 1 Alexa Fluor 488-A ᇭ

Alexa Fluor 488-A

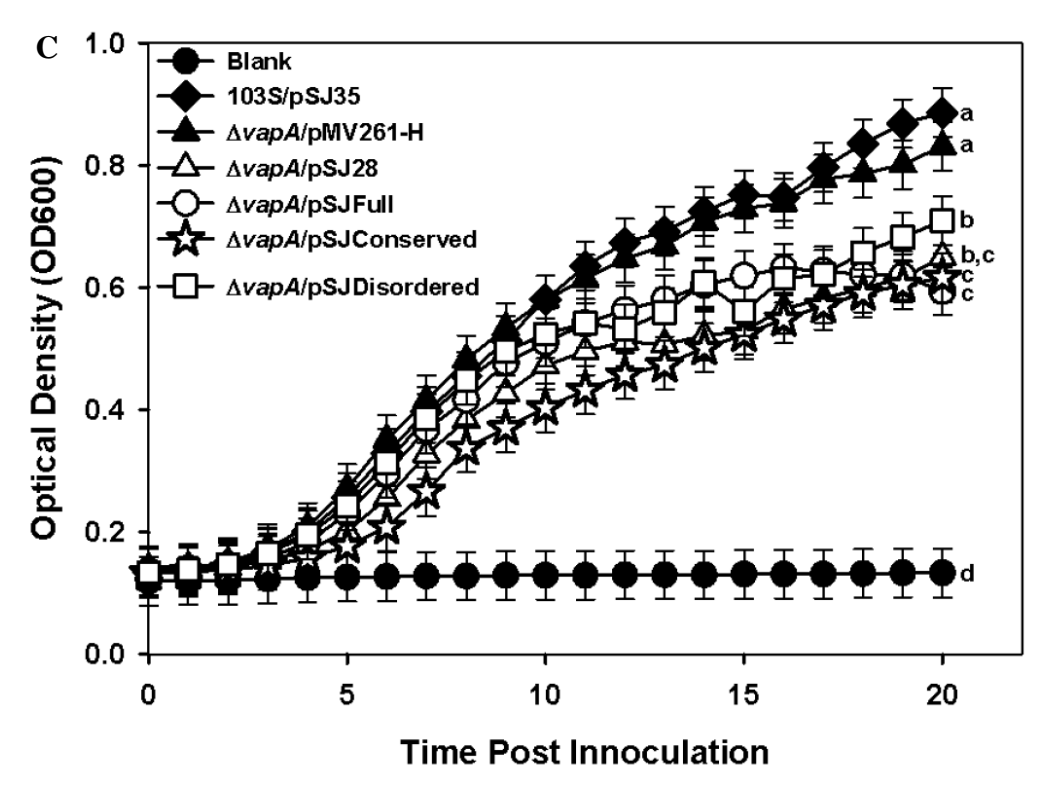


Figure 8. Comparison of  $\Delta vapA$  with strains expressing wild type or mutated versions of vapA. (A) Domains of VapA protein sequence as annotated by Letek and colleagues in 2008 [76]. The specific domain is defined by brackets and the mutated lysine and arginine residues are bolded underlined residues. (B) Flow cytometry profiles of  $\Delta vapA$  expressing wild and mutated versions of the vapA gene. Bacteria were grown at 37°C, washed and incubated with either pre-immune serum (as an irrelevant antibody control) or rabbit polyclonal anti-VapA antisera as primary antibody and thereafter probed with an Alexa Fluor 488-labeled anti-rabbit IgG secondary as described in Material and Methods. The fluorescence profiles of wild type isolate 103S, the  $\Delta vapA$  mutant,  $\Delta vapA/pSJD$ isordered,  $\Delta vapA/pSJC$ onserved,  $\Delta vapA/pSJ28$ , and  $\Delta vapA/pSJFull$  were compared. (C) Bacterial growth was followed for 20hrs by measuring the optical density at 600nm using a Biotek plate reader. Individual time points were assessed in triplicate and the growth comparison assay was done three times. Letters to the right of the curves indicate statistical difference wherein shared letters indicate no statistical difference. Statistical analysis was preformed using repeated measures analysis of variation (ANOVA) with the Holm-Sidak method, significance was considered p < .05.

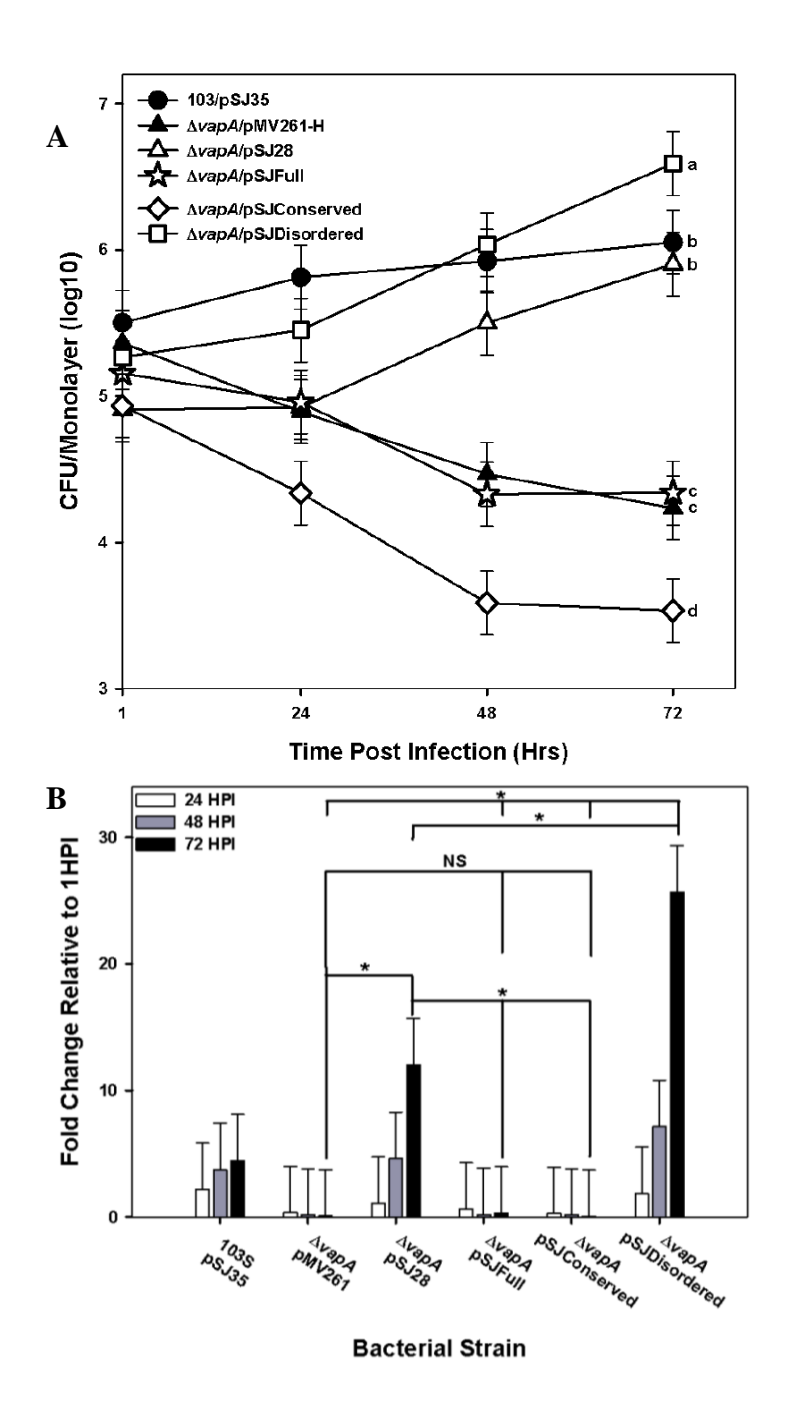
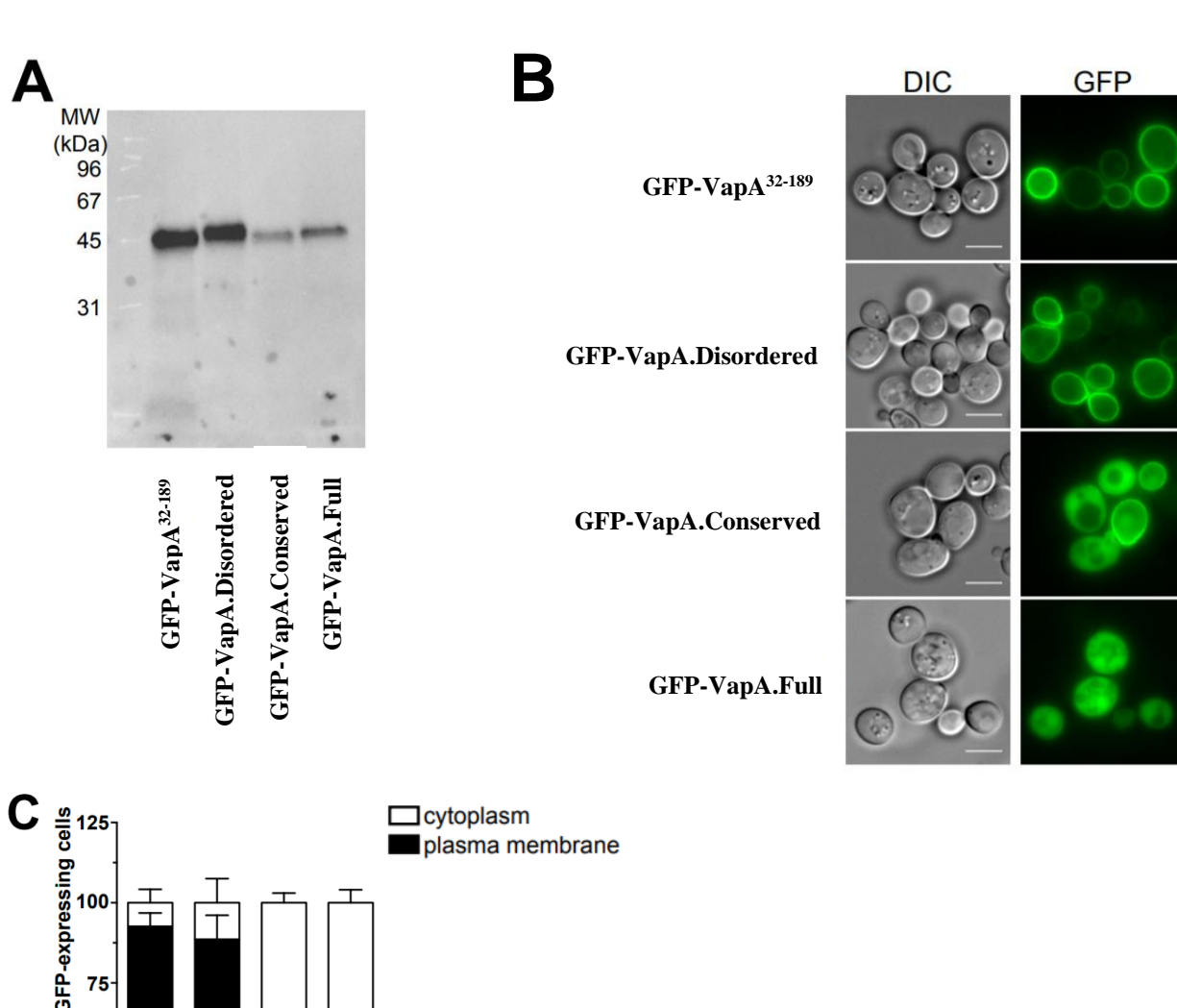
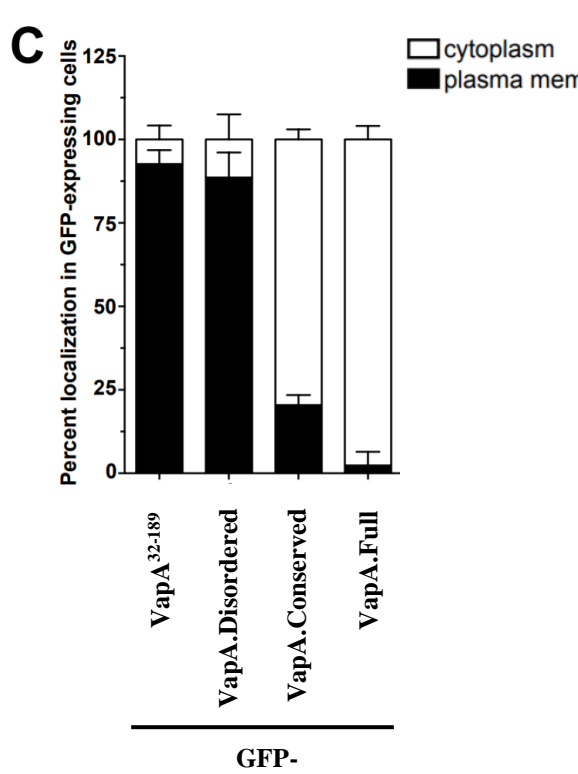


Figure 9. Expression of *vapA* containing mutations within the conserved domain is unable rescue the replication defect of  $\Delta vapA$  R. equi. Murine J774A.1 macrophages were infected with the indicated R. equi strain. Individual time points were performed in triplicate and each experiment was completed on 3 separate occasions. Statistical analysis was performed using repeated measures ANOVA via the Holm-Sidak test. (A) Bacterial colony forming units (CFUs) were quantified over the course of 72 hours by lysis and plating of infected macrophage monolayers. Open symbols denote  $\Delta vapA$  bacterial strains that were expressing a version of the vapA gene off of pSJ28. Letters to the right of each curve denote statistical significance, where the

same letter indicates no statistical difference. Significance was considered a p<.05. (**B**) Bars denote fold change in bacterial strain growth as compared to 1hr post infection. NS = not significant; (\*) = p < .05.





**Figure 10. GFP-VapA mutated within the conserved domain fails to localize to the plasma membrane in** *Saccharomyces cerevisiae*. (**A**) Western blot analysis on lysates of *S. cerevisiae* strain BY4742 expressing variations of GFP-VapA. GFP-VapA proteins were GFP-VapA<sup>32-189</sup> (wild type protein without the putative signal sequence), GFP-VapA.Disordered, GFP-VapA.Conserved, or GFP-VapA.Full. Rabbit polyclonal anti-VapA antibody and goat αrabbit antibody conjugated to horseradish peroxidase (HRP) were used as primary and secondary antibodies to probe for protein expression. (**B**) Fluorescence microscopy evaluating GFP localization on the yeast strains from (**A**). Each bar denotes 5μ. (**C**) Percent quantification of GFP localization from yeast strains in (**A**) where 100 yeast cells were enumerated per each experimental condition.

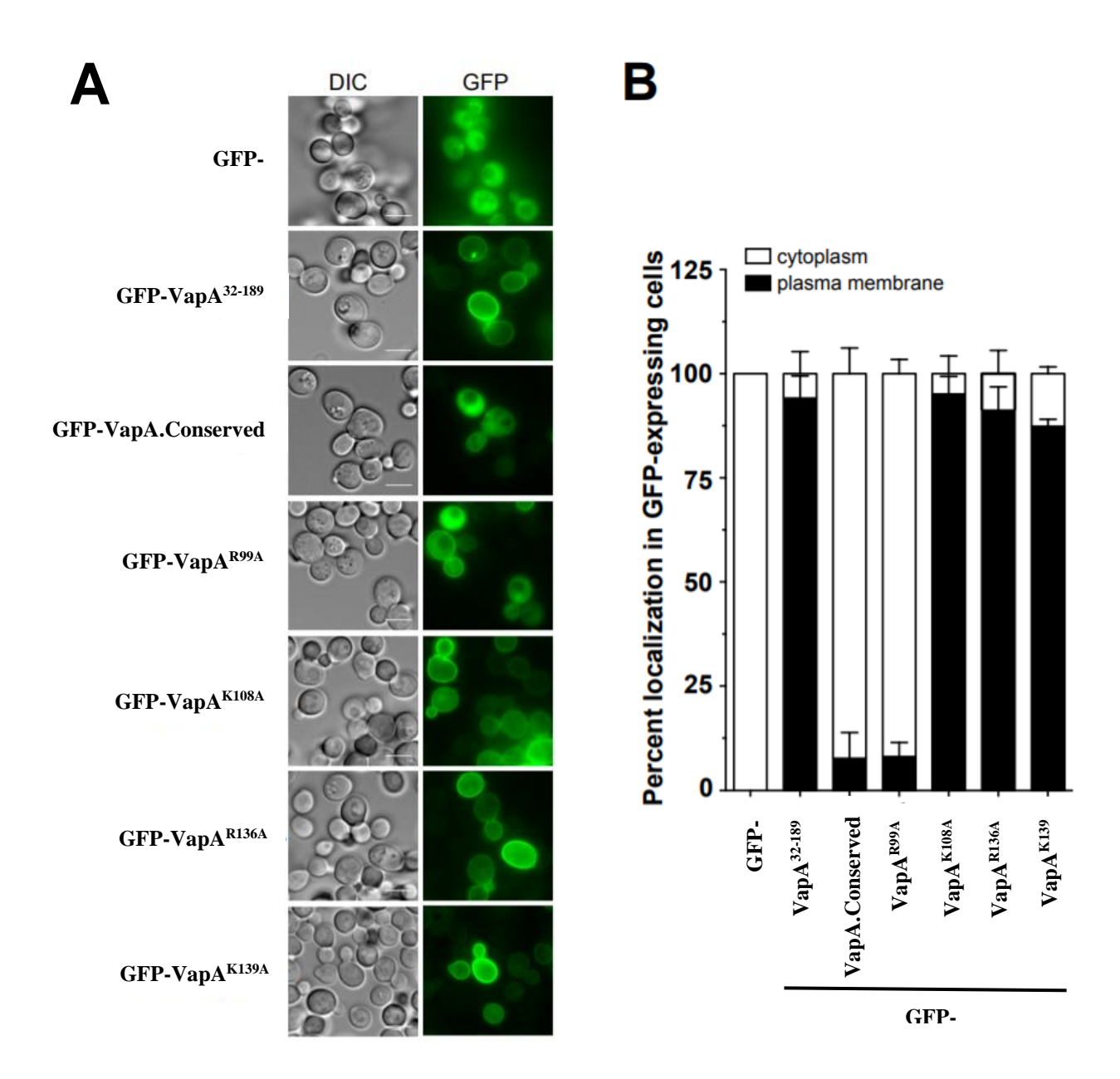


**Figure 11. GFP-VapA**<sup>R99A</sup> mimics the localization of GFP-VapA.Conserved when expressed in *Saccharomyces cerevisiae*. (**A**) Fluorescence microscopy examination of either GFP alone, GFP-VapA<sup>32-189</sup>, GFP-VapA.Conserved, or GFP-tagged VapA containing a single mutated residue of the conserved domain. Each bar denotes 5μ. (**B**). Quantification of GFP-VapA variant localization within yeast (plasma membrane and the cytoplasm), wherein 100 cells were counted per experimental condition.

Table 4. Bacterial and yeast strains.

Bacterial and yeas  Bacteria/Yeast	Description	Source
R. equi	-	
103S	Wild type strain isolated from pneumonic foal (~80kb pVapA type virulence plasmid)	[95]
$\Delta vap A$	103S R. equi variant with vapA deletion; Apr <sup>R</sup>	[82]
103S/pSJ35	103S harboring pSJ35; Hyg <sup>R</sup> Apr <sup>R</sup>	[82]
Δ <i>vapA</i> /pMV261-H	ΔvapA harboring pMV261-H; Hyg <sup>R</sup> and Apr <sup>R</sup>	[82]
Δ <i>vapA</i> /pSJ28	$\Delta vapA$ harboring pSJ28 allowing for $vapA$ expression from its native promoter; Hyg <sup>R</sup> and Apr <sup>R</sup>	[82]
ΔvapA/pSJDisordered	$\Delta vapA$ harboring pSJDisordered allowing for $vapA$ expression off the native promoter with mutations in the disordered domain; Hyg <sup>R</sup> and Apr <sup>R</sup>	This Study
ΔvapA/pSJConserved	$\Delta vapA$ harboring pSJConserved allowing for $vapA$ expression off the native promoter with mutations in the conserved domain; Hyg <sup>R</sup> and Apr <sup>R</sup>	This Study
Δ <i>vapA</i> /pSJFull	Δ <i>vapA</i> harboring pSJFull allowing for <i>vapA</i> expression off the native promoter with mutations in the disordered and conserved domains; Hyg <sup>R</sup> and Apr <sup>R</sup>	This Study
S. cerevisiae BY4742	MATα his3Δ1 leu2Δ0 lys2Δ0 ura3Δ0	GE Dharmacon

Table 5. Primers used in this study.

Name	Sequence	Plasmid Generated	Reference
VapA F (BamHI)	5'GTA <u>GGATCC</u> GACCGTTCT TGATTCCGGTAG-3'	pVapALMW	[131]
VapA R (SalI)	5'-TA <u>GTCGAC</u> CCGGAA GTACGTGCAG-3'	pVapALMW	[131]
VapA K68A F	5'-GTTAAACCTTCAGGCAGA CGAACCGAACGGTCGAGCAAGC-3'	pVapADis, pVapA K68A, pVapAFull	This Study
VapA K68A R	5'-GCTCGACCGTTCGGTTCG TCTGCCTGAAGGTTTAACGAAG-3'	pVapADis, pVapA K68A, pVapAFull	This Study
VapA R74A F	5'-GAAAGACGAACCGAACG GTGCAGCAAGCGATACCGCC-3'	pVapA R74A	This Study
VapA R74A R	5'-GGCGGTATCGCTTGCTGC ACCGTTCGGTTCG-3'	pVapADis, pVapAFull, pVapA R74A	This Study
VapA K68A R74A F	5'-GACGAACCGAACGGTG CAGCAAGCGATACCGCC-3'	pVapADis, pVapAFull	This Study
VapA R99A F	5'-GCGGTCGTCTACCAGGCGT TTCACGTATTCGGGCCAGAAG-3'	pVapACons, pVapAFull, pVapA R99A	This Study
VapA R99A R	5'-GAATACGTGAAACGCCT GGTAGACGACCGCGCTGATG-3'	pVapACons, pVapAFull, pVapA R99A	This Study
VapA K108A F	5'-GGCCAGAAGGAGCGGTCT TCGATGGCGATGC-3'	pVapACons, pVapAFull, pVapA K108A	This Study
VapA K108A R	5'-CATCGCCATCGAAGACCG CTCCTTCTGGCCCGAATAC-3'	pVapACons, pVapAFull, pVapA K108A	This Study
VapA R136A F	5'-CACAAATGACCTTCAGGC GCTCTACAAAGACACCGTCTCG-3'	pVapACons, pVapAFull, pVapA R136A	This Study
VapA R136A F	5'-CGAGACGGTGTCTTTGTA GAGCGCCTGAAGGTCATTTGTG-3'	pVapACons, pVapAFull, pVapA R136A	This Study
VapA R136A K139A F	5'-CTTCAGGCGCTCTACGCAG ACACCGTCTCGTTCCAG-3'	pVapACons, pVapAFull	This Study

VapA R136A K139A R	5'-CTGGAACGAGACGGTGT CTGCGTAGAGCGCCTGAAG-3'	pVapACons, pVapAFull	This Study
VapA K139A F	5'-CACAATGACCTTCAGCGT CTCTACGCAGACACCGTCTCGTTC-3'	pVapA K139A	This Study
VapA K139A R	5'-GTACTGGAACGAGACGGT GTCTGCGTAGAGACGCTGAAG-3'	pVapA K139A	This Study
pSJ28 F End (KpnI)	5'-C <u>GGTACC</u> CTGCGTC GCGCAGTACG-3'	pSJDisordered, pSJConserved, pSJFull	This Study
pSJ28 overlap R	5'- CCACTATTGAGAATCG CACTGCTGCTACCG -3'	pSJDisordered, pSJConserved, pSJFull	This Study
pSJ28 overlap F	5'-CGGTAGCAGCAGTG CGATTCTCAATAGTGG-3'	pSJDisordered, pSJConserved, pSJFull	This Study
pSJ28 R End (ScaI)	5'-AC <u>AGTACT</u> AACTCCA CCGGACTGG-3'	pSJDisordered, pSJConserved, pSJFull	This Study
GFP-VapA NSS F (BglII)	5'ATGGATGAACTATACAAGTC CGGACTC <u>AGATCT</u> ATGACCGTT CTTGATTCCGGTAGC-3'	pGFP-VapA <sup>32-</sup>	[131]
GFP-VapA R (BglII)	5'-GTCGACTGCAGAATTCGAAGCT TGAGCTCG <u>AGATCT</u> CTAGGC GTTGTGCCAGCTAC-3'	pGFP-VapA <sup>32-</sup> <sub>189</sub>	[131]

<sup>&</sup>lt;sup>1</sup>Underlined sequence represents restriction enzyme digestion site

Table 6. Plasmids used in this study.

Name	Purpose	Reference
pHis-Parallel1	E. coli expression plasmid that contains an N-	[204]
	terminal His tag; Carb <sup>R</sup>	
pVapALMW	pHis-Parallel1 background containing <i>vapA</i> (without signal sequence region); Carb <sup>R</sup>	[131]
pVapADis	pVapALMW with lysine 68 and arginine 74	This Study
p + up. 12 15	residues in the disordered domain mutated to alanine; Carb <sup>R</sup>	Tims Staay
pVapACons	pVapALMW with lysines 108 and 139 and arginines 99 and 136 in the conserved domain mutated to alanine; Carb <sup>R</sup>	This Study
pVapAFull	pVapALMW with lysine and arginine residues in the disordered and conserved domains mutated to alanine; Carb <sup>R</sup>	This Study
pVapA R99A	pVapALMW with arginine 99 substituted with alanine within the conserved domain; Carb <sup>R</sup>	This Study
pVapA K108A	pVapALMW with lysine 108 substituted with alanine within the conserved domain; Carb <sup>R</sup>	This Study
pVapA R136A	pVapALMW with arginine 136 substituted with alanine within the conserved domain; Carb <sup>R</sup>	This Study
pVapA K139A	pVapALMW with lysine 139 substituted with alanine within the conserved domain; Carb <sup>R</sup>	This Study
pSJ28	Complementation vector expressing VapA from its native promoter; Hyg <sup>R</sup>	[82]
pSJDisordered	pSJ28 with <i>vapA</i> containing lysine 68 and arginine 74 mutations within the disordered domain; Hyg <sup>R</sup>	This Study
pSJConserved	pSJ28 with <i>vapA</i> containing lysines 108 and 139 and arginines 99 and 136 mutated within the conserved domain; Hyg <sup>R</sup>	This Study
pSJFull	pSJ28 with <i>vapA</i> containing lysine and arginine mutations within both the disordered and conserved domain; Hyg <sup>R</sup>	This Study
pMV261-H	Mycobacterium and E. coli shuttle vector containing oriM and oriE for plasmid replication; Hyg <sup>R</sup>	[82, 209]
pSJ35	pMP176 with added Hygromycin resistance gene;Hyg <sup>R</sup> and Apr <sup>R</sup>	[82]
pGO35	yeast N-terminal GFP fusion expression plasmid; URA	[202, 203]
pGFP-VapA <sup>32-189</sup>	<i>vapA</i> (94-567) in pGO35	[131]
pGFP-VapA.Disordered	vapA(94-567) with lysine 68 and arginine 74 mutated within the disordered domain in pG035	This Study

pGFP-VapA.Conserved	<i>vapA</i> (94-567) with lysines 108 and 139 and arginines 99 and 136 mutated within the	This Study
	conserved domain in pG035	
pGFP-VapA.Full	vapA(94-567) with lysine and arginine	This Study
	mutations within the disordered and conserved	
	domains in pG035	
pGFP-VapA <sup>R99A</sup>	vapA(94-567) with arginine 99 mutated to	This Study
	alanine within the conserved domain in pG035	
pGFP-VapA <sup>K108A</sup>	vapA(94-567) with lysine 108 mutated to	This Study
_	alanine within the conserved domain in pG035	-
pGFP-VapA <sup>R136A</sup>	vapA(94-567) with arginine 136 mutated to	This Study
	alanine within the conserved domain in pG035	
pGFP-VapA <sup>K139A</sup>	vapA(94-567) with lysine 139 mutated to	This Study
	alanine within the conserved domain in pG035	

#### **CHAPTER 5**

#### CONCLUSION

Initial isolation of *Rhodococcus equi* from foals led to recognition of the bacterium as a pathogen causing pyogranulomatous lesions within the lung [2, 95]. Further studies have determined that *R. equi* is capable of causing disease in a wide variety of hosts, most important being human, swine, and bovine species [9, 12, 71, 73]. Virulence is dependent upon the bacterium carrying a virulence associated plasmid, wherein *R. equi* can be equipped with either pVapA, pVapB, or pVapN which tend to infect foals, swine, and bovine respectively [23-25, 69, 73, 95]. Human isolates of *R. equi* have been shown to carry any one of the three plasmid types and it is therefore presumed that exposure of a susceptible host to virulent bacteria predisposes them to disease [9, 71, 206]. Intriguingly, both foals and humans present with pyogranulomatous pneumonia while pigs and cattle have tuberculosis-like lesions in their submaxillary lymph nodes [9, 24, 25, 95]. Since each virulent isolate of *R. equi* examined has been shown to replicate within macrophages, it is unknown if these differences in presentation are due to different routes of exposure, a differing collection of virulence-associated genes, or alternate species anatomy [75].

Within the virulence associated plasmids lies a pathogenicity island, which is presumed to have arisen during horizontal gene transfer events and has led to the acquisition of a novel family of genes known as the *vap* (virulence associated protein) family [48, 76]. Gene deletion analysis has determined the importance of *vapA* (pVapA), *vapK1/K2* (pVapB), and *vapN* (pVapN) during intramacrophage replication of *R. equi*, but bioinformatic analysis of either the

vap genes or their resultant proteins lacks identification of any significant homologs outside of the vap/Vap famly [73, 76, 82, 208]. Therefore, the mechanisms by which certain Vap proteins allow intracellular replication of the bacterium has remained highly elusive. Studies on Vap protein function have predominantly been done on *R. equi* equipped with the pVapA type virulence plasmid, thereby focusing the preceding work on VapA (Virulence Associated Protein A).

Trafficking of pVapA carrying R. equi has previously shown delivery of the bacterium to a late endosomal-like compartment 24-hours post infection, wherein this compartment lacks acidification [122, 124, 129]. The work here studied the progression of a pVapA equipped R. equi strain during a 72-hour macrophage infection by localizing the bacterium, VapA, and LAMP1 (lysosome associated membrane protein 1). The work shown here suggests that the LAMP1 marker is lost at 48 hours post infection and remains unassociated with the R. equi containing vacuole at the 72-hour time point [131]. This could signify the modified phagosomal niche in which the bacterium replicates and should be further characterized to better understand how R. equi alters the phagosome in order to be protected from the microbicidal capacities of the macrophage. The compartment markers that should be assessed regarding this newly identified R. equi containing vacuole (RCV) include autophagy mediators and other late endosomal indicators. Induction of the autophagy pathway would not only provide the excess membrane bilayer seen during the T48-T72 time points, but also essential nutrients the bacterium needs for survival. Produced autophagosomes should eventually fuse with the macrophage lysosome; however, induction of this pathway may hinder lysosomal delivery of R. equi long enough to allow for cellular necrosis. Autophagy initiation during infection may be due to either starvation pathways activated from bacterial signals, phagosome destruction from bacterial replication, or

bacterial escape into the cytoplasm [137]. Release of *R. equi* from the RCV has not been documented however, while unlikely, real time imaging of infections during later time points has not yet ruled out this mechanism. It has been long-accepted that *R. equi*'s ability to replicate within the macrophage is due to inhibition of fusion between the phagosome containing the bacterium and the lysosome [33, 124]. If this is true, then the additional membrane obtained by the RCV could be from further fusion of early or late endosomal compartments. LAMP1 being lost from the RCV at T48 suggests that further adjustments of the phagosome have transpired and therefore late endosomal markers required for fusion with the lysosome should be studied to determine what other alterations have occurred. In either case, knowing the response of the macrophage will help identify the upstream signaling that caused the mis-regulation of phagosomal trafficking.

Deletion of vapA from pVapA carrying R. equi has determined that VapA alters intramacrophage replication and phagosomal acidification [82, 129]. Recent work has begun to focus on the functions of purified recombinant VapA, by evaluating the effects of the protein alone to alter the physiology of cells, to rescue bacteria during macrophage infection, or to bind a host cell component [130, 131, 138]. Rofe and colleagues defined the capacity of incubated recombinant VapA to cause lysosomal swelling and alter the hydrolytic capacity of Normal Rat Kidney cells [130]. Herein, recombinant VapA was incubated with J774A.1 macrophages and then the growth of either  $\Delta vapA$  R. equi or  $Escherichia\ coli$  was examined [131]. The ability of rVapA to rescue the growth defect of  $\Delta vapA$  gives the field a way to confirm isolated protein function and therefore determine if any subsequent findings were caused by rVapA or an artifact of non-functional protein. Interestingly, the addition of rVapA to macrophages before infection with E. coli led to the prolonged survival of the bacterium [131]. Data not presented includes the

inability of rVapA to alter intramacrophage replication or persistence of the equine commensal *Streptococcus equi ssp. zooepidemicus*. It is of interest to note that both *R. equi* and *E. coli* possess a lipid outer membrane while *S. zooepidemicus* is a conventional Gram-positive [35, 46, 210, 211]. Future macrophage infections in the presence of rVapA and various bacteria may determine a trend for the species of bacteria the protein is able to protect within the macrophage. Assessment of different bacterial cell structures, phylogenetic cohorts, and pathogenesis will determine a basis for how the macrophage is interacting with rVapA in relation to certain bacteria. This work could not only aid in determining VapA's mechanism of action but may lend knowledge as to how certain coinfections with *R. equi* are more common [212].

The use of liposome binding assays revealed the ability of VapA to interact with liposomes that contain phosphatidic acid (PA) [131]. Phosphatidic acid has long been defined as a lipid that modifies membrane negative curvature within the cell to promote fusion and fission events during intracellular trafficking [213]. As studies have progressed, PA binding and activation has been determined for several eukaryotic proteins leading to cell signaling events [188, 190-194]. Bacterial alteration of phospholipids has been documented previously as a means to inhabit and grow within host cells [121, 125, 128]. Of specific significance is a *Vibrio parahaemolyticus* protein multivalent adhesion molecule 7 (MAM7), which binds phosphatidic acid to modify RhoA GTPases of intestinal epithelial cells to cause breakdown of the host intestinal barrier and gain access to the blood stream [214]. In contrast, VapA seems to act after phagocytosis by host alveolar macrophages and there has yet to be another intramacrophage pathogen known to target PA. It is possible that VapA is targeting an unknown pathway within macrophage phagolysosomal maturation by interacting with PA, yet it has been established that mTOR, a major regulator in lysosomal biogenesis and cell starvation, is regulated by

phosphatidic acid and is present on the phagosome [215]. If autophagic markers are found in association with the newly modified RCV at T48, then VapA alteration of the mTORC1 complex should be considered. mTORC1 is responsible for the macrophage's response during nutrient deprivation, wherein the cell will undergo autophagy to recycle the nutrients already present as complex molecules within the cell [135]. VapA may promote mTOR inhibition, and therefore autophagy activation, by sequestering the phosphatidic acid present in the bilayer of the phagosome, thereby tricking the macrophage into delivering nutrients and diluting antibacterial components within the RCV (Figure 12). In either case, determining the mechanism by which VapA alters intramacrophage replication of *R. equi* could identify a new means of macrophage machinery exploitation by an intracellular pathogen.

The importance of PA binding by VapA during intramacrophage replication has yet to be examined and will require generating a mutant VapA protein that can no longer bind phosphatidic acid; this mutant protein may be pre-incubated with the macrophage monolayer to test for function or expressed by the Δ*vapA* strain used in a complementation assessment examining reversal of that strain's intracellular growth impairment. The mutational analysis should continue to look at residue 99 within the conserved domain as this GFP-tagged VapA was the only altered residue to mis-localize from the plasma membrane in *Saccharomyces cerevisiae*. Mis-localization of the protein from the plasma membrane might not be equivalent to a lack of function, as the protein domains have so far been defined by computational analysis [76]. Therefore, if VapA no longer binds the RCV membrane but is still able to rescue intramacrophage replication, then it is possible that VapA's localization ability has been altered but a yet to be defined enzymatic function remains. In contrast, if function is absent in a protein

that lacks liposome binding qualities, it could demonstrate that binding of VapA serves to sequester the available phosphatidic acid within the phagosome and allows for deviation from normal phagosomal maturation.

Work previously presented noted that while GFP-tagged VapA was able to localize to the yeast plasma membrane, both GFP-VapB and GFP-VapK2 were dramatically decreased in their ability to traffic to a similar location. It was additionally shown that rVapK2 was able to rescue the vapA deletion mutant of R. equi when protein was pre-incubated with the macrophage monolayer but could not bind PA containing liposomes [131]. Taken together, VapK2 appears to alter the killing capacity of the macrophage but either via a different mechanism or a less proficient means. Feasibly, the lipid binding modality of the protein is required for locating VapA to the surface of the RCV and some yet identified enzymatic function promotes alteration of the maturing phagosome. Therefore, VapK2 may lack the ability to bind phosphatidic acid but still harbor the enzymatic function located within VapA. One cannot forget that the pVapB plasmid also harbors VapK1, which also supports intracellular replication [208]. It is possible that the various virulence associated proteins, which allow for intramacrophage replication of the bacterium, act by alternate means from one another. It is our impression that, while the phagosome containing R.equi equipped with pVapA enlarges to a point where the macrophage is predominated by the RCV, pVapB carrying R. equi do not cause phagosome enlargement and the bacteria stay within close proximity to the phagosomal membrane, suggesting that the *vaps* responsible for intramacrophage growth may function by slightly different mechanisms. Trafficking markers throughout phagosomal maturation should be examined for both pVapB and pVapN carrying R. equi to determine whether bacteria equipped with these plasmids are handled in a similar fashion to pVapA containing R. equi. Protein studies used herein should be

completed with isolated pVapN Vaps, specifically VapN, to determine their ability to bind phosphatidic acid, rescue Δ*vapA*, and localize within *Saccharomyces cerevisiae*. Comparison between VapA and VapN would be less complex then attempting to compare the virulence determinant Vaps between the pVapA and pVapB virulence plasmids, since both VapK1 and VapK2 promote intracellular replication within the pVapB-type virulence plasmid and, as such, both proteins should be present during molecular analysis.

As a whole, these experiments provide a foundation for deciphering the mechanism of action of virulence associated protein A and for analyzing the different mechanisms used by the Vaps necessary for intramacrophage replication. Binding of VapA to phosphatidic acid should be abolished to determine the significance of this property during intramacrophage replication. Doing so will determine whether this function is required for activity or used for localization. Additional testing on the newly identified compartment that pVapA carrying R. equi resides in will help elucidate signaling events which provide the bacterium with an intramacrophage niche. Each of these experiments will progress the understanding of VapA's activity and will discern a new means by which an intracellular pathogen takes advantage of host machinery. Eukaryotic trafficking has been well studied but it is unlikely that the entirety of these processes has been elucidated [125]. Therefore, studies of VapA may identify a new cellular pathway, furthering the understanding of macrophage physiology and phagolysosomal maturation. Comparative studies between pVapA, pVapB, and pVapN carrying R. equi will determine whether the intracellular replication of these bacteria employs the same tactics for survival, wherein this analysis should be expanded to include the

protein aspects discussed previously. This work has opened avenues within the field to help understand the molecular basis of *R. equi*'s pathogenesis and to better define the host:pathogen interaction during intramacrophage replication.

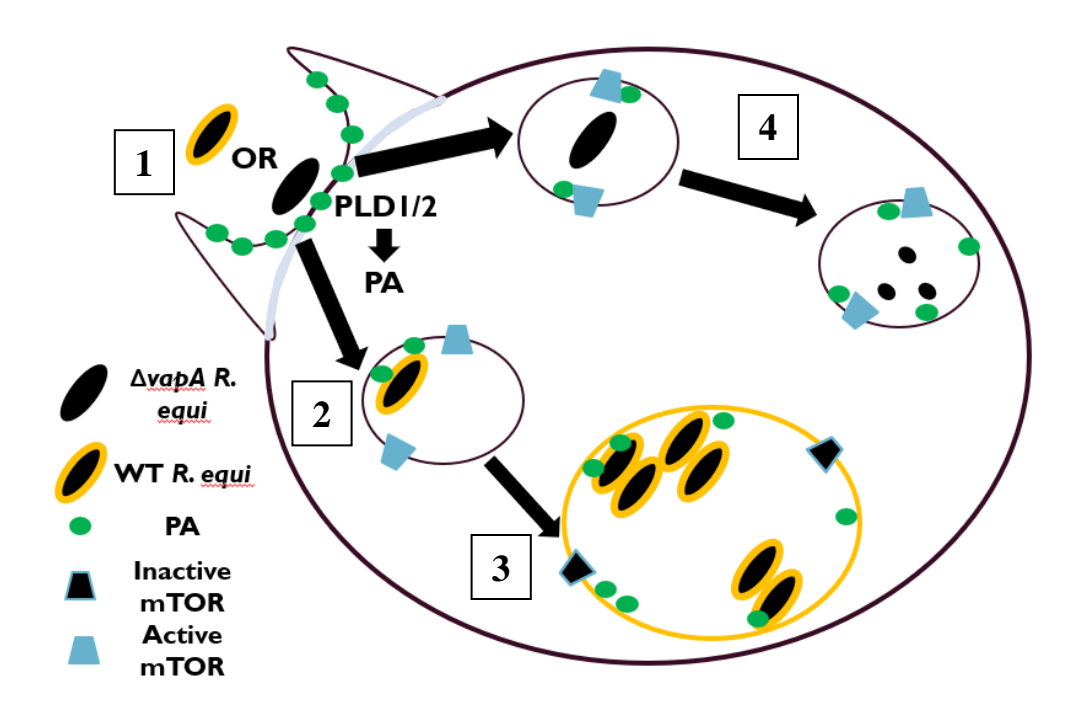


**Figure 12. Model for VapA's mechanism of action during macrophage infection with** *Rhodococcus equi*. (1) Phagocytosis of either bacterium will generate phosphatidic acid through the activation of phospholipase D 1/2 at the phagocytic cup [189]. (2) VapA, located on the surface of the wild type bacterium (gold color) can bind and sequester phosphatidic acid away from mTOR present within the mTORC1 complex [216]. Phosphatidic acid has been suggested as an activator of mTOR and therefore sequestration may lead to its inactivation [215]. (3) VapA on the bacterial surface and novel interaction with the RCV. mTOR inactivation will allow for induction of autophagy, leading to the delivery of additional membrane bilayer, nutrients, and time before the RCV fuses with the lysosome, thereby allowing for further replication of the wild type bacterium [125, 137]. (4) Phagocytosis of the *vapA* deletion mutant of *R. equi* will not inhibit mTOR and the bacteria will be delivered to the lysosome for degradation.

## REFERENCES

- 1. Jones, A.L., I.C. Sutcliffe, and M. Goodfellow, *Prescottia equi gen. nov., comb. nov.: a new home for an old pathogen.* Antonie Van Leeuwenhoek, 2013. **103**(3): p. 655-71.
- 2. Goodfellow, M. and G. Alderson, *The actinomycete-genus Rhodococcus: a home for the* "rhodochrous" complex. J Gen Microbiol, 1977. **100**(1): p. 99-122.
- 3. Goodfellow, M., *The taxonomic status of Rhodococcus equi*. Vet Microbiol, 1987. **14**(3): p. 205-9.
- 4. Mosser, D.M. and M.K. Hondalus, *Rhodococcus equi: an emerging opportunistic pathogen*. Trends Microbiol, 1996. **4**(1): p. 29-33.
- 5. Tindall, B.J., *The correct name of the taxon that contains the type strain of Rhodococcus equi.* Int J Syst Evol Microbiol, 2014. **64**(Pt 1): p. 302-8.
- 6. Garrity, G.M., Conservation of Rhodococcus equi (Magnusson 1923) Goodfellow and Alderson 1977 and rejection of Corynebacterium hoagii (Morse 1912) Eberson 1918. Int J Syst Evol Microbiol, 2014. **64**(Pt 1): p. 311-2.
- 7. Goodfellow, M., et al., Charting stormy waters: A commentary on the nomenclature of the equine pathogen variously named Prescottella equi, Rhodococcus equi and Rhodococcus hoagii. Equine Vet J, 2015. **47**(5): p. 508-9.
- 8. Anastasi, E., et al., *Pangenome and Phylogenomic Analysis of the Pathogenic Actinobacterium Rhodococcus equi*. Genome Biol Evol, 2016. **8**(10): p. 3140-3148.

- 9. Weinstock, D.M. and A.E. Brown, *Rhodococcus equi: an emerging pathogen*. Clin Infect Dis, 2002. **34**(10): p. 1379-85.
- 10. Hughes, K.L. and I. Sulaiman, *The ecology of Rhodococcus equi and physicochemical influences on growth.* Vet Microbiol, 1987. **14**(3): p. 241-50.
- 11. Barton, M.D. and K.L. Hughes, *Ecology of Rhodococcus equi*. Vet Microbiol, 1984. **9**(1): p. 65-76.
- 12. Takai, S., *Epidemiology of Rhodococcus equi infections: a review.* Vet Microbiol, 1997. **56**(3-4): p. 167-76.
- 13. Petry, S., et al., Differential distribution of vapA-positive Rhodococcus equi in affected and unaffected horse-breeding farms. Vet Rec, 2017. **181**(6): p. 145.
- 14. Prescott, J.F., M. Travers, and J.A. Yager-Johnson, Epidemiological survey of
   Corynebacterium equi infections on five Ontario horse farms. Can J Comp Med, 1984.

   48(1): p. 10-3.
- 15. Prescott, J.F., *Rhodococcus equi: an animal and human pathogen*. Clin Microbiol Rev, 1991. **4**(1): p. 20-34.
- 16. Muscatello, G., et al., Associations between the ecology of virulent Rhodococcus equi and the epidemiology of R. equi pneumonia on Australian thoroughbred farms. Appl Environ Microbiol, 2006. **72**(9): p. 6152-60.
- 17. Prescott, J.F., *Epidemiology of Rhodococcus equi infection in horses*. Vet Microbiol, 1987. **14**(3): p. 211-4.
- 18. Chaffin, M.K., et al., Foal-related risk factors associated with development of Rhodococcus equi pneumonia on farms with endemic infection. J Am Vet Med Assoc, 2003. **223**(12): p. 1791-9.

- 19. Muscatello, G., J.R. Gilkerson, and G.F. Browning, *Detection of virulent Rhodococcus* equi in exhaled air samples from naturally infected foals. J Clin Microbiol, 2009. **47**(3): p. 734-7.
- 20. Johnson, J.A., J.F. Prescott, and R.J. Markham, *The pathology of experimental Corynebacterium equi infection in foals following intrabronchial challenge*. Vet Pathol, 1983. **20**(4): p. 440-9.
- 21. Martens, R.J., R.A. Fiske, and H.W. Renshaw, *Experimental subacute foal pneumonia induced by aerosol administration of Corynebacterium equi*. Equine Vet J, 1982. **14**(2): p. 111-6.
- 22. Muscatello, G., et al., *Rhodococcus equi infection in foals: the science of 'rattles'*. Equine Vet J, 2007. **39**(5): p. 470-8.
- 23. Takai, S., et al., *Identification of intermediately virulent Rhodococcus equi isolates from pigs.* J Clin Microbiol, 1996. **34**(4): p. 1034-7.
- 24. Flynn, O., et al., Virulence-associated protein characterisation of Rhodococcus equi isolated from bovine lymph nodes. Vet Microbiol, 2001. **78**(3): p. 221-8.
- 25. Makrai, L., et al., *Isolation and characterisation of Rhodococcus equi from submaxillary lymph nodes of wild boars (Sus scrofa).* Vet Microbiol, 2008. **131**(3-4): p. 318-23.
- 26. Zink, M.C. and J.A. Yager, Experimental infection of piglets by aerosols of Rhodococcus equi. Can J Vet Res, 1987. **51**(3): p. 290-6.
- 27. Golub, B., G. Falk, and W.W. Spink, Lung abscess due to Corynebacterium equi. Report of first human infection. Ann Intern Med, 1967. **66**(6): p. 1174-7.
- 28. Guerrero, R., A. Bhargava, and Z. Nahleh, *Rhodococcus equi venous catheter infection: a case report and review of the literature.* J Med Case Rep, 2011. **5**: p. 358.

- 29. Kedlaya, I., M.B. Ing, and S.S. Wong, *Rhodococcus equi infections in immunocompetent hosts: case report and review.* Clin Infect Dis, 2001. **32**(3): p. E39-46.
- 30. Ayoade, F. and M.U. Alam, *Rhodococcus Equi*, in *StatPearls*. 2017: Treasure Island (FL).
- 31. Takai, S., et al., *Isolation of virulent and intermediately virulent Rhodococcus equi from soil and sand on parks and yards in Japan.* J Vet Med Sci, 1996. **58**(7): p. 669-72.
- 32. Witkowski, L., et al., *Molecular epidemiology of Rhodococcus equi in slaughtered swine,* cattle and horses in Poland. BMC Microbiol, 2016. **16**: p. 98.
- Zink, M.C., et al., Electron microscopic investigation of intracellular events after ingestion of Rhodococcus equi by foal alveolar macrophages. Vet Microbiol, 1987.
   14(3): p. 295-305.
- 34. Prescott, J.F., Capsular serotypes of Corynebacterium equi. Can J Comp Med, 1981.

  45(2): p. 130-4.
- 35. Iain C. Sutcliffe, A.K.B., and Lynn G. Dover, *The Rhodococcal Cell Envelope:*Composition, Organization and Biosynthesis. Biology of Rhodococcus, 2010: p. 29-71.
- 36. Severn, W.B. and J.C. Richards, *The structure of the specific capsular polysaccharide of Rhodococcus equi serotype 4*. Carbohydr Res, 1999. **320**(3-4): p. 209-22.
- 37. Smith, H., *Microbial surfaces in relation to pathogenicity*. Bacteriol Rev, 1977. **41**(2): p. 475-500.
- 38. Takai, S., et al., *Identification of 15- to 17-kilodalton antigens associated with virulent Rhodococcus equi.* J Clin Microbiol, 1991. **29**(3): p. 439-43.
- 39. Sydor, T., et al., *Diversion of phagosome trafficking by pathogenic Rhodococcus equi depends on mycolic acid chain length.* Cell Microbiol, 2013. **15**(3): p. 458-73.

- 40. Sutcliffe, I.C., *Macroamphiphilic cell envelope components of Rhodococcus equi and closely related bacteria.* Vet Microbiol, 1997. **56**(3-4): p. 287-99.
- 41. Sutcliffe, I.C., *Cell envelope composition and organisation in the genus Rhodococcus*.

  Antonie Van Leeuwenhoek, 1998. **74**(1-3): p. 49-58.
- 42. Marrakchi, H., M.A. Laneelle, and M. Daffe, *Mycolic acids: structures, biosynthesis, and beyond.* Chem Biol, 2014. **21**(1): p. 67-85.
- 43. Silhavy, T.J., D. Kahne, and S. Walker, *The bacterial cell envelope*. Cold Spring Harb Perspect Biol, 2010. **2**(5): p. a000414.
- 44. Gebhardt, H., et al., *The key role of the mycolic acid content in the functionality of the cell wall permeability barrier in Corynebacterineae*. Microbiology, 2007. **153**(Pt 5): p. 1424-34.
- 45. Daffe, M., M. McNeil, and P.J. Brennan, *Major structural features of the cell wall arabinogalactans of Mycobacterium, Rhodococcus, and Nocardia spp.* Carbohydr Res, 1993. **249**(2): p. 383-98.
- 46. Hsu, F.F., et al., Characterization of mycolic acids from the pathogen Rhodococcus equi by tandem mass spectrometry with electrospray ionization. Anal Biochem, 2011. **409**(1): p. 112-22.
- 47. Nishiuchi, Y., T. Baba, and I. Yano, *Mycolic acids from Rhodococcus, Gordonia, and Dietzia*. J Microbiol Methods, 2000. **40**(1): p. 1-9.
- 48. Letek, M., et al., *The genome of a pathogenic rhodococcus: cooptive virulence underpinned by key gene acquisitions.* PLoS Genet, 2010. **6**(9): p. e1001145.

- 49. Tan, C., et al., Molecular characterization of a lipid-modified virulence-associated protein of Rhodococcus equi and its potential in protective immunity. Can J Vet Res, 1995. **59**(1): p. 51-9.
- 50. Schlesinger, L.S., S.R. Hull, and T.M. Kaufman, *Binding of the terminal mannosyl units* of lipoarabinomannan from a virulent strain of Mycobacterium tuberculosis to human macrophages. J Immunol, 1994. **152**(8): p. 4070-9.
- 51. Garton, N.J., et al., A novel lipoarabinomannan from the equine pathogen Rhodococcus equi. Structure and effect on macrophage cytokine production. J Biol Chem, 2002. **277**(35): p. 31722-33.
- 52. Pei, Y., et al., Mutation and virulence assessment of chromosomal genes of Rhodococcus equi 103. Can J Vet Res, 2007. **71**(1): p. 1-7.
- 53. Kelly, B.G., et al., *Isocitrate lyase of the facultative intracellular pathogen Rhodococcus equi*. Microbiology, 2002. **148**(Pt 3): p. 793-8.
- Miranda-Casoluengo, R., et al., The hydroxamate siderophore rhequichelin is required for virulence of the pathogenic actinomycete Rhodococcus equi. Infect Immun, 2012.
   80(12): p. 4106-14.
- 55. Navas, J., et al., *Identification and mutagenesis by allelic exchange of choE, encoding a cholesterol oxidase from the intracellular pathogen Rhodococcus equi.* J Bacteriol, 2001. **183**(16): p. 4796-805.
- 56. Wall, D.M., et al., *Isocitrate lyase activity is required for virulence of the intracellular pathogen Rhodococcus equi.* Infect Immun, 2005. **73**(10): p. 6736-41.

- 57. van der Geize, R., et al., A novel method to generate unmarked gene deletions in the intracellular pathogen Rhodococcus equi using 5-fluorocytosine conditional lethality.

  Nucleic Acids Res, 2008. **36**(22): p. e151.
- 58. van der Geize, R., et al., *The steroid catabolic pathway of the intracellular pathogen*Rhodococcus equi is important for pathogenesis and a target for vaccine development.

  PLoS Pathog, 2011. **7**(8): p. e1002181.
- 59. Linder, R. and A.W. Bernheimer, *Oxidation of macrophage membrane cholesterol by intracellular Rhodococcus equi*. Vet Microbiol, 1997. **56**(3-4): p. 269-76.
- Dunn, M.F., J.A. Ramirez-Trujillo, and I. Hernandez-Lucas, *Major roles of isocitrate* lyase and malate synthase in bacterial and fungal pathogenesis. Microbiology, 2009.
   155(Pt 10): p. 3166-75.
- 61. Kondrashov, F.A., et al., Evolution of glyoxylate cycle enzymes in Metazoa: evidence of multiple horizontal transfer events and pseudogene formation. Biol Direct, 2006. 1: p. 31.
- 62. Wandersman, C. and P. Delepelaire, *Bacterial iron sources: from siderophores to hemophores*. Annu Rev Microbiol, 2004. **58**: p. 611-47.
- 63. Huynh, C. and N.W. Andrews, *Iron acquisition within host cells and the pathogenicity of Leishmania*. Cell Microbiol, 2008. **10**(2): p. 293-300.
- 64. Forbes, J.R. and P. Gros, *Divalent-metal transport by NRAMP proteins at the interface of host-pathogen interactions*. Trends Microbiol, 2001. **9**(8): p. 397-403.
- 65. De Voss, J.J., et al., The salicylate-derived mycobactin siderophores of Mycobacterium tuberculosis are essential for growth in macrophages. Proc Natl Acad Sci U S A, 2000. 97(3): p. 1252-7.

- 66. Miranda-CasoLuengo, R., et al., *The intracellular pathogen Rhodococcus equi produces* a catecholate siderophore required for saprophytic growth. J Bacteriol, 2008. **190**(5): p. 1631-7.
- 67. Takai, S., et al., Association between a large plasmid and 15- to 17-kilodalton antigens in virulent Rhodococcus equi. Infect Immun, 1991. **59**(11): p. 4056-60.
- 68. Goldstein, A.L. and J.H. McCusker, *Three new dominant drug resistance cassettes for gene disruption in Saccharomyces cerevisiae*. Yeast, 1999. **15**(14): p. 1541-53.
- 69. Takai, S., et al., *Virulence-associated plasmids in Rhodococcus equi*. J Clin Microbiol, 1993. **31**(7): p. 1726-9.
- 70. Tkachuk-Saad, O. and J. Prescott, *Rhodococcus equi plasmids: isolation and partial characterization*. J Clin Microbiol, 1991. **29**(12): p. 2696-700.
- 71. Ocampo-Sosa, A.A., et al., *Molecular epidemiology of Rhodococcus equi based on traA*, vapA, and vapB virulence plasmid markers. J Infect Dis, 2007. **196**(5): p. 763-9.
- 72. Vazquez-Boland, J.A., et al., *Rhodococcus equi: the many facets of a pathogenic actinomycete*. Vet Microbiol, 2013. **167**(1-2): p. 9-33.
- Valero-Rello, A., et al., An Invertron-Like Linear Plasmid Mediates Intracellular
   Survival and Virulence in Bovine Isolates of Rhodococcus equi. Infect Immun, 2015.
   83(7): p. 2725-37.
- 74. MacArthur, I., et al., Comparative Genomics of Rhodococcus equi Virulence Plasmids Indicates Host-Driven Evolution of the vap Pathogenicity Island. Genome Biol Evol, 2017. **9**(5): p. 1241-1247.
- 75. Willingham-Lane, J.M., et al., *Influence of Plasmid Type on the Replication of Rhodococcus equi in Host Macrophages*. mSphere, 2016. **1**(5).

- 76. Letek, M., et al., Evolution of the Rhodococcus equi vap pathogenicity island seen through comparison of host-associated vapA and vapB virulence plasmids. J Bacteriol, 2008. **190**(17): p. 5797-805.
- 77. Takai, S., et al., DNA sequence and comparison of virulence plasmids from Rhodococcus equi ATCC 33701 and 103. Infect Immun, 2000. **68**(12): p. 6840-7.
- 78. Aberdein, J.D., et al., Alveolar macrophages in pulmonary host defence the unrecognized role of apoptosis as a mechanism of intracellular bacterial killing. Clin Exp Immunol, 2013. **174**(2): p. 193-202.
- 79. Che, D., M.S. Hasan, and B. Chen, *Identifying pathogenicity islands in bacterial pathogenomics using computational approaches*. Pathogens, 2014. **3**(1): p. 36-56.
- 80. Gal-Mor, O. and B.B. Finlay, *Pathogenicity islands: a molecular toolbox for bacterial virulence*. Cell Microbiol, 2006. **8**(11): p. 1707-19.
- 81. Coulson, G.B., S. Agarwal, and M.K. Hondalus, *Characterization of the role of the pathogenicity island and vapG in the virulence of the intracellular actinomycete pathogen Rhodococcus equi*. Infect Immun, 2010. **78**(8): p. 3323-34.
- 82. Jain, S., B.R. Bloom, and M.K. Hondalus, *Deletion of vapA encoding Virulence*Associated Protein A attenuates the intracellular actinomycete Rhodococcus equi. Mol Microbiol, 2003. **50**(1): p. 115-28.
- 83. Byrne, G.A., et al., *Transcriptional regulation of the virR operon of the intracellular pathogen Rhodococcus equi.* J Bacteriol, 2007. **189**(14): p. 5082-9.
- 84. Kakuda, T., et al., VirS, an OmpR/PhoB subfamily response regulator, is required for activation of vapA gene expression in Rhodococcus equi. BMC Microbiol, 2014. **14**: p. 243.

- 85. Ren, J. and J.F. Prescott, *The effect of mutation on Rhodococcus equi virulence plasmid gene expression and mouse virulence*. Vet Microbiol, 2004. **103**(3-4): p. 219-30.
- 86. Russell, D.A., et al., *The LysR-type transcriptional regulator VirR is required for* expression of the virulence gene vapA of Rhodococcus equi ATCC 33701. J Bacteriol, 2004. **186**(17): p. 5576-84.
- 87. Wang, X., et al., *IcgA* is a virulence factor of Rhodococcus equi that modulates intracellular growth. Infect Immun, 2014. **82**(5): p. 1793-800.
- 88. Kakuda, T., et al., Transcriptional regulation by VirR and VirS of members of the Rhodococcus equi virulence-associated protein multigene family. Microbiol Immunol, 2015. **59**(8): p. 495-9.
- 89. Coulson, G.B., et al., *Transcriptome reprogramming by plasmid encoded transcriptional regulators is required for host-niche adaptation of a macrophage pathogen.* Infect Immun, 2015.
- 90. Byrne, G.A., et al., Differential mRNA stability of the vapAICD operon of the facultative intracellular pathogen Rhodococcus equi. FEMS Microbiol Lett, 2008. **280**(1): p. 89-94.
- 91. Boland, C., *Transcriptional regulation of virulence factors in Rhodococcus equi* National University of Ireland, Dublin, 2002.
- 92. Byrne, B.A., et al., Virulence plasmid of Rhodococcus equi contains inducible gene family encoding secreted proteins. Infect Immun, 2001. **69**(2): p. 650-6.
- 93. Takai, S., et al., Virulence-associated 15- to 17-kilodalton antigens in Rhodococcus equi: temperature-dependent expression and location of the antigens. Infect Immun, 1992.

  60(7): p. 2995-7.

- 94. Jacks, S., S. Giguere, and J.F. Prescott, *In vivo expression of and cell-mediated immune responses to the plasmid-encoded virulence-associated proteins of Rhodococcus equi in foals*. Clin Vaccine Immunol, 2007. **14**(4): p. 369-74.
- 95. Giguere, S., et al., Role of the 85-kilobase plasmid and plasmid-encoded virulence-associated protein A in intracellular survival and virulence of Rhodococcus equi. Infect Immun, 1999. **67**(7): p. 3548-57.
- 96. Okoko, T., et al., Structural characterisation of the virulence-associated protein VapG from the horse pathogen Rhodococcus equi. Vet Microbiol, 2015.
- 97. Geerds, C., et al., Structure of Rhodococcus equi virulence-associated protein B (VapB) reveals an eight-stranded antiparallel beta-barrel consisting of two Greek-key motifs.

  Acta Crystallogr F Struct Biol Commun, 2014. **70**(Pt 7): p. 866-71.
- 98. Whittingham, J.L., et al., Structure of the virulence-associated protein VapD from the intracellular pathogen Rhodococcus equi. Acta Crystallogr D Biol Crystallogr, 2014. **70**(Pt 8): p. 2139-51.
- 99. Shi, Y., A glimpse of structural biology through X-ray crystallography. Cell, 2014. **159**(5): p. 995-1014.
- 100. Kamal Gandhi, A.K., Saurabh Gosewade, Ravinder Kaushik, Darshan Lal, *X-RayCrystallography and Its Applications in Dairy Science: a Review.* STM Journals, 2013.2(1): p. 2319-3409.
- 101. Aderem, A. and D.M. Underhill, *Mechanisms of phagocytosis in macrophages*. Annu Rev Immunol, 1999. **17**: p. 593-623.
- 102. Hondalus, M.K., et al., *The intracellular bacterium Rhodococcus equi requires Mac-1 to bind to mammalian cells.* Infect Immun, 1993. **61**(7): p. 2919-29.

- 103. Noris, M. and G. Remuzzi, *Overview of complement activation and regulation*. Semin Nephrol, 2013. **33**(6): p. 479-92.
- 104. Bolger, M.S., et al., *Complement levels and activity in the normal and LPS-injured lung*.

  Am J Physiol Lung Cell Mol Physiol, 2007. **292**(3): p. L748-59.
- 105. Watford, W.T., A.J. Ghio, and J.R. Wright, *Complement-mediated host defense in the lung*. Am J Physiol Lung Cell Mol Physiol, 2000. **279**(5): p. L790-8.
- 106. Law, S.K. and A.W. Dodds, *The internal thioester and the covalent binding properties of the complement proteins C3 and C4*. Protein Sci, 1997. **6**(2): p. 263-74.
- 107. Croize, J., et al., Activation of the human complement alternative pathway by Listeria monocytogenes: evidence for direct binding and proteolysis of the C3 component on bacteria. Infect Immun, 1993. **61**(12): p. 5134-9.
- 108. Ernst, J.D., *Macrophage receptors for Mycobacterium tuberculosis*. Infect Immun, 1998. **66**(4): p. 1277-81.
- 109. Darrah, P.A., et al., *Innate immune responses to Rhodococcus equi*. J Immunol, 2004. **173**(3): p. 1914-24.
- 110. Dawson, D.R., et al., Effects of opsonization of Rhodococcus equi on bacterial viability and phagocyte activation. Am J Vet Res, 2011. **72**(11): p. 1465-75.
- 111. Zink, M.C., et al., *The interaction of Corynebacterium equi and equine alveolar macrophages in vitro*. J Reprod Fertil Suppl, 1982. **32**: p. 491-6.
- 112. Anderson, C.L., et al., *Alveolar and peritoneal macrophages bear three distinct classes of Fc receptors for IgG*. J Immunol, 1990. **145**(1): p. 196-201.
- 113. Guilliams, M., et al., *The function of Fcgamma receptors in dendritic cells and macrophages*. Nat Rev Immunol, 2014. **14**(2): p. 94-108.

- 114. Hietala, S.K. and A.A. Ardans, *Interaction of Rhodococcus equi with phagocytic cells* from R. equi-exposed and non-exposed foals. Vet Microbiol, 1987. **14**(3): p. 307-20.
- 115. Kawai, T. and S. Akira, *Toll-like receptors and their crosstalk with other innate receptors in infection and immunity*. Immunity, 2011. **34**(5): p. 637-50.
- 116. Kawai, T. and S. Akira, *The role of pattern-recognition receptors in innate immunity:*update on Toll-like receptors. Nat Immunol, 2010. **11**(5): p. 373-84.
- 117. Blander, J.M. and R. Medzhitov, *Regulation of phagosome maturation by signals from toll-like receptors*. Science, 2004. **304**(5673): p. 1014-8.
- 118. Fratti, R.A., J. Chua, and V. Deretic, *Induction of p38 mitogen-activated protein kinase reduces early endosome autoantigen 1 (EEA1) recruitment to phagosomal membranes.* J Biol Chem, 2003. **278**(47): p. 46961-7.
- 119. Kuhlman, M., K. Joiner, and R.A. Ezekowitz, *The human mannose-binding protein functions as an opsonin.* J Exp Med, 1989. **169**(5): p. 1733-45.
- 120. Matsushita, M., Y. Endo, and T. Fujita, *Structural and functional overview of the lectin complement pathway: its molecular basis and physiological implication*. Arch Immunol Ther Exp (Warsz), 2013. **61**(4): p. 273-83.
- 121. Diacovich, L. and J.P. Gorvel, *Bacterial manipulation of innate immunity to promote infection*. Nat Rev Microbiol, 2010. **8**(2): p. 117-28.
- 122. Toyooka, K., S. Takai, and T. Kirikae, *Rhodococcus equi can survive a phagolysosomal environment in macrophages by suppressing acidification of the phagolysosome*. J Med Microbiol, 2005. **54**(Pt 11): p. 1007-15.
- 123. Hondalus, M.K. and D.M. Mosser, *Survival and replication of Rhodococcus equi in macrophages*. Infect Immun, 1994. **62**(10): p. 4167-75.

- 124. Fernandez-Mora, E., et al., *Maturation of Rhodococcus equi-containing vacuoles is* arrested after completion of the early endosome stage. Traffic, 2005. **6**(8): p. 635-53.
- 125. Flannagan, R.S., G. Cosio, and S. Grinstein, *Antimicrobial mechanisms of phagocytes* and bacterial evasion strategies. Nat Rev Microbiol, 2009. **7**(5): p. 355-66.
- 126. Fairn, G.D. and S. Grinstein, *How nascent phagosomes mature to become phagolysosomes*. Trends Immunol, 2012. **33**(8): p. 397-405.
- 127. Vieira, O.V., R.J. Botelho, and S. Grinstein, *Phagosome maturation: aging gracefully*. Biochem J, 2002. **366**(Pt 3): p. 689-704.
- 128. Ham, H., A. Sreelatha, and K. Orth, *Manipulation of host membranes by bacterial effectors*. Nat Rev Microbiol, 2011. **9**(9): p. 635-46.
- 129. von Bargen, K., et al., *Rhodococcus equi virulence-associated protein A is required for diversion of phagosome biogenesis but not for cytotoxicity*. Infect Immun, 2009. **77**(12): p. 5676-81.
- 130. Rofe, A.P., et al., *The Rhodococcus equi virulence protein VapA disrupts endolysosome* function and stimulates lysosome biogenesis. Microbiologyopen, 2017. **6**(2).
- 131. Wright, L.M., et al., *VapA of Rhodococcus equi binds phosphatidic acid.* Mol Microbiol, 2017. **107**(3): p. 428-444.
- 132. Khalkhali-Ellis, Z. and M.J. Hendrix, *Two Faces of Cathepsin D: Physiological Guardian Angel and Pathological Demon.* Biol Med (Aligarh), 2014. **6**(2).
- 133. Chandramani-Shivalingappa, P., et al., *Induction of Reactive Intermediates and Autophagy-Related Proteins upon Infection of Macrophages with Rhodococcus equi.*Scientifica (Cairo), 2017. **2017**: p. 8135737.

- 134. Sardiello, M., et al., *A gene network regulating lysosomal biogenesis and function*. Science, 2009. **325**(5939): p. 473-7.
- 135. Settembre, C., et al., *TFEB links autophagy to lysosomal biogenesis*. Science, 2011. **332**(6036): p. 1429-33.
- 136. Dall'Armi, C., et al., *The phospholipase D1 pathway modulates macroautophagy*. Nat Commun, 2010. **1**: p. 142.
- 137. Levine, B., N. Mizushima, and H.W. Virgin, *Autophagy in immunity and inflammation*.

  Nature, 2011. **469**(7330): p. 323-35.
- 138. Sangkanjanavanich, N., et al., Rescue of an intracellular avirulent Rhodococcus equi replication defect by the extracellular addition of virulence-associated protein A. J Vet Med Sci, 2017. **79**(8): p. 1323-1326.
- 139. Luhrmann, A., et al., *Necrotic death of Rhodococcus equi-infected macrophages is regulated by virulence-associated plasmids*. Infect Immun, 2004. **72**(2): p. 853-62.
- 140. Mosser, D.M. and J.P. Edwards, *Exploring the full spectrum of macrophage activation*.

  Nat Rev Immunol, 2008. **8**(12): p. 958-69.
- 141. von Bargen, K., et al., Nitric oxide-mediated intracellular growth restriction of pathogenic Rhodococcus equi can be prevented by iron. Infect Immun, 2011. **79**(5): p. 2098-111.
- 142. Darrah, P.A., et al., Cooperation between reactive oxygen and nitrogen intermediates in killing of Rhodococcus equi by activated macrophages. Infect Immun, 2000. **68**(6): p. 3587-93.
- 143. Arango Duque, G. and A. Descoteaux, *Macrophage cytokines: involvement in immunity and infectious diseases*. Front Immunol, 2014. **5**: p. 491.

- 144. Schroder, K., M.J. Sweet, and D.A. Hume, *Signal integration between IFNgamma and TLR signalling pathways in macrophages*. Immunobiology, 2006. **211**(6-8): p. 511-24.
- 145. Giguere, S. and J.F. Prescott, *Cytokine induction in murine macrophages infected with virulent and avirulent Rhodococcus equi*. Infect Immun, 1998. **66**(5): p. 1848-54.
- 146. Giguere, S., B.N. Wilkie, and J.F. Prescott, *Modulation of cytokine response of pneumonic foals by virulent Rhodococcus equi*. Infect Immun, 1999. **67**(10): p. 5041-7.
- 147. Berghaus, L.J., et al., Effects of priming with cytokines on intracellular survival and replication of Rhodococcus equi in equine macrophages. Cytokine, 2017. **102**: p. 7-11.
- 148. Giguere, S., et al., *Rhodococcus equi: clinical manifestations, virulence, and immunity.* J Vet Intern Med, 2011. **25**(6): p. 1221-30.
- 149. Dawson, T.R., et al., Current understanding of the equine immune response to Rhodococcus equi. An immunological review of R. equi pneumonia. Vet Immunol Immunopathol, 2010. **135**(1-2): p. 1-11.
- 150. Nordmann, P., E. Ronco, and C. Nauciel, *Role of T-lymphocyte subsets in Rhodococcus equi infection*. Infect Immun, 1992. **60**(7): p. 2748-52.
- 151. Hietala, S.K. and A.A. Ardans, *Neutrophil phagocytic and serum opsonic response of the foal to Corynebacterium equi*. Vet Immunol Immunopathol, 1987. **14**(3): p. 279-94.
- 152. Yager, J.A., et al., *The effect of experimental infection with Rhodococcus equi on immunodeficient mice*. Vet Microbiol, 1991. **28**(4): p. 363-76.
- 153. Yager, J.A., *The pathogenesis of Rhodococcus equi pneumonia in foals.* Vet Microbiol, 1987. **14**(3): p. 225-32.
- 154. Martens, R.J., et al., *Rhodococcus equi foal pneumonia: protective effects of immune plasma in experimentally infected foals.* Equine Vet J, 1989. **21**(4): p. 249-55.

- 155. Sanz, M.G., A. Loynachan, and D.W. Horohov, *Rhodococcus equi hyperimmune plasma decreases pneumonia severity after a randomised experimental challenge of neonatal foals.* Vet Rec, 2016. **178**(11): p. 261.
- 156. Madarame, H., et al., Virulent and avirulent Rhodococcus equi infection in T-cell deficient athymic nude mice: pathologic, bacteriologic and immunologic responses. FEMS Immunol Med Microbiol, 1997. **17**(4): p. 251-62.
- 157. Kanaly, S.T., S.A. Hines, and G.H. Palmer, Failure of pulmonary clearance of Rhodococcus equi infection in CD4+ T-lymphocyte-deficient transgenic mice. Infect Immun, 1993. **61**(11): p. 4929-32.
- 158. Ross, T.L., et al., Role of CD4+, CD8+ and double negative T-cells in the protection of SCID/beige mice against respiratory challenge with Rhodococcus equi. Can J Vet Res, 1996. **60**(3): p. 186-92.
- 159. Kanaly, S.T., S.A. Hines, and G.H. Palmer, *Cytokine modulation alters pulmonary clearance of Rhodococcus equi and development of granulomatous pneumonia*. Infect Immun, 1995. **63**(8): p. 3037-41.
- 160. Hines, M.T., et al., *Immunity to Rhodococcus equi: antigen-specific recall responses in the lungs of adult horses.* Vet Immunol Immunopathol, 2001. **79**(1-2): p. 101-14.
- 161. Cohen, N.D., Rhodococcus equi foal pneumonia. Vet Clin North Am Equine Pract, 2014.30(3): p. 609-22.
- 162. Sanz, M., et al., *The effect of bacterial dose and foal age at challenge on Rhodococcus equi infection.* Vet Microbiol, 2013. **167**(3-4): p. 623-31.
- 163. Huber, L., et al., Development of septic polysynovitis and uveitis in foals experimentally infected with Rhodococcus equi. PLoS One, 2018. **13**(2): p. e0192655.

- 164. Giguere, S., et al., *Diagnosis, treatment, control, and prevention of infections caused by Rhodococcus equi in foals.* J Vet Intern Med, 2011. **25**(6): p. 1209-20.
- 165. Kinoshita, Y., et al., Development of a loop-mediated isothermal amplification method for detecting virulent Rhodococcus equi. J Vet Diagn Invest, 2016. **28**(5): p. 608-11.
- 166. Takai, S., et al., Monoclonal antibody specific to virulence-associated 15- to 17-kilodalton antigens of Rhodococcus equi. J Clin Microbiol, 1993. **31**(10): p. 2780-2.
- 167. Anastasi, E., et al., Novel transferable erm(46) determinant responsible for emerging macrolide resistance in Rhodococcus equi. J Antimicrob Chemother, 2015. **70**(12): p. 3184-90.
- 168. Fines, M., et al., Characterization of mutations in the rpoB gene associated with rifampin resistance in Rhodococcus equi isolated from foals. J Clin Microbiol, 2001. **39**(8): p. 2784-7.
- 169. Xu, L., et al., *Inhibition of host vacuolar H+-ATPase activity by a Legionella pneumophila effector*. PLoS Pathog, 2010. **6**(3): p. e1000822.
- 170. Li, W. and J. Xie, Role of mycobacteria effectors in phagosome maturation blockage and new drug targets discovery. J Cell Biochem, 2011. **112**(10): p. 2688-93.
- 171. Vergne, I., et al., *Mechanism of phagolysosome biogenesis block by viable Mycobacterium tuberculosis.* Proc Natl Acad Sci U S A, 2005. **102**(11): p. 4033-8.
- 172. Kolodziejek, A.M. and S.I. Miller, *Salmonella modulation of the phagosome membrane*, role of SseJ. Cell Microbiol, 2015. **17**(3): p. 333-41.
- 173. Steele-Mortimer, O., *The Salmonella-containing vacuole: moving with the times*. Curr Opin Microbiol, 2008. **11**(1): p. 38-45.

- 174. Arasaki, K., D.K. Toomre, and C.R. Roy, *The Legionella pneumophila effector DrrA is sufficient to stimulate SNARE-dependent membrane fusion*. Cell Host Microbe, 2012.

  11(1): p. 46-57.
- 175. Botstein, D. and G.R. Fink, *Yeast: an experimental organism for modern biology*. Science, 1988. **240**(4858): p. 1439-43.
- 176. Botstein, D. and G.R. Fink, *Yeast: an experimental organism for 21st Century biology*. Genetics, 2011. **189**(3): p. 695-704.
- 177. Siggers, K.A. and C.F. Lesser, *The Yeast Saccharomyces cerevisiae: a versatile model system for the identification and characterization of bacterial virulence proteins.* Cell Host Microbe, 2008. **4**(1): p. 8-15.
- 178. Sato, H., et al., *The mechanism of action of the Pseudomonas aeruginosa-encoded type III cytotoxin, ExoU*. EMBO J, 2003. **22**(12): p. 2959-69.
- 179. Sisko, J.L., et al., *Multifunctional analysis of Chlamydia-specific genes in a yeast expression system.* Mol Microbiol, 2006. **60**(1): p. 51-66.
- 180. Curak, J., J. Rohde, and I. Stagljar, *Yeast as a tool to study bacterial effectors*. Curr Opin Microbiol, 2009. **12**(1): p. 18-23.
- 181. Cox, D.L.N.a.M.M., *Principles of Biochemistry*. 5th ed. 2008, New York: W. H. Freeman and Company. 1-1158.
- 182. van Meer, G., D.R. Voelker, and G.W. Feigenson, *Membrane lipids: where they are and how they behave.* Nat Rev Mol Cell Biol, 2008. **9**(2): p. 112-24.
- 183. Bohdanowicz, M. and S. Grinstein, *Role of phospholipids in endocytosis, phagocytosis, and macropinocytosis.* Physiol Rev, 2013. **93**(1): p. 69-106.

- 184. Fahy, E., et al., *A comprehensive classification system for lipids*. J Lipid Res, 2005. **46**(5): p. 839-61.
- 185. Dennis, E.A., et al., *A mouse macrophage lipidome*. J Biol Chem, 2010. **285**(51): p. 39976-85.
- 186. Teng, O., C.K.E. Ang, and X.L. Guan, *Macrophage-Bacteria Interactions-A Lipid-Centric Relationship*. Front Immunol, 2017. **8**: p. 1836.
- 187. Putta, P., et al., *Phosphatidic acid binding proteins display differential binding as a function of membrane curvature stress and chemical properties.* Biochim Biophys Acta, 2016. **1858**(11): p. 2709-2716.
- 188. Lemmon, M.A., *Membrane recognition by phospholipid-binding domains*. Nat Rev Mol Cell Biol, 2008. **9**(2): p. 99-111.
- 189. Corrotte, M., et al., *Dynamics and function of phospholipase D and phosphatidic acid during phagocytosis*. Traffic, 2006. **7**(3): p. 365-77.
- 190. Jenkins, G.H., P.L. Fisette, and R.A. Anderson, *Type I phosphatidylinositol 4-phosphate*5-kinase isoforms are specifically stimulated by phosphatidic acid. J Biol Chem, 1994.

  269(15): p. 11547-54.
- 191. Wang, X., et al., *Signaling functions of phosphatidic acid.* Prog Lipid Res, 2006. **45**(3): p. 250-78.
- 192. Lim, H.K., et al., *Phosphatidic acid regulates systemic inflammatory responses by modulating the Akt-mammalian target of rapamycin-p70 S6 kinase 1 pathway*. J Biol Chem, 2003. **278**(46): p. 45117-27.
- 193. Liu, Y., Y. Su, and X. Wang, *Phosphatidic acid-mediated signaling*. Adv Exp Med Biol, 2013. **991**: p. 159-76.

- 194. Frondorf, K., et al., *Phosphatidic acid is a leukocyte chemoattractant that acts through S6 kinase signaling*. J Biol Chem, 2010. **285**(21): p. 15837-47.
- 195. Poerio, N., et al., *Liposomes loaded with bioactive lipids enhance antibacterial innate immunity irrespective of drug resistance*. Sci Rep, 2017. **7**: p. 45120.
- 196. Auricchio, G., et al., *Role of macrophage phospholipase D in natural and CpG-induced antimycobacterial activity*. Cell Microbiol, 2003. **5**(12): p. 913-20.
- 197. Manifava, M., et al., Differential binding of traffic-related proteins to phosphatidic acidor phosphatidylinositol (4,5)- bisphosphate-coupled affinity reagents. J Biol Chem, 2001. **276**(12): p. 8987-94.
- 198. Vicogne, J., et al., Asymmetric phospholipid distribution drives in vitro reconstituted SNARE-dependent membrane fusion. Proc Natl Acad Sci U S A, 2006. **103**(40): p. 14761-6.
- 199. Komijn, R.E., et al., Granulomatous lesions in lymph nodes of slaughter pigs bacteriologically negative for Mycobacterium avium subsp. avium and positive for Rhodococcus equi. Vet Microbiol, 2007. **120**(3-4): p. 352-7.
- 200. Giguere, S., *Treatment of Infections Caused by Rhodococcus equi*. Vet Clin North Am Equine Pract, 2017. **33**(1): p. 67-85.
- 201. Hooper-McGrevy, K.E., B.N. Wilkie, and J.F. Prescott, *Immunoglobulin G subisotype* responses of pneumonic and healthy, exposed foals and adult horses to Rhodococcus equi virulence-associated proteins. Clin Diagn Lab Immunol, 2003. **10**(3): p. 345-51.
- 202. Burd, C.G. and S.D. Emr, *Phosphatidylinositol(3)-phosphate signaling mediated by specific binding to RING FYVE domains*. Mol Cell, 1998. **2**(1): p. 157-62.

- 203. Odorizzi, G., M. Babst, and S.D. Emr, *Fab1p PtdIns(3)P 5-kinase function essential for protein sorting in the multivesicular body*. Cell, 1998. **95**(6): p. 847-58.
- 204. Sheffield, P., S. Garrard, and Z. Derewenda, *Overcoming expression and purification* problems of RhoGDI using a family of "parallel" expression vectors. Protein Expr Purif, 1999. **15**(1): p. 34-9.
- 205. Burton, A.J., et al., *Efficacy of liposomal gentamicin against Rhodococcus equi in a mouse infection model and colocalization with R. equi in equine alveolar macrophages.*Vet Microbiol, 2015. **176**(3-4): p. 292-300.
- 206. Bryan, L.K., et al., *Detection of vapN in Rhodococcus equi isolates cultured from humans*. PLoS One, 2018. **13**(1): p. e0190829.
- 207. Takai, S., et al., Effect of growth temperature on maintenance of virulent Rhodococcus equi. Vet Microbiol, 1994. **39**(1-2): p. 187-92.
- 208. Willingham-Lane, J.M., Host Species Tropism and the Genetic Requirement for Intracellular Replication of Rhodococcus equi, in Infectious Diseases. 2016, University of Georgia
- 209. Stover, C.K., et al., *New use of BCG for recombinant vaccines*. Nature, 1991. **351**(6326): p. 456-60.
- 210. Huang, K.C., et al., *Cell shape and cell-wall organization in Gram-negative bacteria*.

  Proc Natl Acad Sci U S A, 2008. **105**(49): p. 19282-7.
- 211. Jorm, L.R., et al., Genetic structure of populations of beta-haemolytic Lancefield group C streptococci from horses and their association with disease. Res Vet Sci, 1994. **57**(3): p. 292-9.

- 212. Giguere, S., et al., Relationship of mixed bacterial infection to prognosis in foals with pneumonia caused by Rhodococcus equi. J Vet Intern Med, 2012. **26**(6): p. 1443-8.
- 213. Kooijman, E.E., et al., *Spontaneous curvature of phosphatidic acid and lysophosphatidic acid.* Biochemistry, 2005. **44**(6): p. 2097-102.
- 214. Stones, D.H. and A.M. Krachler, *Dual function of a bacterial protein as an adhesin and extracellular effector of host GTPase signaling*. Small GTPases, 2015. **6**(3): p. 153-6.
- 215. Veverka, V., et al., Structural characterization of the interaction of mTOR with phosphatidic acid and a novel class of inhibitor: compelling evidence for a central role of the FRB domain in small molecule-mediated regulation of mTOR. Oncogene, 2008.
  27(5): p. 585-95.
- 216. Saxton, R.A. and D.M. Sabatini, *mTOR Signaling in Growth, Metabolism, and Disease*. Cell, 2017. **169**(2): p. 361-371.